Brain-Computer Interfaces for Inducing Brain Plasticity and Motor Learning: Implications for Brain-Injury Rehabilitation

A Dissertation
Presented to
The Academic Faculty
By

Karolyn O. Babalola

In Partial Fulfillment of the Requirements for the Degree
Doctor of Philosophy in Electrical Engineering

School of Electrical and Computer Engineering
Georgia Institute of Technology
August 2011

Brain-Computer Interfaces for Inducing Brain Plasticity and Motor Learning: Implications for Brain-Injury Rehabilitation

Approved by:

Dr. **Robert J. Butera**, Advisor
School of Electrical and Computer Engineering
Georgia Institute of Technology

Dr. **Melody Moore-Jackson**, Co-Advisor
College of Computing
Georgia Institute of Technology

Dr**. Stephen DeWeerth**
School of Electrical and Computer Engineering
Georgia Institute of Technology

Dr. **Ayanna M. Howard**
School of Electrical and Computer Engineering
Georgia Institute of Technology

Dr. **Elliot Moore**
School of Electrical and Computer Engineering
Georgia Institute of Technology

Dr. **Boris Prilutsky**
School of Applied Physiology
Georgia Institute of Technology

Date Approved: July 5, 2011

Dedication

This body of work is dedicated to all families have been affected by stroke or traumatic brain injury. Whether in the loss of a family member or the observance of a loved-one's debilitation, the devastation of brain injury is much more far-reaching that just the patient. I pray that the contributions of this dissertation and my future work will help to make a significant improvement in rehabilitative options and improve the lives of stroke and brain injury survivors and their families.

This dissertation is also dedicated to the African American students who have taken on the difficult task of pursuing higher education despite the personal, social and psychological challenges that can be particular to our group. My prayer is that over time, our support system in higher learning will continue to grow stronger so that our research goals and needs are met.

Finally I would like to dedicate this research to my father, Dr. Banji Babalola, who has been an inspiration, a mentor, and a role model. I know he is watching me from somewhere; as I take on his title, Dr. Babalola, I hope to make him proud.

Acknowledgements

First and foremost, I would like to express an extensive amount of gratitude to the Most High. Over the last few months, I have felt an overwhelming amount of divine intervention in every area of my life. This intervention has played a pivotal role in getting me through this Ph.D. process and I am grateful.

I am grateful for my advisors, Dr. Robert Butera and Dr. Melody Jackson, for their continued support and willingness to help me through this process. It has been a long road that I could not have traveled without them believing in me.

I would like to thank my committee members, Dr. Stephen DeWeerth, Dr. Ayanna Howard and Dr. Elliot Moore and Dr. Boris Prilutsky, whose genius, expertise and critical statements have helped me to become a better researcher.

I would like to thank Dr. Andrew Butler who has been an invaluable mentor and a friend. I truly appreciate the lessons he has given me and the words of inspiration. I am also grateful for the Atlanta Department of Veterans Affairs Center of Excellence who supported the last year and a half of my Ph.D. work!

I would like to thank Arun Elangovan for his voice of reason and unwavering help and support; no one can ask for a better friend. I hope he remembers me when he takes over the world! I am also grateful for the assistance of Dr. Chip Mappus. I am grateful for and indebted to Dr. Ashley Johnson for referring some wonderful volunteers! I am also grateful for the hours of time and assistance afforded me by Matt Wilczynski, who was my statistics guru!

I would like to thank Dr. Linda Harley who designed the motor learning assessment protocol that I used in this investigation and gave me an enormous amount of help with the motor learning data processing.

I would like to thank my cousin, Dr. Olusimidele Akinsiku. The chocolate covered fruit she sent me helped me to stop crying and continue writing. I can't wait to see the great things she will inevitably do!

My BGSA crew, Dr. Jacqueline Fairley, Dr. Sekou Remy, Dr. Otis Smart, Dr. Christal Gordon, Dr. Brett Matthews, Makayah Royal, Adrienne Prysock, Dr. Monique Hite, Crystal Gilpin, Dr. Kwaku Eason, Dr. Chris Green, Dr. Tammy McCoy, Dr. Manu Platt, Dr. Christiana Taylor, Dr. Clyde Lettsome, Dr. Cornelius Ejimifor and many others, have all inspired me in some way. Most of them do not know how much of an impact they have had on my life, but I am truly grateful!

I would like to thanks Dr. Ayodeji Fajebe; I am grateful for the words of encouragement and the Yoruba lessons!

My inspiring mentors, Dr. Janet Rutledge, Dr. Freeman Hrabowski, Dr. Gary May, Dr. Donna Llewellyn, Dr. Marion Usselman, Dr. Comas Haynes and the rest of the FACES committee, and the many other sources of support, inspiration and reassurance. They believed in me at times when I did not; that has truly helped to keep me moving.

I am extremely grateful for my yoga family, Tiffany Campbell, Kemiko Lawrence Octavia Raheem, Brooke Murray, Bethany Vaughn, Maya Bruer and my yoga retreat sisters and all of my wonderful students; they have helped me to keep the love and the light.

My best buddy, Elton Holmes, the math genius, has kept me laughing at times when I wanted to cry. I can always count on him to turn a bad day into a big joke.

I am grateful for my rock of support, my family. My Mom has always told me to persevere in spite of the all the challenges; she reminds me to keep my eyes on my goals and to not allow the obstacles to sidetrack me. My sister, Yetunde, has always been willing to offer

words of wisdom and hope. My brother, Bunmi, has been an inspiration for me to both set an example and to learn to be more laid back. My sister, Tope, has always been there for me from day one; she is my best friend, my strongest adviser and my greatest supporter; I cannot wait to see her become the doctor she was always meant to be!

Finally, I am grateful for my Dad who has given me his spirit, his dry wit and his dreams.

Table of Contents

List of Tables

List of Figures

List of Keywords and Abbreviations

BCI	Brain-Computer Interface
CAR	Common Average Reference Spatial Filter
CIMT	Constraint-Induced Movement Therapy
E_{ld}	Total Estimated Learning Error
E_{ad}	Total Estimated Adapted Error
E_{cd}	Estimated Degree of Adaptation
D_{eld}	Daily Reduction in Learning Error
D_{ead}	Daily Reduction in Adapted Error
EEG	Electroencephalogram
ERP	Event Related Potential
FLD	Fisher's Linear Discriminate
FLDwPCA	Fisher's Linear Discriminate with Principle Component Analysis
fMRI	Functional Magnetic Resonance Imaging
KINARM	Kinesiological Instrument for Normal and Altered Reaching Movement Robot
PID	Proportional Integrative Differential Controller
r^2	Coefficient of Determination
RBF	Radial Basis Function Kernel
SCP	Slow-Cortical Potential
SMR	Sensorimotor Rhythms
SVM	Support Vector Machine
TCP/IP	Transfer Control Protocol/Internet Protocol
UDP	User Datagram Protocol

Summary

The goal of this investigation was to explore the efficacy of implementing a rehabilitation robot controlled by a noninvasive brain-computer interface (BCI) to influence brain plasticity and facilitate motor learning. The motivation of this project stemmed from the need to address the population of stroke survivors who have few or no options for therapy.

A stroke occurs every 40 seconds in the United States and it is the leading cause of long-term disability [1-3]. In a country where the elderly population is growing at an astounding rate, one in six persons above the age of 55 is at risk of having a stroke. Internationally, the rates of strokes and stroke-induced disabilities are comparable to those of the United States [1, 4-6]. Approximately half of all stroke survivors suffer from immediate unilateral paralysis or weakness, 30-60% of which never regain function [1, 6-9]. Many individuals who survive stroke will be forced to seek institutional care or long-term assistance.

Clinicians have typically implemented stroke rehabilitative treatment using active training techniques such as constraint induced movement therapy (CIMT) and robotic therapy [10-12]. Such techniques restore motor activity by forcing the movement of weakened limbs. That active engagement of the weakened limb movement stimulates neural pathways and activates the motor cortex, thus inducing brain plasticity and motor learning. Several studies have demonstrated that active training does in fact have an effect on the way the brain restores itself and leads to faster rehabilitation [10, 13-15]. In addition, studies involving mental practice, another form of rehabilitation, have shown that mental imagery directly stimulates the brain, but is not effective unless implemented as a supplemental to active training [16, 17]. Only stroke survivors retaining residual motor ability are able to undergo active rehabilitative training; the

current selection of therapies has overlooked the significant population of stroke survivors suffering from severe control loss or complete paralysis [6, 10].

A BCI is a system or device that detects minute changes in brain signals to facilitate communication or control. In this investigation, the BCI was implemented through an electroencephalograph (EEG) device. EEG devices detect electrical brain signals transmitted through the scalp that corresponded with imagined motor activity. Within the BCI, a linear transformation algorithm converted EEG spectral features into control commands for an upper-limb rehabilitative robot, thus implementing a closed-looped feedback-control training system. The concept of the BCI-robot system implemented in this investigation may provide an alternative to current therapies by demonstrating the results of bypassing motor activity using brain signals to facilitate robotic therapy.

In this study, 24 able-bodied volunteers were divided into two study groups; one group trained to use sensorimotor rhythms (SMRs) (produced by imagining motor activity) to control the movement of a robot and the other group performed the 'guided-imagery' task of watching the robot move without control. This investigation looked for contrasts between the two groups that showed that the training involved with controlling the BCI-robot system had an effect on brain plasticity and motor learning.

To analyze brain plasticity and motor learning, EEG data corresponding to imagined arm movement and motor learning were acquired before, during, and after training. Features extracted from the EEG data consisted of frequencies in the 5-35Hz range, which produced amplitude fluctuations that were measurably significant during reaching. Motor learning data consisted of arm displacement measures (error) produced during an motor adaptation task performed daily by all subjects.

The results of the brain plasticity analysis showed persistent reductions in beta activity for subjects in the BCI group. The analysis also showed that subjects in the Non-BCI group had significant reductions in mu activity; however, these results were likely due to the fact that different EEG caps were used in each stage of the study. These results were promising but require further investigation.

The motor learning data showed that the BCI group out-performed non-BCI group in all measures of motor learning. These findings were significant because this was the first time a BCI had been applied to a motor learning protocol and the findings suggested that BCI had an influence on the speed at which subjects adapted to a motor learning task. Additional findings suggested that BCI subjects who were in the 40 and over age group had greater decreases in error after the learning phase of motor assessment. These finding suggests that BCI could have positive long term effects on individuals who are more likely to suffer from a stroke and possibly could be beneficial for chronic stroke patients.

In addition to exploring the effects of BCI training on brain plasticity and motor learning this investigation sought to detect whether the EEG features produced during guided-imagery could differentiate between reaching direction. While the analysis presented in this project produced classification accuracies no greater than ~77%, it formed the basis of future studies that would incorporate different pattern recognition techniques.

The results of this study show the potential for developing new rehabilitation therapies and motor learning protocols that incorporate BCI.

Chapter 1: Introduction

1.1. Motivation

1.1.1. Stroke

Strokes are the leading cause of partial paralysis and long-term adult disability in the United States [1-3]. With approximately 795,000 occurrences per year, 500,000 of which are first-time cases, and a total estimated cost amounting to over 57.9 billion dollars, it is clear that strokes have a very critical impact on the general well-being of the population [1, 2]. Because of modern medical advances, a stroke is more likely to result in chronic disability rather than death; therefore, the cost of healthcare and assistance for stroke survivors is of growing concern [2, 3]. It is estimated that one in six people over the age of 55 run the risk of suffering a stroke, and currently over 1.1 million Americans over the age of 65 have reported that disabilities from one or more strokes have left them dependent on outside care [2, 18].

Even children run a risk of developing disabilities due to a stroke as the incidence of strokes among children between infancy and toddler age is rising [19]. For infants under the age of 30 days, the rate of stroke occurrence is 26.4 in every 100,000 with 42% experiencing a moderate to severe deficit in physical abilities [20, 21]. With the aging baby boomers increasing the senior population at a disproportionate rate, and the increase in the rate of strokes among children, the concerns of stroke-related disability are only going to increase over time.

Despite the overall devastation of strokes, the number of survivors has increased by 37% since the 1970s, implying that there is a greater demand on resources needed for the assistance of individuals with disabilities resulting from the disorder [2].

A stroke occurs when the regular supply of oxygen to the brain is suddenly disrupted, causing a localized infarction or an accumulation of dead brain cells. There are two major types of strokes: ischemic strokes, which are characterized by a blockage of blood flow to the brain, and hemorrhagic strokes, which are characterized by bleeding in the brain, usually due to the bursting of a blood vessel. Of all new stroke cases, 88% are ischemic, which are more likely to result in long-term disability than death [2].

Depending on the locations in the brain where the lesions resulting from an ischemic stroke occur, a patient can suffer from any number of disruptions to neurological function including loss of eyesight or laziness of the eyes; aphasia, an inability to understand and/or communicate language; a loss of balance; and, most commonly, partial or complete physical paralysis.

Approximately half of all ischemic strokes are accompanied by hemiparesis, an increased weakness on one side of the body, or hemiplegia, paralysis on one side of the body [18]. Unilateral paralysis is due to the presence of lesions in a single hemisphere of the motor cortex, the side of the motor cortex contralateral, or opposite the side of paralysis (also referred to as the ipsilesional hemisphere).

Only approximately 60% of those suffering from hemiparesis after a stroke are expected to regain full functional independence; those with hemiplegia have an even lower rate of recovery [19]. Because of the large population of paralyzed stroke survivors, it is necessary to produce treatment methods that are as focused as possible, directly targeting areas of the brain

that are causing the disability [22]. Unfortunately, most rehabilitation techniques today are only effective if the subject retains some residual motor activity in the effected limb; therefore, individuals with severe hemiparesis and hemiplegia are left with very few options for treatment.

1.2. Problem Definition

The goal of this investigation is to explore the efficacy of using a rehabilitation robot controlled by a noninvasive brain-computer interface (BCI) to induce brain plasticity and facilitate motor learning. A BCI is a system or device that detects minute changes in brain signals to provide communication or facilitate control of a device. In this study an electroencephalograph (EEG) device detects signals on the scalp that correspond with imagined motor activity (motor imagery). A linear transformation algorithm converts the EEG frequency signals into control commands for a rehabilitative robot, thus implementing a closed-looped feedback-control training system. The closed-loop system, or BCI-robot system, implemented in this project operates as mental training instrument that invokes activity in areas of the brain that correspond with limb movement. The objective of this research is to determine whether the brain activity induced by training on the BCI-robot system has a measurable influence on brain plasticity and motor learning.

The Georgia Institute of Technology BrainLab works with BCI technologies to give the physically disabled new ways to communicate and control devices by engaging their direct brain signals [23, 24]. People suffering from brain injury and neurodegenerative diseases enjoy a higher level of independence that they otherwise would not have been able to experience thanks to technological advances with non-invasive BCIs [24-27].

Some of the BCI technologies used in the BrainLab require subject training that involves focusing on hand and limb movement to evoke changes in a brain signal called sensorimotor rhythm (SMR), 8-30Hz signals that can be adjusted with motor imagery or actual motor activity [28-31]. In several cases, after training, paralyzed subjects had shown increased motor ability in parts of the body on which they were asked to focus their attention. While anecdotal, these observations demonstrated that mental activity involved in operating a BCI may promote neural reorganization similar to that which occurs when using active training [16, 32-34]. Given the previous evidence, exploring whether the addition of BCI technology to a traditional rehabilitation technique can provide any improvement to overall rehabilitation was a logical next step.

Recent studies have suggested that technological developments may provide new options for rehabilitation in the form of combining robot-assisted therapies with BCIs [35-40]. While robotic rehabilitation has shown some promise for patients with weakened limbs, the control of a rehabilitative robot with a BCI can provide the closed-loop system needed to significantly influence brain activity to advance severely paralyzed patients past the movement threshold needed to undergo regular rehabilitation. In several studies, people with severe paralysis have controlled external devices, such as computer cursors and wheelchairs, by intentionally adjusting the activity of their brains [25, 41]. Thus, BCI technology could potentially empower stroke patients with severe upper limb paralysis to operate external devices such as robotic arms.

In this study, able-bodied volunteers performed active reaching of a rehabilitative robot arm using only motor imagery. This study assessed changes in the brain by evaluating statistical changes in electroencephalogram (EEG) activity. In addition, this study assessed motor learning

data to determine whether relevant changes in brain activity might correlate with an improvement in motor function.

1.3. Thesis Statement

Training on a BCI-controlled robot can influence neural plasticity and motor learning.

The investigation has sought to show that subjects who train to control a robot arm with the closed-loop feedback-controlled BCI-robot system implemented in this study would demonstrate more statistically significant changes in EEG and motor learning data during and after training than subjects who did not train in the closed-loop BCI-robot system. In addition, this investigation has begun the discussion of whether reaching directionality is detectable in EEG data corresponding to guided-imagery.

1.4. Method Overview

The methodology of this study is illustrated in Figure 1.4-1 Twenty-four volunteers participated in this study. Twelve subjects trained to control the BCI-robot system (BCI group); the other twelve formed the control group that performed a guided-imagery task with no BCI control (Non-BCI). All participants gave informed consent after receiving full disclosure of all components of the study. This study was approved by the Georgia Institute of Technology Institutional Review Board.

Members of each group were randomly placed and not aware of their group assignment. The entire protocol involved seven sessions of data collection, four of which were training. The first meeting was a screening session in which each volunteer participated prior to training; during this session, subjects were asked to perform real and imagined reaching in the robot while

wearing an EEG cap. After screening, subjects returned for five consecutive days of motor learning data collection and either BCI training or guided-imagery (Non-BCI) training. The seventh day of the protocol occurred approximately four weeks after the last day of training. This was a follow-up session where, once again, subjects performed reaching activities in the robot with the EEG; in addition subjects performed their final motor learning data collection task. The details of all components of training are explained in **Chapter 3**, Section **3.3**.

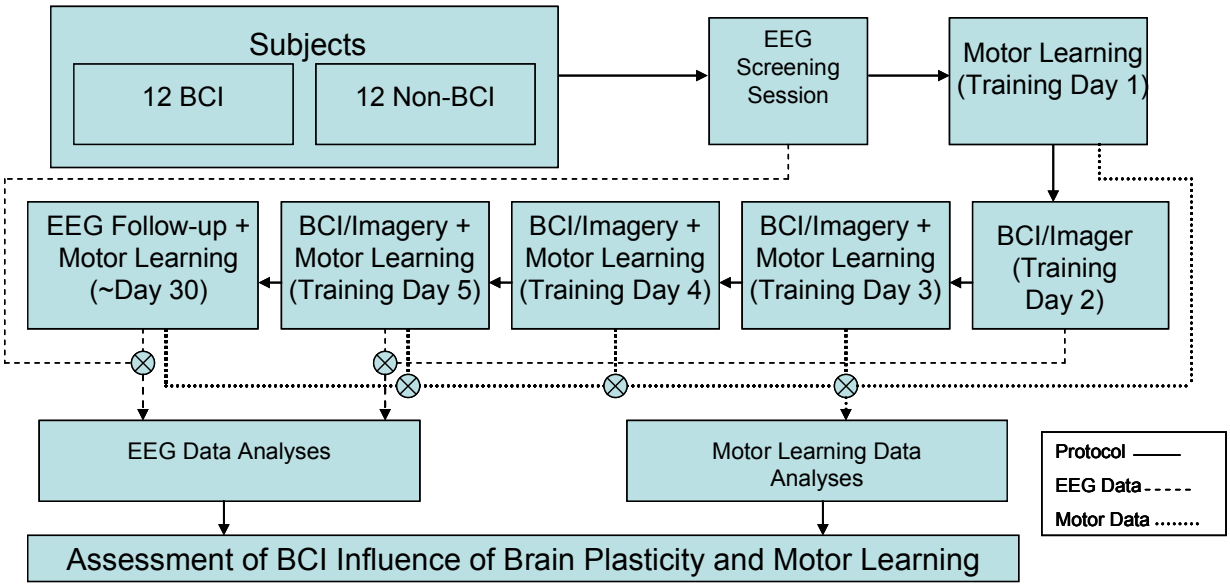

Figure 1.4-1. Diagram outlining the methodological steps of the study protocol. Dashed lines indicate data flow (EEG and motor learning).

1.5. Contributions

The results of this study form the basis for investigating new rehabilitation protocols that incorporate non-invasive BCI. The expected contributions of this study include:

1. *A proof of the hypothesis that BCI control can influence brain plasticity*- Several past studies have performed EEG statistical analysis to extract features for BCI applications; however, none have analyzed changes in EEG features as a measurement of brain

plasticity, particularly in comparison with EEG features of individuals who have no BCI experience [24, 25, 41-49]. This investigation takes advantage of the neurological underpinnings of EEG signals to make a claim for BCI-induced brain plasticity.

2. *A proof of the hypothesis that BCI control influences motor learning*- This investigation one of the first to combine a BCI protocol with a motor learning protocol. This is also the first time a motor learning analysis was performed to validate a BCI study. While the motivation for this research stems from stroke rehabilitation, the impact of this work can be more far-reaching. Considering that the subjects in this study are able-bodied, demonstrating that BCI has statistically significant effects on their motor learning could initiate the development of physical training protocols that incorporate BCI for improving motor performance in the able-bodied as well as in the disabled
3. *An analysis of EEG features corresponding to a novel guided-imagery reaching task*- The unique nature of the guided-imagery tasks performed in this study provides a new frontier for BCI discovery. The guided-imagery task represented by the robot movement updates previous methods used to evoke motor imagery. A feature-based analysis of the guided-imagery tasks performed by subjects during the seventh session of study forms the basis for future studies of EEG features produced while performing such tasks.
4. *A data repository consisting of BCI-robot training, guided-imagery training and related motor leaning data*.- The data collected in this study was made available to the engineering and science community for further analysis with the hopes of producing more novel contributions in BCI control, guided-imagery and motor learning. Data from this study can be accessed using the instructions outlined in Appendix C.

Chapter 2: Origin and History of the Problem

2.1. Stroke and Post-Stroke Paralysis

2.1.1. Post-Stroke Paralysis

Half of all stroke survivors suffer from hemiparesis or hemiplegia with only approximately 60% of those suffering from hemiparesis expected to regain enough motor ability for functional independence [19]. The devastating effects of a brain lesion are often not the only causes of paralysis; inter-hemispheric inhibition is another possible contributor. Already an inherent part of the natural operation of the brain, inter-hemispheric inhibition is believed by many to become more pronounced after brain injury; the increased effect causes overcompensation of the uninjured side of the brain by assuming the duties of both the paralyzed and the unaffected arm [50, 51]. Over time, stroke survivors develop a "learned non-use" of the paralyzed limb because of the natural tendency of the unaffected part of the brain to take over the functions of the lesion side of the brain [15, 50, 52].

2.2. Post-Stroke Cortical Plasticity and Rehabilitation Techniques

Historically, clinicians have instituted stroke rehabilitative treatments using compensatory training techniques that produced significant clinical results [10]. Recently stroke rehabilitation techniques have relied on manipulating neural plasticity to restore activity in areas of the brain that have lesions [10, 53, 54]. Techniques such as constraint-induced movement therapy, robotic therapy and mental practice have taken varied approaches to influencing

movement and brain plasticity with positive results. Such techniques, however, tend to impose the hefty requirement that patients retain some residual movement after having a stroke, a requirement that eliminates approximately 80% of the hemiplegic population [10, 53, 54].

2.2.1. Post-Stroke Cortical Plasticity

Cortical plasticity is a general term that refers to any physiological changes that occur in the brain, whether with natural experience or in response to training. Cortical plasticity often results in functional changes over time [55]. Studies have shown that immediately following a stroke, the brain demonstrates a natural capacity to reorganize itself to counterbalance the effect of a lesion; however, without some intervention, brain plasticity can lead to an overcompensation of unaffected limbs and a reduction in the cortical representation of weakened limbs [56-58]. Rehabilitation interventions are, therefore, often applied immediately after a patient experiences a stroke. Such interventions use limb-associated sensory input to influence plasticity while taking advantage of post-stroke plasticity [53, 59, 60]. The notion that sensory input influences plasticity is valid since the neural mechanisms underlying plasticity are often attributed to Hebbian learning, long-term activation or depression of synaptic processes in the brain that lead to associations of motor activities with specific cortical locations [61-63]. Evidence of successful rehabilitative training following a stroke is demonstrated by an increase in local cortical activation and an improvement in muscle capability in a paretic limb [10]. Some of the more prominent stroke rehabilitation techniques are outlined below.

2.2.2. Constraint-Induced Movement Therapy

Constraint-induced movement therapy (CIMT) is a common intervention for post-stroke hemiparesis. The quantity of studies involving CIMT with positive outcomes has been growing significantly since 1980 [64-67]. CIMT involves limiting the use of an opposing able limb and forcing the movement of a chronic paretic limb to reestablish muscle activity. Research suggests that CIMT increases activity in areas of the motor cortex surrounding those injured during a stroke, thus taking advantage of the plasticity of the brain and possibly reinstating the neural control of motor activity that was lost due to lesions in the brain caused by the stroke [52, 64, 68].

CIMT also reduces post-stroke interhemispheric inhibition, a neural-physiological phenomenon that may contribute to reduced function in a paretic limb. Interhemispheric inhibition is a natural response to brain injury; the uninjured part of the brain takes over most activity by having the non-paralyzed limb inherit the functions of the paralyzed limb. CIMT counters this effect by having the patient force the paralyzed limb to perform activities, thus evoking activity in the ipsilesional (contralateral) hemisphere and countering the learned non-use that results from being inhibited by the contralesional (ipsilateral), uninjured side of the brain [14, 50].

Previous CIMT studies have generally assumed the same common approach [10, 14, 15, 65]. Subjects in past studies have had newly-developed hemiparesis, having typically suffered from stroke no less than six months prior to CIMT therapy. These subjects are required to eliminate the use of an able limb by constraining the limb with a sling or some other means of inhibition (Figure. 2.2-1). Constraint is typically induced during all waking hours for a preset time period, ranging from one to 10 weeks. The subjects undergo regular daily training where

they are asked to perform everyday tasks with the weakened limb such as picking up objects and opening doors; in some studies, the subjects are also exposed to movement shaping exercises to force precision while performing everyday tasks [14, 67]. Most studies have reported patients' improvements in standard movement assessment tests after CIMT.

CIMT is the most common approach to post-stroke rehabilitation; however, this type of therapy has limitations. CIMT relies heavily on the need for subjects to have some residual motor ability in the paretic limb, often as considerable as 20% of the average range of motion; therefore, patients whose level of paresis exceeds that required for effective training are not able to benefit from CIMT [12]. Another caveat of CIMT is the free form nature by which subjects are instructed to perform tasks; in some cases, the lack of specificity in instruction leads to the subject developing compensating movements to enable the paretic limb to perform tasks, rather than actually activating the muscles that have lost function [10, 69]. In addition, the long-term constraint of an able limb can significantly reduce the quality of life of the subject, thus driving him/her to interfere with the study by removing the constraint of the able limb during waking hours. Because of these limitations, many have sought to augment or replace CIMT with other forms of rehabilitative training.

Figure 2.2-1. Patient undergoing CIMT is compelled to use left hand to write while right hand is constrained (http://whsc.emory.edu/_pubs/em/2001spring/brain.html).

2.2.3. Robotic Therapy

The field of robotic therapy has grown as a complement to CIMT as well as a stand alone method [10]. In the current healthcare environment, where efficient therapies require less direct supervision and faster results, robotic rehabilitation potentially fulfills a growing need and has several unique benefits. Recent advances in robotic technology, specifically the development of back-drivable robots (i.e., robots that move when they are pushed), allow for safe interactions between the robotic devices and people. This new robotic technology has been demonstrated to have great potential for physical rehabilitation of patients with muscle and/or neurological injuries [70, 71]. The advantages offered by robot-assisted therapy include the ability to assist in moving an impaired limb while supporting limb weight and setting precise resistance to limb motion for added training. In addition, robots that assist in therapy have the ability to quantify the amount and intensity of an intervention while monitoring the progress of therapy over time. To date, several studies have shown that robot-assisted technology can be successfully applied to restoring locomotion and to rehabilitating upper extremity function [70].

Several studies involving robotic therapy with stroke patients have demonstrated positive results [72]. Examples of robotic devices that are currently being used in clinical trials include the MIT-Manus [73], a two-joint manipulandum; the Mirror Image Movement Enhancer (MIME) [74], a six degree-of-freedom robot arm; and the Assisted Rehabilitation and Measurement (ARM) guide [75].

MIT-Manus was the first device to undergo considerable clinical tests (Figure 2.2-2). An initial pilot study involving 20 participants showed that there were no adverse responses to robot rehabilitation and that robot rehabilitation likely had a positive effect on brain reorganization [76]. The study showed improvements among patients who had suffered from a stroke within three months prior to the study and had developed hemiparesis as a result. Follow-up studies showed that patients retained the improvements up to three years following the initial study [77]. Successive studies of 60 and over 90 subjects confirmed the results of the first study [78]. The inaugural MIT-Manus trial was the first study to demonstrate that robotic rehabilitation is a useful rehabilitative tool; however, it also showed that robotic therapy was not particularly more beneficial than other conventional methods such as CIMT.

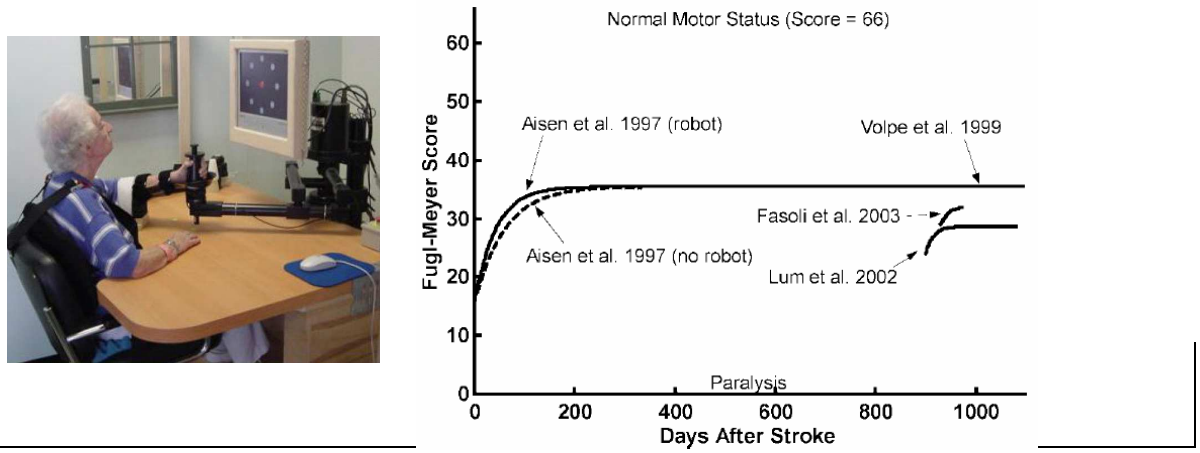

Figure 2.2-2. MIT-MANUS Study: 20 stroke patients received 5 1-h sessions a week for up to 9 weeks using the MIT-MANUS robot beginning 3 weeks after a single stroke. Left panel: Robot-assisted training with the MIT-MANUS device. Right panel: Plot demonstrating effects of rehabilitation with (continuous line) and without (dashed line) robot assistance [76].

The MIME robot studies were the first to show that robot rehabilitative therapy could possibly be more effective than conventional techniques [70, 74]. In the initial MIME study, 27 subjects, all of whom had hemiparesis resulting from strokes they had suffered within six months prior to the study, were divided into two groups. In one group subjects did extensive shoulder/elbow movements using the MIME robot; in the other group, subjects received conventional therapy and only minimal exposure to the robot. The immediate results showed that the robotic therapy subjects had a greater improvement in their Fugle-Meyer (FM) scores and in their strength and reaching capabilities (the Fugle-Meyer score is based on a quantitative scale developed through research performed by Twitchell and Brunnstrom regarding sequential stages of motor recovery in the hemiplegic stroke patient) [79-82]. After six months, the FM scores among all subjects were comparable; however, the overall functional ability of the robot subjects was still greater based on Function Independence Measures [69].

The ARM robot study sought to determine the similarities and differences between mechanical versus conventional rehabilitative assistance. The results of the initial study, however, were somewhat ambiguous. Initially, the patients who received robotic assistance showed greater improvements in almost all function and strength tests after two months of intervention. However, after six months, the degree of improvements gained by individuals receiving conventional rehabilitation had caught up with those who had received robotic rehabilitation. The authors postulated that the improvements could be attributed to personal interactions with the conventional therapists and because conventional patients were encouraged continue rehabilitation activities at home on their own [70, 74, 75].

Overall, robotic therapy has been shown to be beneficial and comparable to conventional rehabilitative techniques, such as CIMT. The approach, however still has its limitations. All of

the studies mentioned above had protocols that made use of patient movement to activate the robot's assistance; unfortunately, many patients have no residual movement and, therefore, cannot benefit from such a protocol. Also, as was demonstrated in the ARM study, patients' extra-curricular involvement in the intervention amplified the effects on rehabilitation so much that those who underwent conventional therapies were able to catch up to those who showed faster initial improvements with robotic therapy. The results outlined above suggest that robotic therapy is very useful for patients who retain significant sensory ability in their weakened limbs and are able to physically participate in their own intervention; however, the results also suggest that there are few, if any benefits to robotic rehabilitation for people with very little or no sensory ability.

2.2.4. Mental Practice

Mental practice is a relatively new field that works almost entirely on the premise of influencing brain plasticity to restore motor ability. Also referred to as mental imagery or mental training, mental practice involves using the process of engaging motor imagery to encourage the brain to activate specific areas associated with movement of certain body parts. This approach to rehabilitation is supported by studies that have shown that the same areas activated in the brain during motor activity are activated during the imagination *or* observation of motor activity [83-86]. Currently mental imagery is not heavily used in brain rehabilitation, but several pilot studies have shown that the addition of mental practice to an intervention can produce significant benefits.

In one study, two patients were given two different types of visual cues to stimulate the mental imagery of wrist movement [87]. The first type used a movie generated on the computer

to instruct the patients on how to move their wrists. The other practice involved using a mirror (Figure 2.2-3) to reflect the image of the patient's non-disabled hand performing activities. The patient's observation of the reflection invoked the *mirror neuron system* in the pre-motor cortex, thus causing the patient to produce brain signals corresponding to left-hand movements [86, 88, 89]. After both interventions, the patients' hands showed measurable improvements. The use of a mirror image to force mental imagery follows well with the findings of a study that suggests that mental imagery can be induced via movement intention *or* observation [90].

A more recent study involved 32 subjects who had mental practice combined with physical rehabilitation. The combination of therapies was compared to physical rehabilitation alone [33]. All subjects underwent a physical rehabilitation process; however, half of the group received a muscle flexing/relaxation period afterward, while the other half received a muscle flexing/relaxation period *plus* mental practice. For the mental practice group, rather than having visually guided imagery, patients were guided using a recording of a male voice. Patients in the mental practice group were instructed to imagine the physical practice they had previously performed. All subjects received treatment twice a week for six weeks. The study concluded with the mental practice patients showing greater improvements in their Action Research Arm tests (ARA), an arm reaching ability test [91], and FM scores [79]. Given the clinical significance of the patients' improvements, this study gave conclusive evidence that including mental practice in rehabilitation can have a significant impact on the outcome [33].

Figure 2.2-3. Subjects performs movements with the right hand and observe the movements in a mirror to evoke imagery of left hand movement [85].

Investigators are now seeking a more detailed understanding of the neural underpinnings of rehabilitation and particularly that which includes mental practice. Butler et al. recently published the results of a study that showed that individuals who received a combination of mental practice and CIMT showed not only increased functional ability, but also that mental practice may have a distinct influence on neural plasticity [16]. The study demonstrated that individuals who had performed mental practice had increased neural activation in the intact side of the brain and plasticity in the side of the brain containing the lesion [16]. This study introduced significant questions and has considerable implications for correlating mental practice with brain plasticity [16, 17, 92]. One glaring reality of mental practice, however, is that it has not been shown to be an effective means of intervention on its own. Mental practice shows more promise when combined with another intervention.

The promise and limitations of mental practice motivate the exploration of the idea that using mental imagery controlled rehabilitation therapy could have significant results that may begin to address some of the limitations of conventional therapies. One possible means of implementing this mental imagery controlled rehabilitation is through a brain computer interface.

2.3. BCI Techniques, History and Operation

2.3.1. Background

Brain computer interfaces translate externally-recorded brain activity to convey messages or commands to the external world [25]. Several invasive and noninvasive approaches to human BCI have been successfully used to communicate information and control external devices. These approaches take advantage of a number of different signals produced by the brain. Some of the intra-cortical brain signals employed within invasive BCIs include single neural action potentials and synaptic and extra-cellular field potentials [26, 27, 93, 94]. Extra-cortical signals, which are manipulated in non-invasive BCIs, include slow cortical potentials (SCPs), SMR, event-related potentials (ERPs), and blood oxygen levels [25, 29, 94-99]. Successful animal studies that employ invasive techniques have proven to be relatively effective for their purposes; however, for the sake of this review, only non-invasive approaches will be discussed [25, 30, 31, 41].

The origin of non-invasive BCI begins with the predictions of the pioneers of EEG. Hans Berger, who developed the human EEG in 1929, proposed in his review, the "Elektrenkephalogramm," that "sophisticated mathematics" may someday enable the reading of human thoughts. Grey Walter, who discovered the expectancy wave in 1964, attempted to distinguish covert thoughts from human language when he engineered the first frequency analyzer [41, 100-102]. Both were moving toward the general approach to BCI today, which plays on the concept of computationally transforming information obtained directly from the brain for technological applications. Because of its high time resolution, relatively inexpensive setup and well-known standard, the EEG is the primary non-invasive tool used to acquire signals

from BCI subjects and the International 10-20 system is the standard EEG electrode montage (Figure 2.3-2).

A BCI system is, generally, composed of three stages: signal acquisition, signal processing, and application control [25, 103]. During the signal acquisition stage, EEG electrodes measure electrical potentials on the scalp; the BCI system then transfers those EEG signals to an amplifier of comparable impedance to the electrodes; the amplifier interfaces with a computer that, finally, translates the acquired scalp signal to a command or communication signal. SMRs and SCPs are the primary signals translated for control. P300, an oddball response signal detected in parietal cortex, can administer control when combining its binary nature with specially designed software; this review will only discuss how SMR translation, transformation and mapping can control a cursor.

"Mu" SMRs are EEG signals that, when converted from time series to frequency signals, show measurable fluctuations in the 8-12 Hz range when a person performs or imagines motor activity (Figure 2.3-1.) [25, 104, 105]. Not to be confused with alpha rhythms, which contain the same bandwidth, but reside mainly in parietal cortex, mu activity is extracted over motor cortex [106]. Mu SMRs are sometimes coupled with or replaced by "beta" SMRs, which lay in the 18-26Hz bandwidth and have similar characteristics [25, 105]. The signal processing step in BCI uses the variability of mu amplitudes to control a device.

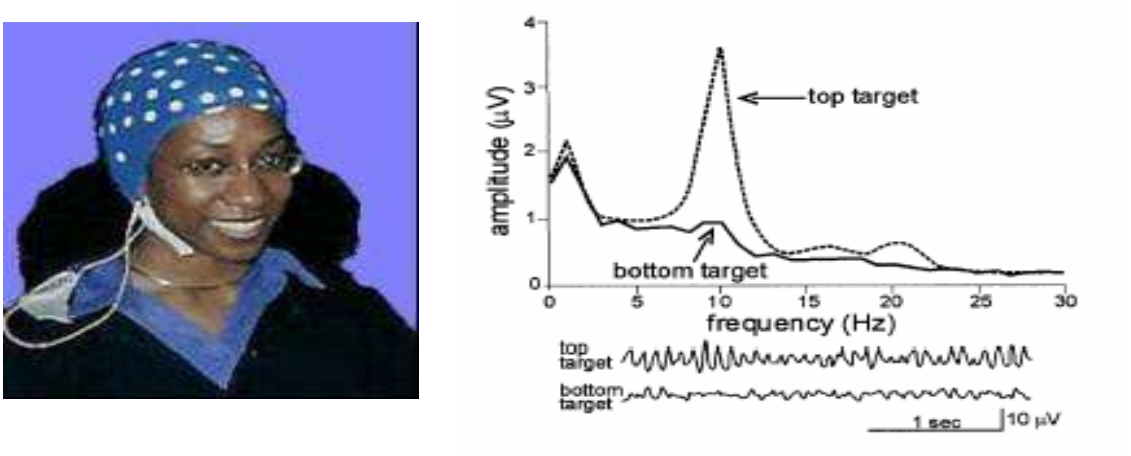

Figure 2.3-1. Left: BrainLab student modeling 64-Channel EEG cap. **Right:** Example of (SMR) activity, top graph is amplitude of mu in frequency domain; bottom is EEG data.

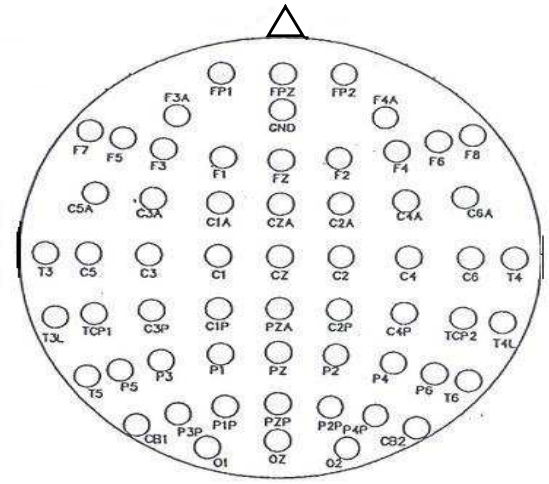

Figure 2.3-2. Standard 64-channel EEG electrode layout (International 10-20 system) [103].

For the task of controlling an external device using SMRs, patients undergo some operant conditioning, or training, that over time enables the patient to deliberately elicit specific cortical activity that will be processed and routed to an adaptive transformation algorithm. This transformation algorithm is the signal processing step, which produces the output that is interpreted in the application control step. The training process requires that subjects receive feedback (i.e. visual or touch) that communicates to them when they have produced the correct

signal amplitudes [25]. Over time, the subjects learn to control motor imagery to consistently produce SMR signals that correlate with their intentions.

2.3.2. BCI Computational Methods

One can take several approaches to process mu signals for BCI; however, for the purposes of this review, only the method employed by *BCI2000*, the software used in the BrainLab, is discussed; this should provide a sufficient description of the general computational approach taken for processing SMR-based BCIs. The signal processing methods outlined in this review are implemented in the ARSignalProcessing application of the *BCI2000* software package developed in the Wadsworth Center for Laboratories and Research at the New York State Department of Health [45, 107].

In this investigation, EEG data were transmitted to a 16-channel Guger Technologies g.USBamp biosignal amplifier that had a 0.1Hz high-pass filter and a 58Hz-62Hz notch filter and was sampled at 256Hz. During the *BCI2000* signal processing step, a small Laplacian reference filter spatially filtered the raw EEG signal (the Laplacian filter is explained in more detail in Section 3.4.1) [42, 108]. For real-time operation, *BCI2000* extracted 200ms windows every 100 milliseconds; therefore each window had a 50% overlap. To obtain spectral information, a 20-order autoregressive model was fit to each window of data using the Burg maximum entropy method and the respective spectral density of the window was estimated with a 256-length FFT [42, 109]. Specific frequency bands, typically in the 5-30Hz range, were then filtered out of the signal to extract the pre-set frequency parameter amplitudes; these were selected as features and linearly combined to produce a control signal, c_t (typically, the log of the control signal is used because of its normal distribution). The coefficients of the linear equation were determined by

offline analysis of previously acquired data. To account for the non-stationary nature of the EEG signal, c_t was normalized using the mean, μ, and standard deviation, σ, of a pre-selected sample of previous signals; so the resulting signal, x_t, was [42]:

$$x_t = \frac{c_t - \mu}{\sigma} \qquad (1).$$

The control signal was then linearly transformed into a scalar that is translated into a positive or negative cursor movement (or control of some other device).

SMRs from left and right motor cortex can be combined to produce a two-dimensional cursor movement from linear combinations of mu and beta amplitudes. For instance, once a control signal was produced using the method above, the cursor position would be determined by

$$\Delta V = b_V(x_{t\text{-}mu} - a_V) \quad \text{and} \quad \Delta H = b_H(x_{t\text{-}beta} - a_H) \qquad (2)$$

where ΔV and ΔH are vertical and horizontal movement of the cursor in terms of pixels, respectively, b_V and b_H are the scaling factors corresponding to vertical and horizontal movement in relation to the resolution of the screen (in this investigation, the screen resolution was 512x512), and $x_{t\text{-}mu}$ and $x_{t\text{-}beta}$ are signals produced from (1) separately using mu and beta feature combinations respectively [44].

Figure 2.3-3 outlines the topographical locations and amplitudes of mu and beta SMRs extracted to produce a two-dimensional cursor movement; the SMRs extracted from both right and left-hand motor cortex were linearly combined to produce horizontal movement and vertical movement separately. Users were initially trained to move the cursor in a one-dimensional horizontal space then in a one-dimensional vertical space. Later the BCI combined the horizontal and vertical movements to produce the two-dimensional cursor task.

Raw EEG signals are controlled by the trained subject. The subject's level of EEG control is directly proportional to the squared difference between the maximum and minimum mu amplitudes (*r2*). The *r2* measurement is useful because of the variable nature of EEG signals. It is estimated that some 80-93% of the population has the ability to control mu amplitudes yielding at least a 60% level of accuracy in control [43].

With the operational methods described above and the statistics mentioned on usability of BCIs, it is very clear that the applications for SMR-based BCIs are endless. The mechanisms used to control BCIs can easily be interfaced with the rehabilitation approaches discussed earlier in this chapter. With recent rehabilitation therapies adapting to directly target brain plasticity, the inclusion of BCI in investigating and developing new forms of therapy is promising.

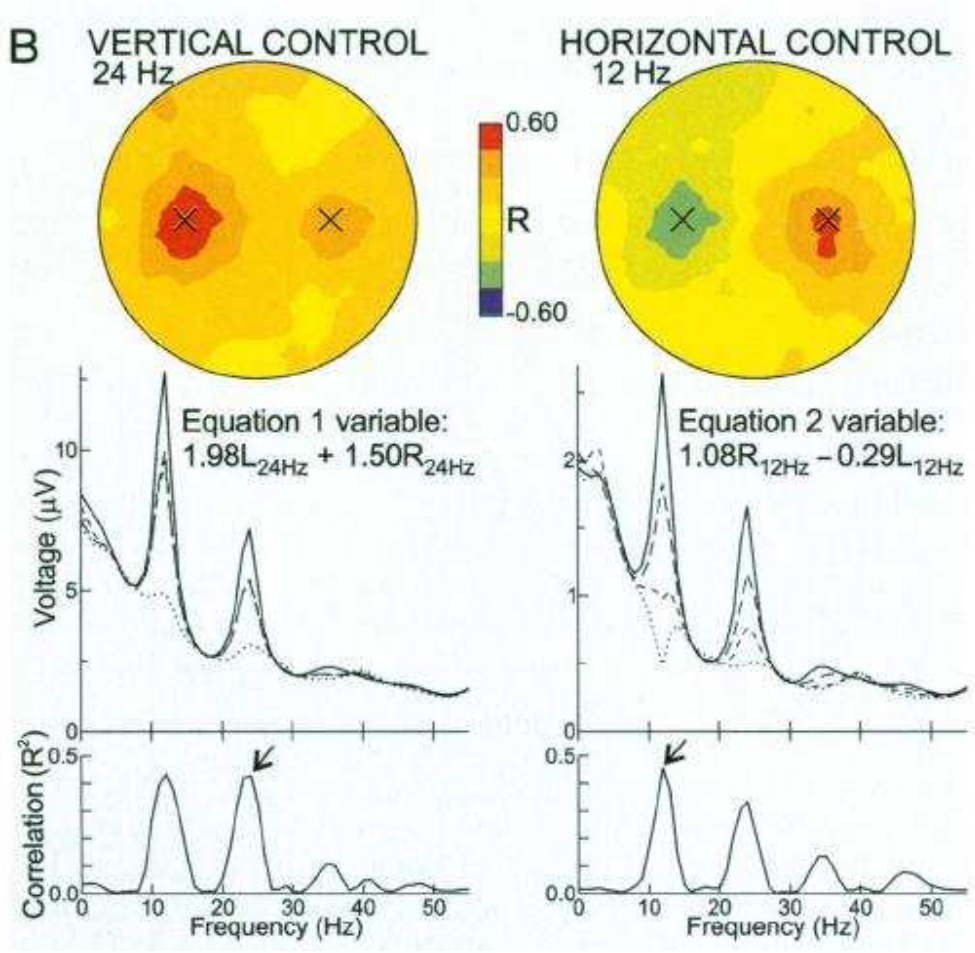

Figure 2.3- 3. Feature space of a two-dimensional BCI. **Top**: Topographical mapping of *r2* values of the 24Hz and 12Hz signals (note significant values over motor cortices). **Middle**: Frequency amplitudes of mu and beta features. **Bottom**: Corresponding *r2* values of mu and beta features [103].

Chapter 3: Methodology

3.1. Project Overview and System Development

The overall goal of this research was to determine whether subjects can demonstrate a measurable effect on brain plasticity and motor learning as a result of training to control a rehabilitation robot with a BCI. In addition to the overall goal, this project explores the possibility of detecting reaching directionality (forward vs. backward) in EEG data collected during a real-time guided-imagery task for future developments in BCI-robotic interfaces.

To achieve the goals of this investigation, the project was divided into the following **three specific aims**:

1. *Analyze BCI effects on brain plasticity* – After training, feature-based statistical analyses of EEG activity was used to determine if there were correlations among the changes that observed in subjects who performed BCI and whether those correlations were unique to the BCI group participants. The statistical analysis is explained in section 3.4.

2. *Analyze BCI effects on motor learning* – All subjects engaged in daily MLAs that consisted of loaded reaches with catch-trials; these assessments tested their rate of motor learning during training and several weeks after. The goal of this aim was to analyze the motor learning data to determine whether there was a statistically significant difference between measures of motor learning for the BCI group and that of the non-BCI group.

3. *Determine whether forward and backward guided-imagery can be detected in EEG.* EEG data collected during the Follow-up session were recorded while subjects were prompted to imagine arm reaching based on the movement of the robot. The classification techniques discussed at the end of this chapter deconstructed this EEG data to determine whether real-time detection of forward and backward movement was feasible given the previously processed feature set (Aim 1). Success in this endeavor would help to improve BCI transducer methods for robotic rehabilitation and to initiate the development of BCI-robot therapy protocols. The data acquisition portion of this project (Section 3.3) fostered the development of a data repository containing EEG data extracted during guide-imagery tasks. This repository will be available for investigators interested in performing alternate analysis of this novel motor imagery task.

The discussion below will explain the methodology in a chronological format. Section 3.4 will give a more detailed explanation the data analysis addressed the three specific aims.

3.2. BCI-Robot System Development

The environment in which this investigation took place was a hybrid system that incorporated an upper-limb, two degree-of-freedom rehabilitation robot called the KINARM; the KINARM was integrated with a SMR-based BCI, which was implemented through *BCI2000*. The integration of the two systems is detailed below.

3.2.1. KINARM Robot Overview

The KINARM (Kinesiological Instrument for Normal and Altered Reaching Movement; BKIN

Technologies, Inc., Ontario, Canada) is a motorized exoskeleton that monitors and manipulates arm motion in a horizontal plane. The robotic system includes two arm trays suitable for both left- and right-handed arm movements. The KINARM system integrates a virtual target presentation system implemented by the BKIN Dexterit-E software, which controls behavioral paradigms and data acquisition. The KINARM is capable of producing assistive or resistive forces while moving the arms around in the horizontal work plane; the KINARM is also capable of collecting data on angular displacement, velocity, acceleration of movements and joint torques with respect to the elbow, shoulder, linear displacement, velocity and acceleration of the hand. The system provides a general platform to perform a broad range of SMR and cognitive tasks. Subjects elbow and shoulder joints are typically aligned with the KINARM robot's joints. Visual feedback is provided to the subject by projecting the images onto a reflective screen in the work space, thus creating a realistic training environment. The KINARM can be used as an exoskeleton and is capable of moving automatically. As an exoskeleton, the hands of the subject are free which allows interaction with objects in the environment or a limitation in proprioceptive feedback to the subject.

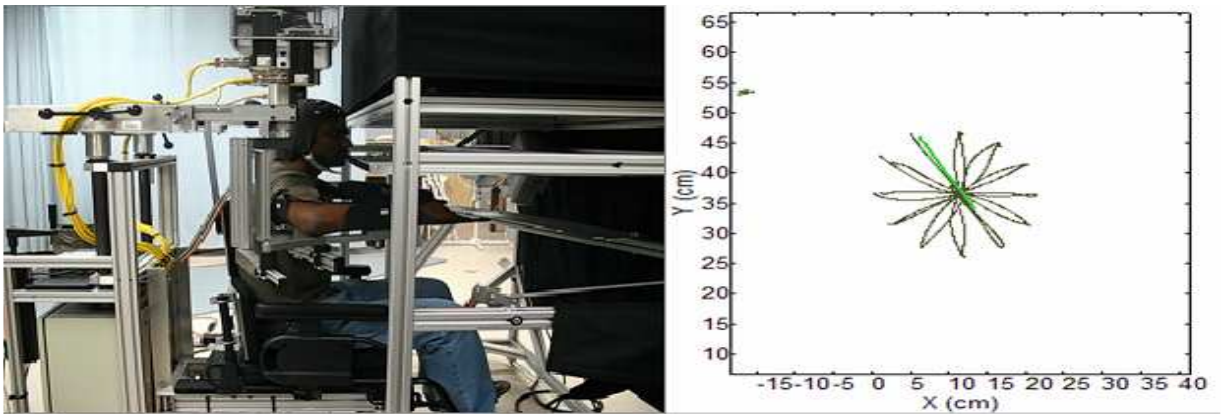

Figure 3.2-1. The KINARM™ robotic device located in Georgia Institute of Technology Biomechanics and Motor Control Lab. Left: A subject performing reaching tasks. Right: Trajectories of the endpoint of the arm during reaching to 12 targets in the KINARM™ (Note: This 12-target reach was a separate task performed in a practice session unrelated to this investigation).

3.2.2. BCI System Overview

This investigation employed *BCI2000* to implement the BCI interface. *BCI2000* is a public-domain BCI software environment developed by the Wadsworth Center at the State University of New York; *BCI2000* has been incorporated into several studies implemented by the BrainLab. *BCI2000* is divided into four modules: an operator program with three other independent processes, which communicate through transmission control protocol (TCP/IP). Those independent processes are the data acquisition, signal processing and application programs (Figure 3.2-2). *BCI2000* provides several signal processing methods with multiple approaches to spatial and temporal filtering of signals. BCI applications provided by *BCI2000* range from those that use evoked signals, such as P300, to make discreet selections to those that use SMR to move a cursor continuously on a screen.

The SMR signal processing component in *BCI2000* is called ARSignalProcessing; it is typically interfaced with Cursor Task, an application that uses SMR to implement a one-dimensional version of the cursor control detailed in **BCI Computational Methods** in **Chapter 2**. The control signal produced in ARSignalProcessing increments the position of the cursor displayed to the user on a computer monitor; then Cursor Task, the real-time application, updates the *BCI2000* system on its activity by means of a vector of state variables detailed in Table 3.2-1. This state vector can be passed to outside programs for device control or execution of external applications as was performed in this project.

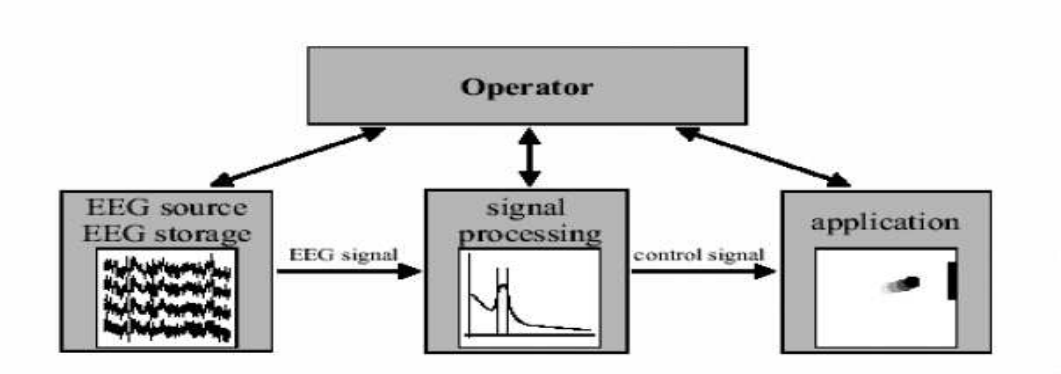

Figure 3.2-2. High level overiew of modules in BCI2000 (BCI2000 Manual, 2007).

3.2.3. System Integration

In this project, the cursor movement in the Cursor Task application was interfaced with the KINARM so that subjects were able to control the movement of the KINARM using SMR. The KINARM's movement was adjusted based on the continuous update of its two-dimensional feedback position; therefore, *BCI2000* transferred the position state variables of the cursor in Cursor Task to the KINARM for interpretation of where to relocate the arm. The state variables 'x_pos' and 'y_pos' corresponded to the position of the cursor on a 512x512 pixel screen in Cursor Task. In this project's BCI-Robot implementation, x_pos and y_pos were routed by user datagram protocol (UDP) to the robot control system implemented in *MATLAB*® xPC Target™ and Simulink®. The cursor position was converted from the 512x512 pixel to a 50x55cm space for use by the robot's proportional integrative differential (PID) controller. *BCI2000* also received feedback from the robot control system on the status of the variables 'CurrentTarget', 'CurrentRunning' and 'CurrentRest' to update the status of each trial and to keep the two systems operating synchronously.

Offline Analysis

Incorporating one-dimensional cursor movement methods similar to those outlined in *BCI Computational Methods*, EEG SMR features rendered forward and backward KINARM movement from a starting point placed 25 centimeters in front of the user. The transformation function used in ARSignalProcessing produced a linear mapping of spectral amplitudes to positive and negative arm movement based on spectral parameters obtained during offline analysis of screening data (described in detail in section 3.3).

The spectral parameters were entered in terms of numbered bins that were three Hertz wide. The numbering started at 0Hz and continued up to 35Hz; this resulted in a total of 12 frequency bins. The *BCI2000* interface (Figure 3.2-3) took bin numbers and channel numbers as inputs to the transformation algorithm. For instance, if offline analysis showed that a subject consistently demonstrated having greatest r^2 correlations in the third and fourth frequency bins (6-8Hz and 9-11Hz) in C3 (reference Figure 2.3-2), the parameter input into *BCI2000* would have been as illustrated in the center square window in Figure 3.2-3; this was the classifier parameter matrix. The linear transformation for the implementation illustrated in Figure 3.2-3 would have been:

$$c_\tau = (a_1 z_{3,3,\tau} + a_2 z_{3,4,\tau}) \qquad (3),$$

where $z_{3,j,t}$ were the amplitudes of the spectral bins in channel C3 (channel 3 on the 16-channel EEG montage) during the specific time block, τ and a_i were the weights determined by the during the first day of training (discussed in section 3.3). x_τ was determined using Equation (1). x_τ determined vertical cursor or robot arm movement using the equation

$$\Delta V = b_v x_\tau \quad (4).$$

ΔV was the arm/cursor movement, and b_v was a scaling factor. Note that 'τ' represented a time block or 0.1 seconds and not a time sample; the real-time systems implemented in *BCI2000* computed Equations (3) and (4) every 100ms using 200ms overlapping windows.

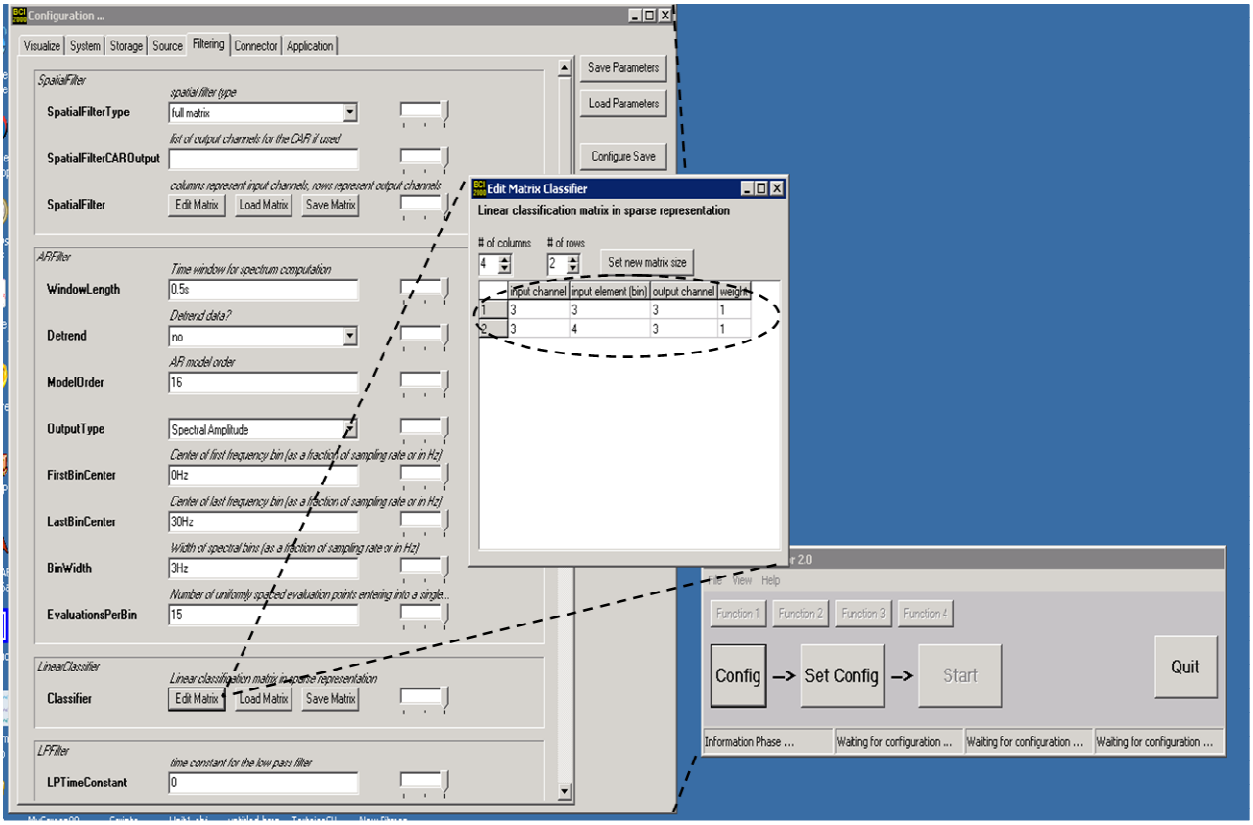

Figure 3.2-3. *BCI2000* user interface. The small window on the lower right section of the image is the operator interface; the config button intatiates the large parameter interface window on the left. Parameters for the classifier were specified using a classifier matrix illustrated by the square box in the middle.

Real-time and Offline Adaptation

Because EEG signals were known to be non-stationary and plastic changes of the brain were anticipated, the classifier adapted to spatial and temporal changes in EEG representation of arm movement [25]. In addition to performing the normalization step in Equation (1) that adjusted for

non-stationarity during real-time operation, the parameter estimation methods outlined in the screening process (discussed in Section 3.3 below) were performed daily to detect plasticity-induced parameter changes over time. Any changes to offline parameter estimates were incorporated into the BCI system at the beginning of each day of training.

Table 3.2-1. List of BCI2000 state variables.

State	Description
CurrentStimulusTime	Current time of feedback display (i.e. cursor) in ms relative to the start of each trial.
CurrentTarget	Code for target being displayed '1-4' for target, '0' for blank screen.
FeedbackTime	The maximum time for display of cursor.
CurrentFeedback	'1' if cursor is on the screen, '0' otherwise.
CurrentIti	'1' if in the inter-trial interval, '0' otherwise.
CurrentRunning	'1' once cursor task is started, '0' when program is between tasks
CurrentRest	'0' when cursor task is started, '1' when task is not running.
x_pos	X position of the cursor (0 if no cursor displayed)
y_pos	Y position of the cursor (0 if no cursor displayed)
CurrentXadapt	The X adaptation coordinate of the target (offset from center).
CurrentYadapt	The Y adaptation coordinate of the target (offset from center).
CurrentAdaptCode	Adaptation code of target displayed ('0' if no target displayed.

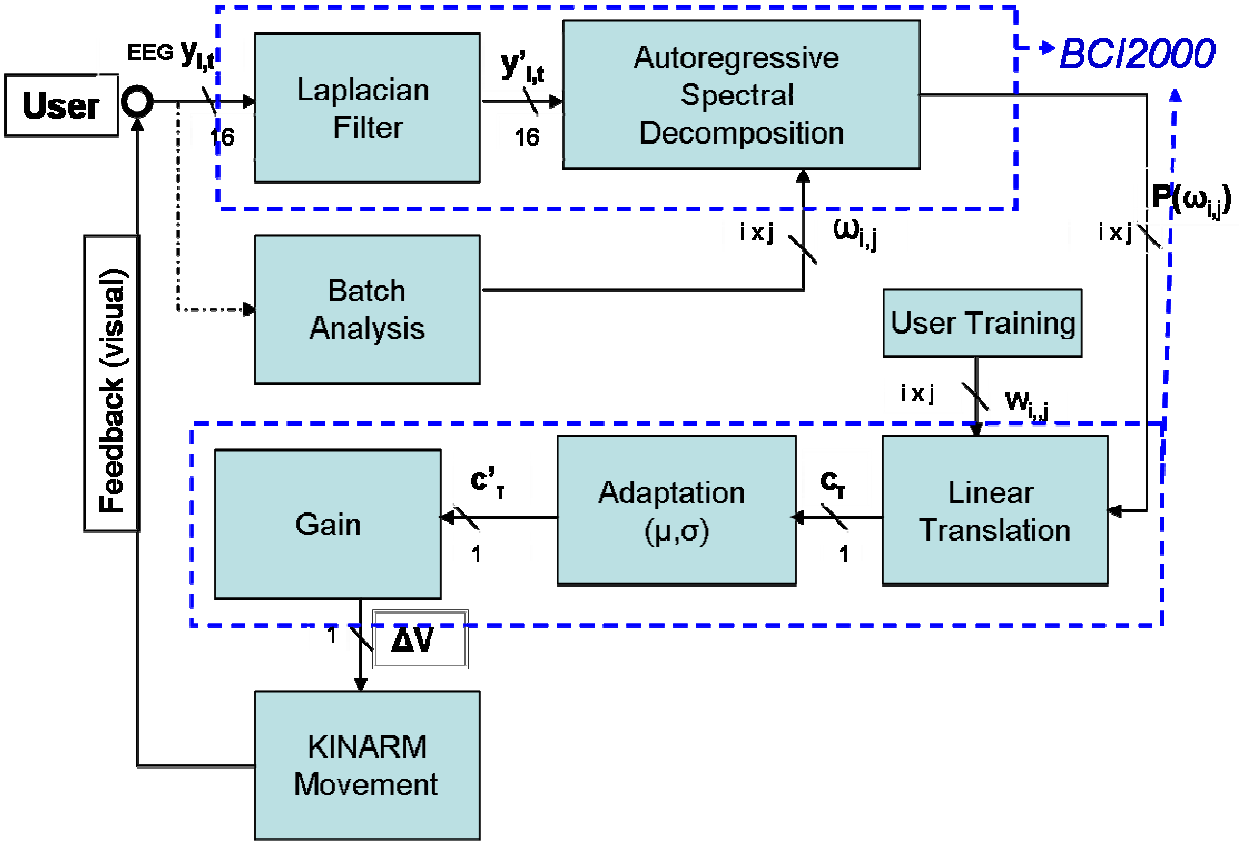

Figure 3.2-4. Diagram of the online operation process for the BCI-robot system mplemented in this investigation.

3.3. Data Acquisition

The data acquisition portion of this study took place in three major stages for each subject: Screening, Training and Follow-up. During all stages, each subject performed real or imagined reaching in the KINARM while wearing a 20-channel, double-banana montage EEG cap; this channel arrangement was used to increase the spatial resolution of the channels located above the sensory and (pre)motor cortices. It should be noted, that some Non-BCI subjects performed the Screening segment of the study (described below) using a similar, yet slightly different EEG montage because the new cap was not available when the study began. Both EEG caps were interfaced with a 16-channel Guger Technologies g.USBamp biosignal amplifier that had a 0.1Hz high-pass filter and a 58Hz-62Hz notch filter and was sampled at 256Hz. Figure 3.3-1

illustrates the locations of the 16 transmitted channels on the two different caps; the small-Laplacian spatial filter implemented during the data analysis allowed for co-registration of the channels of the older montage with that of the double-banana montage (discussed in section 3.4.1).

The discussion below explains the relevance of each stage of the study, the EEG and motor data acquisition protocols and the data analyses performed after each stage. Some subjects were excluded from the EEG analysis because of excess noise or loss of data.

This study enrolled twenty-four right-handed able-bodied volunteers. Each volunteer provided informed consent under the approval of the Georgia Institute of Technology Internal Review Board. The volunteers were randomly divided into two study groups, a test (BCI) group and a control (Non-BCI) group. All EEG and motor adaptability data were de-identified prior to analyses. Subject information, including the group associations, EEG analysis exclusion and whether they performed the Screenings tasks with the older EEG montage, is outlined in Table 3.3-1.

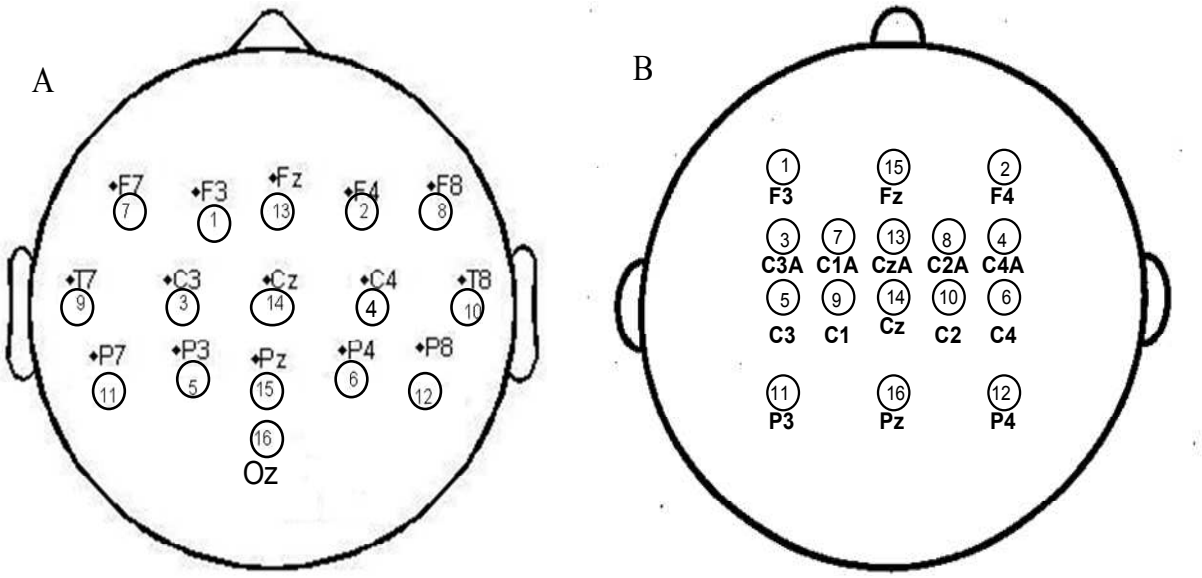

Figure 3.3-1. 16-channel EEG channel montages. A. Old montage used during the Screening stage for a subset of the Non-BCI group. B. Updated 16-channel EEG double-banana channel montage. Spatially similar channels were validly co-registered after using a small-Laplacian filter. Both EEG caps had 20 channels; however, the channels labeled above were the only channels that were transmitted for operation and analysis.

Table 3.3-1. Study participant identifiers.

BCI Subjects			Non-BCI Subjects		
Number (Random)	**Subject Code (Random)**	**EEG Analysis**	**Subject Code (Random)**	**EEG Analysis**	**Older EEG Montage Used**
1	10041210	Yes	09110609	Yes	Yes
2	11061010	Yes	10033010	Yes	No
3	12021910	Yes	10111209	Yes	Yes
4	12041210	Yes	10111309	Yes	Yes
5	01033110	Yes	12033010	Yes	No
6	03071610	Yes	12111009	Yes	Yes
7	04060610	Yes	02022410	Yes	No
8	04092010	Yes	04111809	Yes	Yes
9	05021010	Yes	06111109	Yes	Yes
10	05091510	Yes	02111909	Yes	Yes
11	09021110	Yes	08111109	Removed	Yes
12	02110609	Removed	08110609	Removed	Yes

3.3.1. Screening

During the first stage of data acquisition, all subjects performed a series of reaching tasks in the robot while wearing the EEG cap. Each reaching task was aimed at giving subjects comprehensive training in operating the KINARM and associating KINARM movement with real arm movement. The EEG data collected in this stage was used to determine individual subject parameters for the operation of *BCI2000* and to represent pre-training brain activity during the post-training analyses.

Table 3.3.1 outlines the different real and imagined reaching tasks performed and the amount of trials completed during the screening protocol. The term 'Real' refers to a reaching task during which the subjects were instructed to physically move the KINARM robot to a randomly displayed front or back target. 'Img' refers to the guided-imagery task during which subjects kept their hands in their laps as they observed the movement of the robot and imagined that their arm was in the KINARM. 'ImgNew' refers to a task during which subjects had their arms in the KINARM and were told to reach for a centering target, then to imagine reaching towards a second randomly presented target without actually reaching. Figure 3.3-2 illustrates the three different types to screening tasks.

Table 3.3-2. Screening Task Nomenclature and Descriptions.

Task	Description	Trials/Subject
Real	Single reach where subjects are physically moving the KINARM, first to a centering target, then towards a randomly chosen front or back target.	**10**
Img	Single reach where subjects are watching the KINARM reach for random targets while their hands are in their laps. Subjects are instructed to imagine they are performing the actions the KINARM is performing	**10**
ImgNew	Single Reach where subjects have their arms in the KINARM and are instructed to reach for an initial centering target, then imagine reaching for a second target without actually performing the movement.	**10**
RealSeries	Real reaches performed in the KINARM for a series of random targets rather than a single target.	**20**
ImgSeries	Img reaches performed for a series of random targets rather than a single target.	**20**
ImgNewSeries	ImgNew reaches performed for a series of random targets rather than a single target.	**20**

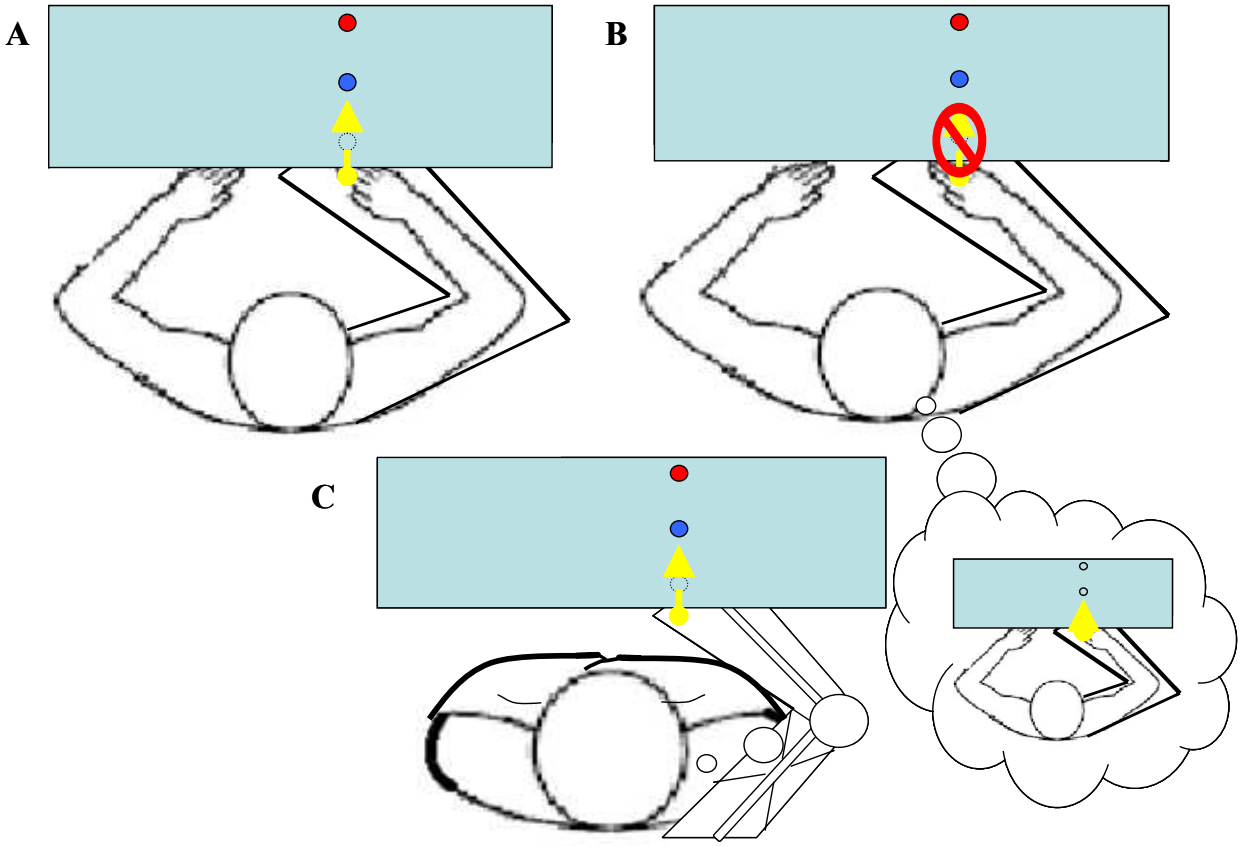

Figure 3.3-2. Screening tasks. A.'Real' reaching task; subjects reach for randomly displayed targets. B. 'ImgNew' imagery task; subjects keep arm in KINARM and imagine reaching for targets without moving. C. 'Img' imagery task; subjects keep arms in lap and observe the KINARM moving while imagining performing the task (guided imagery).

Data acquisition approach

To acquire EEG reaching data, subjects were outfitted with a 20-channel EEG cap and calibrated with the robot. Once calibrated, the KINARM projected a light blue dot over the subject's right index finger for visual feedback (Figure 3.3-3). In each task, the finger-feedback dot started at centered starting position (displayed as a blue or red circle 2 cm in diameter in front of the body). Then one of two targets (red circles each 2 cm in diameter) was projected either in front of or behind the starting position (Figure 3.3-3) on the KINARM heads-up display; the targets were

displayed randomly. Subjects, or the automated KINARM, completed a reach by aligning the finger-feedback dot with the target; the subject or the KINARM then returned to the starting circle and kept the finger-feedback dot at rest for 1.5 seconds in the starting circle before a new target was displayed. To keep the subject motivated during 'Real' reaches, the target color changed from red to green if they reached the target within one second. Each reach for a random target was considered a trial. Each subject performed 10 trials of 'Real', 'Img' and 'ImgNew' reaches, resting for 2 minutes between blocks of five reaches; this produced a total of 30 single reach trials. The subjects then performed three sets of series reaching tasks where the targets were continuously displayed for a set of 20 trials in each task. This resulted in a total of 60 series trials in addition to the single trials. All EEG and robot data were compiled and time-stamped for processing.

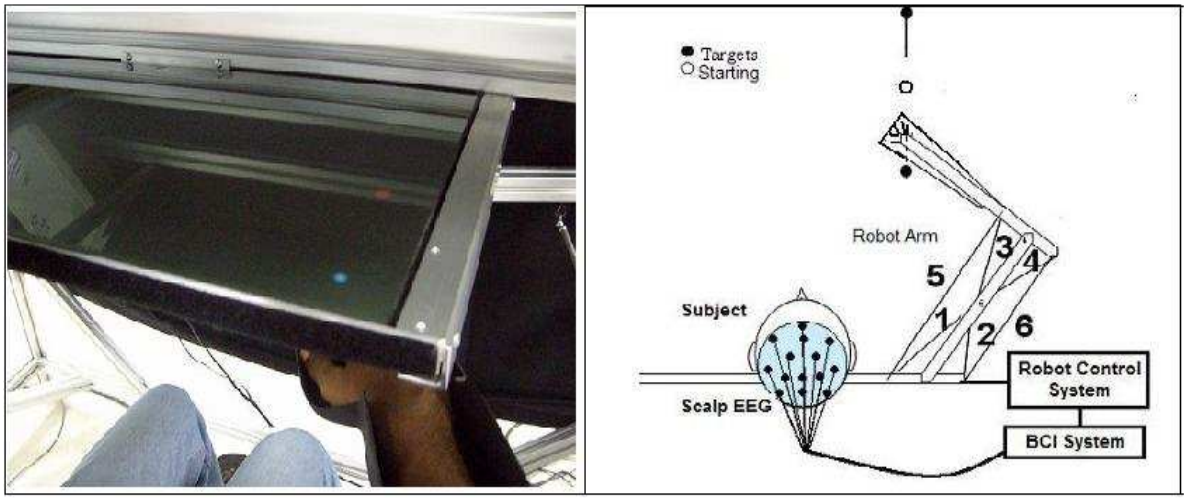

Figure 3.3-3. KINARM Heads up display and BCI operation. **Left:** Subject viewing KINARM heads up display with target (red) and index finger projection (blue). **Right:** BCI-KINARM reaching task diagram.

Offline Analysis

This offline analysis was adapted for this study to measure features pertaining to arm reaching rather than the standard hand movement task required for *BCI2000* screening; the methods outlined below were implemented in *MATLAB*®. The EEG data acquired during the screening process was used to develop the *initial* parameters needed for the for *BCI2000* ARSignalProcessing classifier. As was mentioned in section 3.2, the classifier required frequency bins of specific channels that had higher r^2 correlations relative to arm reaching. To determine these parameters, the data acquired during screening was processed using *MATLAB*® code that calculated the r^2 correlations for each individual frequency from 5- 35Hz in each channel.

The r^2 estimation started with extracting the raw 16-channel data, $y_{i,t}$ ($i \in [1,..,16]$ and t = 1/256s). The signals were spatially filtered using a common average reference (CAR) filter, which does well in accounting for spatial increases in brain activation and has proven to be a highly effective method of increasing signal-to-noise ratios in EEG based BCIs [108]. The CAR filter produced a signal represented by the following equation:

$$y'_{i,t} = y_{i,t} - 1/n \sum_{j=1}^{n} y_{j,t} \qquad (5)$$

where $y_{j,t}$ is the filtered 16-channel EEG data, which is the voltage at each electrode with respect to an ear reference and n was 16. The data were converted to an adaptive autoregressive (AR) equation using the Burg algorithm [109-111]. The autoregressive model represented the data according to the following equation:

$$y''_{i,t} = a_{i,1,t}\, y'_{i,t-1} + a_{i,2,t}\, y'_{i,t-2} + \ldots + a_{i,p,t}\, y'_{i,t-p} + E_{i,t} \qquad (6)$$

Where $a_{i,1,t} - a_{i,p,t}$ are the AR coefficients, and $E_{i,t}$ is the error, which assumed to be white noise. The order, p, was determined to produce an optimal output at 20.

The power spectrum, P(ωi,j), of the signal was derived directly from the AR model using a 256-length FFT. The individual frequencies from 5-35Hz were chosen as features and input into the *MATLAB*® principle components analysis algorithm, princomp; one of the outputs of princomp was the Hotelling t^2 statistic. R^2 was derived from the Hotelling t^2 statistic using the formula

$$r^2 = \frac{t^2}{t^2 + df} \tag{7}$$

where *df* refers to the degrees of freedom of the features space (N-1); since the EEG features space included 16 channels of 31 frequencies, *df* was estimated to be 495 (i.e. 16*31 – 1) [112, 113]. This r^2 amplitude derivation gave a basic assessment of which frequencies contributed the greatest amount of variance to the overall signal during real or imagined reaching. The individual frequencies that contained the highest r^2 values (>0.2, p ≈ .000) with respect to the overall mean were chosen as parameters for the initial subject training session. To reduce the complexity of making adjustments during the initial training session, this process chose the five maximally contributing frequency bins. The investigator recalculated r^2 values daily to determine if any adjustments needed to be made to the parameters.

3.3.2. Training

During this stage of data acquisition, the two study groups (BCI and non-BCI) performed separate training protocols (Figure 3.3-4). All subjects performed either BCI or motor imagery training in addition to daily MLAs (MLAs). For each subject, the training stage lasted five

consecutive days. This training time allowed for the integration of the motor learning protocol with a sufficient BCI/mental imagery training protocol. Past mental imagery studies have had training periods ranging from 5-12 hours over two weeks; this study incorporated a similar training time, while slightly augmenting a motor catch trial protocol [16, 32, 33, 114, 115]. Table 3.3-3 outlines the training protocols for the two groups.

Day One

On the first day of training, all subjects in both groups performed a long set of four motor tasks. Subjects started the session by placing their hands in the KINARM with the feedback dot placed approximately 20 centimeters away from their shoulders. Subjects then performed three sets of non-weighted reaches towards eight randomly placed radial targets for a total of 400 trials; these three tasks were designed to get subjects acclimated to using the KINARM. Then, in the final task, subjects performed a motor learning assessment (MLA) that consisted of 240 loaded reaches with catch-trials. The first 176 reaches had an added perturbation that was a right-directed perpendicular force applied at the endpoint of each reach; the final 64 reaches contained three sets of eight catch-trials, which were unperturbed. After the 176th trial, the task alternated between loaded and unloaded cycles of eight reaches. This final task was designed to assess motor adaptation. *The MLA protocol was designed by Dr. Linda Harley in the Georgia Institute of Technology School of Applied Physiology.* It should be noted that the subjects performed a two-dimensional reaching task towards eight radial targets as opposed to just reaching forward and backward; subjects only performed this two-dimensional task during the daily MLAs.

Figure 3.3-5 illustrates the reaching trajectories corresponding to different stages the subjects experienced during the first day. The trajectories in Figure 3.3-5.B correspond to the

first 400 reaches, were there was no perpendicular force applied to the KINARM; therefore, the subjects' reaches remained relatively straight. Figure 3.3.2-2.C illustrates the beginning of the final set, the loaded reaches with catch-trials, where the subjects were newly introduced to the perpendicular force. Figure 3.3.2-2.D demonstrates how the reaching trajectories typically changed after several trials; the subjects had adapted to the perturbation. Figure 3.3.2-2.E illustrates reaching trajectories performed during catch-trials where the perpendicular perturbation was removed; here subjects typically had adapted to the perturbed task so significantly that when the perturbation was removed they reached overwhelmingly in the opposite direction of the perturbation. The catch-trials are designed to measure the degree to which subjects had learned the task.

The first day of training was the only day where subjects performed the unloaded reaches. Loaded reaches with catch-trials (MLAs) were performed on the first, third, fourth and fifth days of training (Table 3.3-3). The second day of training, as is mentioned below, was dedicated to accommodating subjects to the motor imagery task (BCI or Non-BCI); therefore, there were no MLAs performed on the second day.

Day Two

BCI and mental imagery training started on the second day of the five-day training stage. Day two was the point where the protocols started to differ between the two groups. Figure 3.3.2-1 gives a general illustration of this part of the training stage.

All subjects were fitted with the 20-channel EEG cap and calibrated with the KINARM. Subjects in the non-BCI group sat in the KINARM with their arms in their laps. The KINARM was programmed to perform 10 sets of 60 reaches where random front and back targets were

displayed and the finger feedback reached for the targets (Figure 3.3-4); this was identical to the 'Img' task from screening. The non-BCI subjects were then instructed to observe the KINARM finger feedback and imagine that they were moving the KINARM themselves. Non-BCI subjects were not told that the KINARM was automated; however, most non-BCI subjects mentioned (after being questioned after training) that they had determined at some point during training that they were not controlling the KINARM. The 10 sets of reaches typically took about 1.5 hours to complete and this was the only task that non-BCI subjects performed on the second day of training.

The second day of training for BCI subjects was slightly more involved. All BCI subjects were fitted with the 20-channel EEG cap and calibrated with the KINARM. Once in the robot, BCI subjects placed their arms in their laps, just as the non-BCI subjects had done. At this point, the parameters collected during the Screening stage were entered into *BCI2000* and given initial weights of -1 each. Then the *BCI2000* Cursor Task application was launched to control the movement of the KINARM with the subject's SMR. The SMR-controlled Cursor Task allowed for real-time operation of the KINARM by refreshing its position every 1/10 of a second.

BCI subjects were told imagine reaching forward, reaching backward or resting to influence the KINARM finger feedback so that it moved in the direction of a randomly-placed front or back target; subjects had 25 seconds to reach the target. After the first four or five trials, if the subject noticed that he/she had more influence moving in one direction over the other, the investigator toggle the weights from -1 to 1 before the next trial. During the first set, the subjects were also encouraged to narrow their control down to two types of motor imagery: either forward reaching vs. backward reaching or reaching vs. resting.

During the second set of trials the subjects were instructed to perform the more narrowed imagery task (reaching forward vs. reaching backward or reaching vs. resting) (two tasks) while continuing to adjust motor imagery to influence the arm toward the target in real-time. If the subject's influence over the direction of the arm is still greater in one direction over the other, the weights of the parameters were manually toggled back to -1 one parameter at a time until there was no noticeable difference between the subject's influence over the direction of the movement of the arm. Final weights were typically fixed by the end of the second set. The subject then completed three to four more sets. Each set consisted of twenty reaches, but the first two sets were paused to adjust the weights. BCI training lasted approximately 1.5 hours on the second day of the training stage.

Day Three and Day Four

On the third day of training subjects in both groups performed slightly shortened sets of the mental imagery or BCI training. The Non-BCI subjects performed seven sets of 60 reaches, which lasted approximately one hour to one hour and 15 minutes. The BCI subjects performed one hour and 15 minutes of training also, which approximated to four to five sets of training. Once each subject completed his/her one hour of training, he/she then removed the EEG cap and performed MLA. This process was repeated on the fourth day of training.

Day Five

On the fifth and final day of training was very similar to the third and fourth days. All subjects completed one hour of either mental imagery training or BCI training; however, prior to

removing the EEG cap and performing the motor catch-trials, the subjects performed five sets of 20 'Real' reaches for post-training analyses.

During the training stage all subjects underwent approximately five hours of BCI or mental imagery training and four MLA sessions. Five hours of BCI training was a minimally sufficient time for BCI subjects to obtain a relatively high level of KINARM (cursor) control accuracy (>80%), but the goals of this investigation did not require subjects to demonstrate a high level of accuracy [42, 43, 105].

3.3.3. Follow-up

Subjects returned after approximately 30 days for a follow-up visit. This stage was added to determine whether there were notable persistent effects of training on brain plasticity and motor learning.

All subjects, regardless of study group, performed the same protocol during this stage. They were fitted with the EEG cap and calibrated with the KINARM. Subjects then performed eight sets of 20 'Real' reaches and five sets of 59 'Img' reaches. The EEG cap was then removed and all subjects performed one final MLA. All data were declassified prior to analysis.

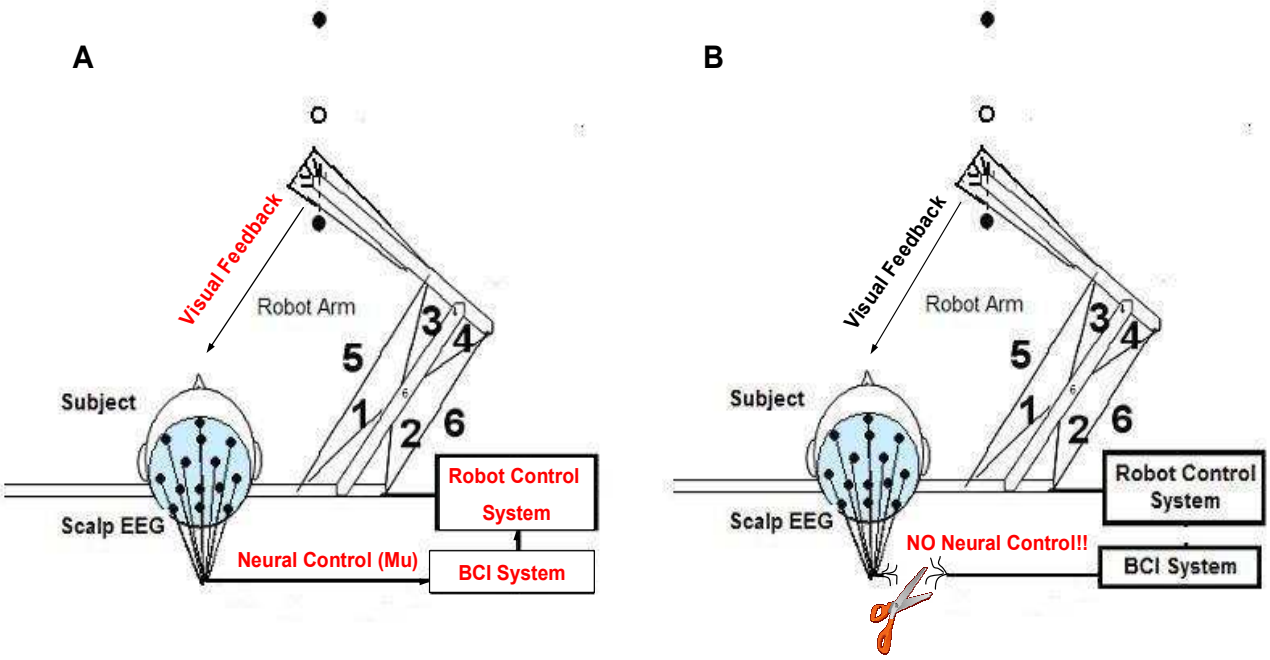

Figure 3.3-4. Project diagram for the training stage. A. Closed loop system used by BCI group subjects. Subjects were trained to control their mu signals and thus control the movement of the robot arm. B. Open loop system used by Non-BCI group subjects. Subjects observed the movement of the robot arm while unknowingly not having control over the arm.

Table 3.3-3. Screening, Training and Follow-up Protocols for BCI and Non-BCI Subjects.

	BCI Group	Non-BCI Group
Screening	See Table 3.3-2	See Table 3.3-2
Day 1	**Motor Tasks:** 400 unloaded reaches + 240 loaded reaches with catch-trials	**Motor Tasks:** 400 unloaded reaches + 240 loaded reaches with catch-trials
Day 2	**Imagery Training (BCI):** 1.5 hours (~six sets of 20 reaches)	**Imagery Training (Non-BCI):** Ten sets of 60 reaches (~1.5 hours)
Day 3	**Imagery Training (BCI):** 1.25 hours (~five sets of 20 reaches)	**Imagery Training (Non-BCI):** Seven sets of 60 reaches (~1.25 hours)
	Motor Tasks: 240 loaded reaches with catch-trials	**Motor Tasks:** 240 loaded reaches with catch-trials
Day 4	**Imagery Training (BCI):** 1.25 hours (~five sets of 20 reaches)	**Imagery Training (Non-BCI):** Seven sets of 60 reaches (~1.25 hours)
	Motor Tasks: 240 loaded reaches with catch-trials	**Motor Tasks:** 240 loaded reaches with catch-trials
Day 5	**Imagery Training (BCI):** 1.25 hours (~five sets of 20 reaches)	**Imagery Training (Non-BCI): S**even sets of 60 reaches (~1.25 hours)
	Reach Screening: 100 'Real' reaches	**Reach Screening**: 100 'Real' reaches
	Motor Tasks: 240 loaded reaches with catch-trials	**Motor Tasks:** 240 loaded reaches with catch-trials
Follow-up	**Reach Screening:** 160 'Real' reaches + 300 'Img' reaches	**Reach Screening:** 160 'Real' reaches + 300 'Img' reaches
	Motor Tasks: 240 loaded reaches with catch-trials	**Motor Tasks:** 240 loaded reaches with catch-trials

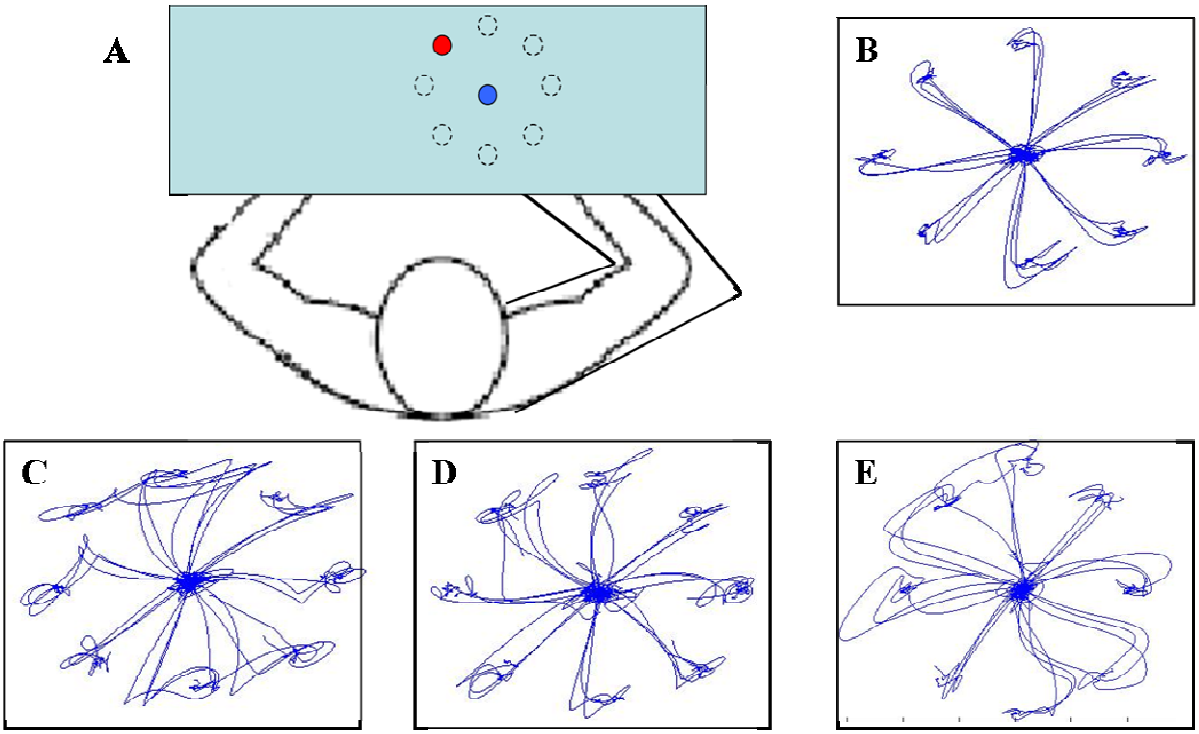

Figure 3.3-5. MLA in the KINARM. A: The subject was instructed to reach as quickly and accurately as possible from a starting position (center blue dot) to one of 8 targets, which appeared randomly on KINARM heads-up display (red dot). When the target was reached it changed color based on speed; the subject then waited for the starting target (center blue dot) to reappear before moving the arm back. B: When the subject performed reaches in a null-force field, the reaching trajectories remained close to a straight line from starting target to endpoint. C: When the subject started the MLA, he/she was performing reaches in a perturbed field and, therefore deviated significantly from a straight path from starting target to endpoint (note the curved trajectories of the finger tip). The force field was imposed on the arm through the KINARM external torques applied at the shoulder and elbow joints. D: After several trials with the perturbed field, the subject began to adapt (note that finger tip trajectories became straighter than in C). E: After the subject had adapted to the task, 3 null-force field trials (catch trials) were offered to measure degree of adaptation (note the opposite deviation of the finger tip trajectories compared C) [116].

3.4. Data Analysis

This section discusses the data analysis in terms of the three specific aims.

3.4.1. Aim I: Analysis of BCI-Robot Training Effects on Brain Plasticity

To link motor learning improvements with brain activity, this investigation searched for statistically significant evidence of BCI-influenced brain plasticity. To measure changes in brain activity, spectral and spatial patterns in EEG data were extracted and statistically analyzed. All analyses contrasted the 'before and after' effects of training on each individual subject. Some aggregate (inter-subject/inter-group) comparisons helped to add post-hoc inferences; however, because of the variability between subject data, such comparisons were not the focus of this investigation.

The guided-imagery EEG data collected during Screening ('Img', 'ImgNew', 'ImgSeries' and 'ImgNewSeries') were statistically analyzed by performing several comparisons with the guided-imagery data extracted during the 30-day Follow-up ('Img'). Statistical tests were performed between the first and last days of training for each subject. The results of each individual's statistical assessment were analyzed to determine whether the distribution of subjects who underwent BCI training produced more significant spatial and spectral changes in comparison to those who completed Non-BCI training.

The EEG data were extracted as mentioned in Section 3.3.3. To precondition the EEG data for analysis, all EEG channels were spatially filtered using a small Laplacian filter [108]. Spatially filtering the data using a small Laplacian formula helped to localize EEG activity by eliminating the average signal of the EEG channels surrounding each channel (Figure 3.4-1);

after each channel was filtered with the small Laplacian its representation was modeled by the equation

$$V_i^{Out} = V_i^{In} - \sum_{j \varepsilon Si} g_{ij} V_j^{In} \tag{8}$$

where V_i^{In} was the potential at the input channel, *Si* was the set of all channels surrounding the input channel, V_j^{In} was the potential at an individual channel in the set *Si* and V_i^{Out} was the output of the filter [108, 117]. The weight g_{ij} was calculated for each of the surrounding channels using the formula

$$g_{ij} = \frac{\frac{1}{d_{ij}}}{\sum_{j \varepsilon Si} \frac{1}{d_{ij}}} \tag{9}$$

where d_{ij} was the distance between V_i^{In} and V_j^{In}.

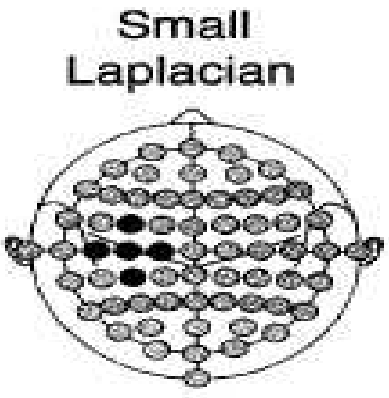

Figure 3.4-1. Example of small Laplacian spatial filter on a 64-channel EEG montage. Of the five bolded channels, the activity of the four outer channels were averaged and subtracted from the activity of the center channel. This calculation was performed on all interior channels [108].

Two seconds of data were processed for each reach, the one-second period before the target was displayed to the subject (rest) and the one second period after the target was displayed (reach). Each period was then divided into 200ms windows overlapped by 50%, so that a sample of data were taken every 10^{th} of a second. A 20-order AR model was used to estimate spectral power at each frequency from 5Hz to 35Hz within each of 16 EEG channels within each window; this gave a total of 11 samples of each frequency in each EEG channel within each one-second period to use for analysis.

To determine the amount of variance attributed to each frequency in each channel, the r^2 values were extracted using two different methods. The first method was the method outlined above in Section 3.3.3.; using the Hotelling t^2 metric (calculated using *MATLAB*® princomp function), r^2 was derived by applying Equation (7) to the post-target period distribution of frequency measures. This estimation of r^2 was called the 'intra-reach' correlation because it measured the degree to which all frequencies varied from the overall mean and was only calculated over the reach period [112, 118]. All intra-reach r^2 values that exceeded 0.2 were accepted as features.

The intra-reach calculation typically produced a fairly large feature space (~100); therefore, to reduce the feature space a second r^2 measure was calculated and cross-referenced with the intra-reach feature space. An 'inter-reach' r^2, was calculated using a method that relates the reach period frequencies to those which occurred during rest period in each trial [118, 119]. In this case, the rest period was used as a model of an average EEG signal for each subject. A basic equation that describes this r^2 calculation method is

$$r^2 = \frac{\sigma_{Pp}^2}{\sigma_P^2 \sigma_p^2} \tag{10}$$

which calculates the ratio of the covariance, σ^2_{Pp}, of the distribution of frequencies comprising a pre-target period, P, and during a post-target period, p, and the product of the individual variances of each period, $\sigma^2_P\sigma^2_p$ [112, 113]. To achieve the output of Equation (10), r^2 was determined for each period by calculating the correlation coefficient, r, of the frequency-channels of the pre-target period with the corresponding frequency-channels in the post-target period. The correlation coefficient, r, was estimated by the *MATLAB*® function corrcoef, which compared the 11 samples (windows) of each reach segment to determine the correlation coefficient of each of the 496 features (16 channels and 31 frequencies). The details of this calculation are described in Appendix A. *Corrcoef* output the r values and estimated probabilities of insignificance (i.e. p values) of each outcome. Squaring r produced the coefficient of determination, r^2. This method chose significant features by keeping channels and frequencies that had r^2 values greater than 0.2. To further reduce the feature space, of the selected features, only those that had p-values below 0.05 were kept as inter-reach r^2 features. The interception of the 'intra-reach' features and the 'inter-reach' features determined the feature set that would represent the significant spectral content of each reach.

Statistical Analyses

Each reach that each subject performed produced a finite set of the features extracted using the methods described above. Each subject's feature sets were compiled for each stage of the study: Screening, Training and Follow-up. To determine statistical significance, this investigation made several comparisons of the feature sets.

EEG signals are highly variable from subject to subject; therefore, the statistical analyses and conclusions were drawn from paired intra-subject tests. Post-hoc observations determined

whether common changes, whether spatial or spectral, occurred within a specific study group that would imply that BCI training had some effect on plasticity.

Paired tests of EEG content only involved contrasting EEG signals that were extracted while performing similar activities. Therefore, the motor imagery tasks performed during the screening session were statistically compared with those performed during the 30-day Follow-up session. To determine whether short-term statistical changes occurred while in training, EEG data extracted during Day One of training were compared to EEG data extracted during Day Four. The training protocols differed for each group; therefore, quantitative post-hoc tests could not contrast the BCI group and the Non-BCI group. Most analyses in Aim I of investigation drew statistical inferences of between-group differences from the intra-subject training data analysis.

This investigation took a two-fold approach to assessing plasticity. The first approach, the spectral analysis, looked at the average frequency distribution of the signals extracted while subjects performed motor imagery. The second approach, the spatial analysis, analyzed the distribution of significant features within channels that aligned with the motor cortex. These aspects of EEG data were chosen, because they are the major components of SMR-based BCI. Details of the statistical analyses are outlined in Table 3.4-1.

Spectral Analysis

The analysis of spectral content looked at the power (r^2/coefficient of determination), and proportion of the feature set frequencies that laid within the mu band (8-14Hz) and the beta band (18-26Hz). Wilcoxon signed rank tests performed comparisons as outlined in Table 3.4.1 between Screening and Follow-up and between Training Day One and Training Day Four [120,

121]. The statistical analysis tested for changes that occurred within the feature data extracted using the methods described above. Significant increases or decreases in the mean r^2 of the mu and/or beta frequencies, or the proportion of mu and/or beta features were considered in the final analysis of trends. Figure 3.4-2 illustrates one BCI subject's frequency proportion data for Screening and Follow-up. Figure 3.4-3 illustrates the same subject's frequency power (r^2) data. Both figures show that activity tends to accumulate close to the mu and beta bands. The distinction between mu and beta are less prominent in the frequency power comparison; this may result in more significant statistical changes between stages for the frequency power.

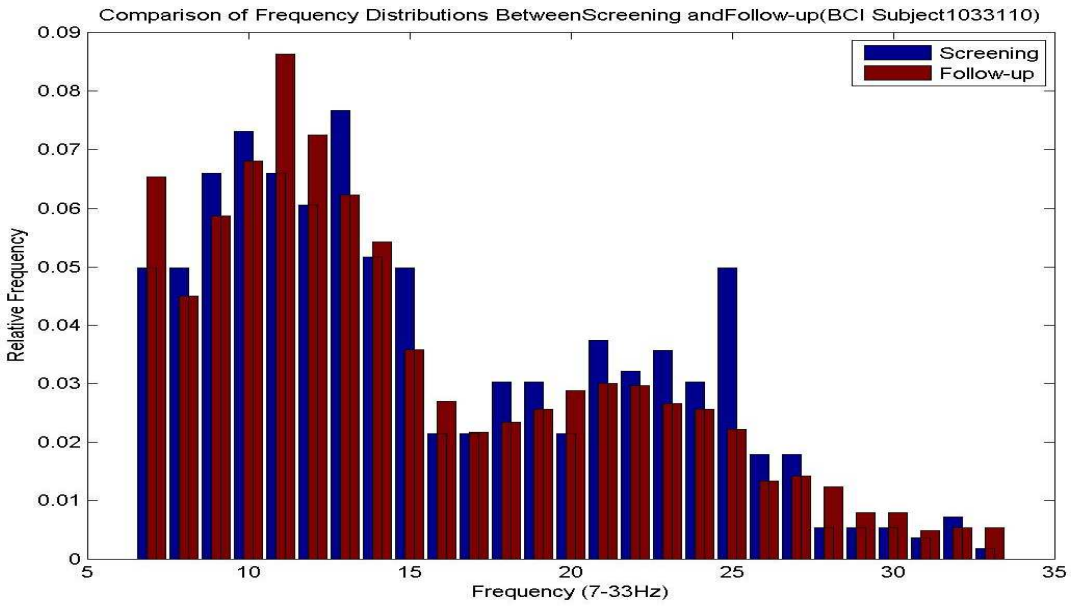

Figure 3.4-2. Single subject frequency proportion data for Screening vs. Follow-up.

Table 3.4-1. Brain Plasticity Statistical Analyses

Intra-subject Comparison	Data	Paired Intra-subject Tests	Paired Aggregate Tests (BCI vs. Non-BCI)
Screening vs. Follow-up	Spectral Proportion/Power (Mu/Beta)	Wilcoxon tests (Nonparametric t-tests)	Observation
	Spatial Mu Power/Proportion Distribution (*Left-brain*/*Motor strip*)	Wilcoxon tests (Nonparametric t-tests)	Observation
	Spatial Beta Power/Proportion Distribution (*Left-brain*/*Motor strip*)	Wilcoxon tests (Nonparametric t-tests)	Observation
Training Day One vs. Training Day Four	Spectral Proportion/ Power (Mu/Beta)	Wilcoxon tests (Nonparametric t-tests)	Observation
	Spatial Mu Power/Proportion Distribution (*Left-brain*/*Motor strip*)	Wilcoxon tests (Nonparametric t-tests)	Observation
	Spatial Beta Power/Proportion Distribution (*Left-brain*/*Motor strip*)	Wilcoxon tests (Nonparametric t-tests)	Observation

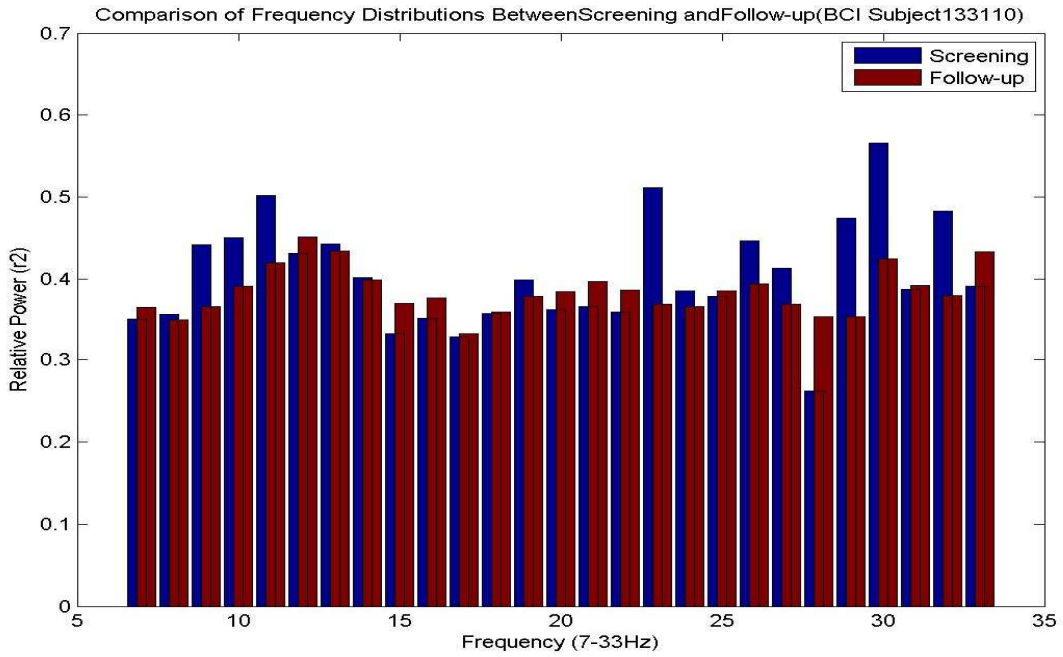

Figure 3.4-3. Single subject frequency power (r^2) data for Screening vs. Follow-up.

Spatial Analysis

Spatial changes were assessed by analyzing changes in the mu and beta content of the channels that laid in or near right-hand motor cortex. This particular analysis was important because eight of the Non-BCI subjects used the older EEG montage (Figure 3.3-1A) for Screening. Because not all channels on the older montage co-registered exactly with the double-banana montage, the investigation implemented two separate paired tests to characterize the statistical spatial changes, the *left-brain* test and the *motor strip* test. The *motor strip* comparison included the channels that were located on the left side of the brain next to and including Cz (i.e. C1 and C3 on the double-banana montage and C3 on the older montage, reference Figure 3.3-1); *left-brain* included *motor strip* and the channels CZA, C1A, C3A, FZ and F1 The older montage used CZ, C3, FZ and F3 for the *left-brain* analysis. Wilcoxon tests compared the mean proportions and mean powers of mu and beta features within the *left-brain* and motor channels.

Once again, the comparisons determined whether significant changes occurred between Screening and Follow-up and/or Training Day One and Day Four.

Figure 3.4-4 illustrates the scalp topographies for the mu proportion of Screening (Figure 3.4-4A) and Follow-up (Figure 3.4-4B) with an illustration of the difference between the two (Figure 3.4-4C). The color intensity in Figure 3.4-4C corresponds to the relative quantitative difference in mean proportion between the different stages of the study. The color scale range changes for each subject; however, deep blue colors typically indicate a negative difference between the two stages, and, thus, a decrease in the proportion (or power other cases). Deep red indicates an increase in the mean proportion from the first stage (in this case, Screening) to the second stage (in this case, Follow-up).

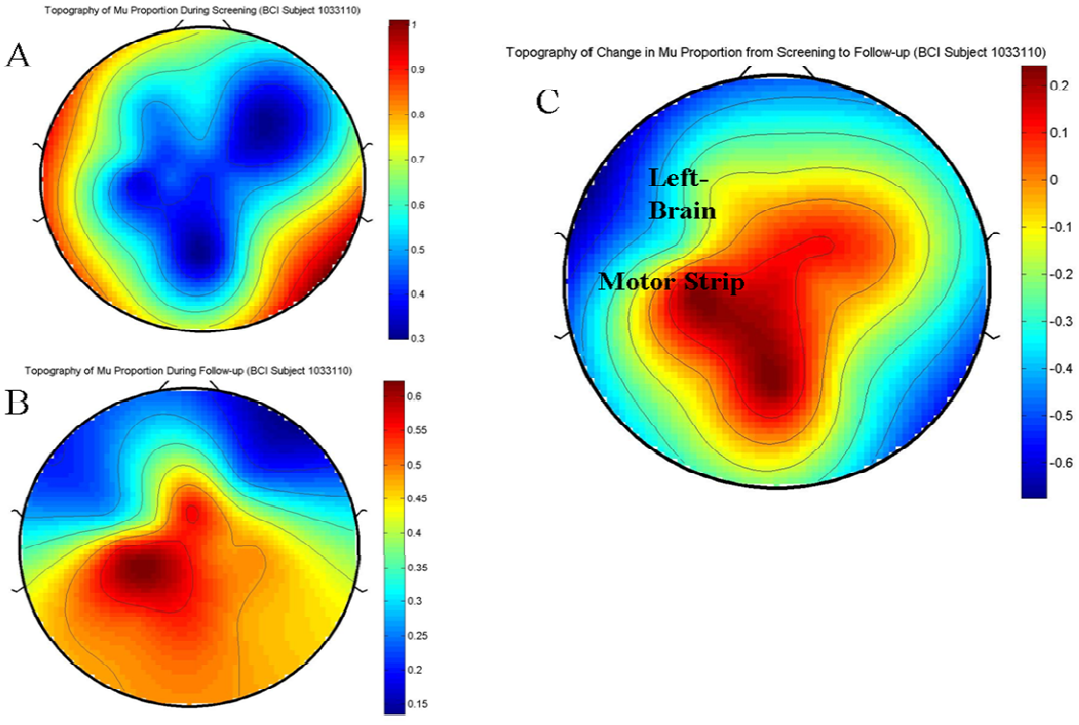

Figure 3.4-4. Single subject scalp topographies that show the relative mu proportion of each channel. A. Screening mu proportions. B. Follow-up mu proportion. C. Quantitative difference between Screening and Follow-up (i.e. Follow-up minus Screening).

3.4.2. Aim II: Determining the Effect of BCI Training on Motor Learning

This investigation employed several analyses to determine whether evidence of greater or more profound motor learning occurred in the BCI group. Those analyses included looking at the rate of adaptation, a measure that implied the speed at which subjects adapted to the KINARM task, and how that rate changed daily in each subject, looking at the change in total estimated error that each subject produced on each day of training and how that change was characterized during two stages of the task, and finally, looking at the degree to which subjects adapted to the task by measuring the amount of error during motor catch-trials.

Rate of Adaptation

Motor learning was assessed by analyzing several features of the loaded reaching and catch-trial data. The first feature involved measuring rate of error reduction (rate of adaptation) and analyzing how that rate changed with each day of training.

Motor adaptation was assessed by plotting the reaching error as a function of the trial number. Reaching error was quantified by taking the ratio of the minor axis and the major axis of each the subjects' reaching trajectory [114, 115]. The major axis was the straight line between the starting point and endpoint of the subject's finger tip location during a single reach; the minor axis was the distance of maximum deviation of the reaching trajectory from the major axis. Figure 3.4-5 uses parts C and D of Figure 3.3-5 to illustrate the how the ratio of the minor axis over the major axis should decrease over several trials, showing that the subject is learning the task.

When plotted over several trials, the reaching error had an approximate exponential decay that was modeled by the equation

$$y_t = ae^{-bt} \quad (11)$$

where *b* was the rate of adaptation and *a* was the estimated starting point [114]. To produce this output with the given data, each daily set of motor data were processed and ordered; the minor/major axes ratios were quantified and plotted. Only four of the eight targets presented during each trial were used for the full analysis; the upper right diagonal, the lower left diagonal and the horizontal targets were removed due to bias (Figure 3.4-6). The exclusion resulted in a total of 120 reaches used for analysis of each day of training. All reaching error data were normalized by dividing by the error of the first reach of the first day of training; this minimized the variance within subjects and scaled down the data so the maximum error was one.

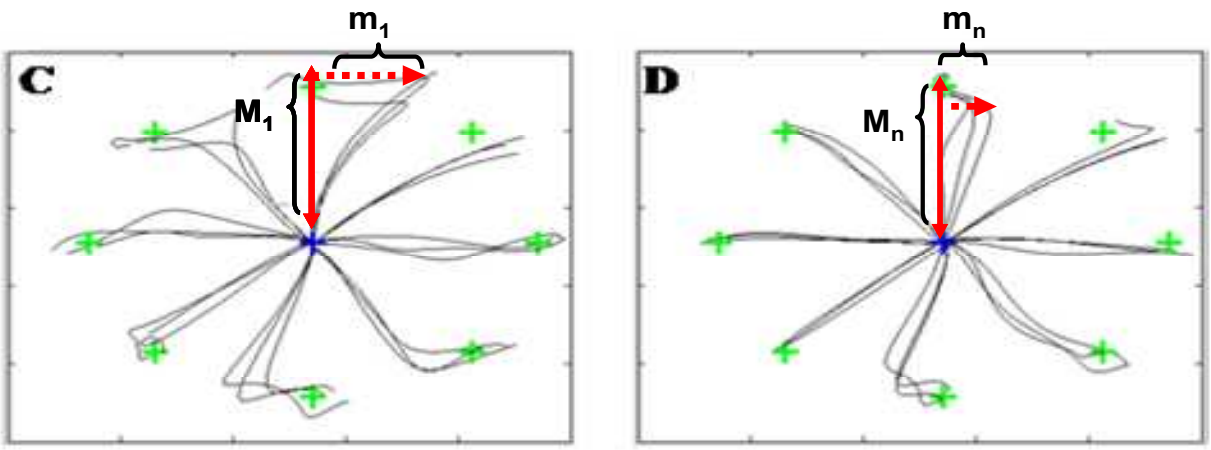

Figure 3.4-5. KINARM reaching trajectories at different times during one run. C. Reaching trajectories during the first three reaches of a MLA. M_1 refers to the major axis of the first reach; m_1 refers to the minor axis of the first reach. D. Reaching trajectories after several trials during the same run.

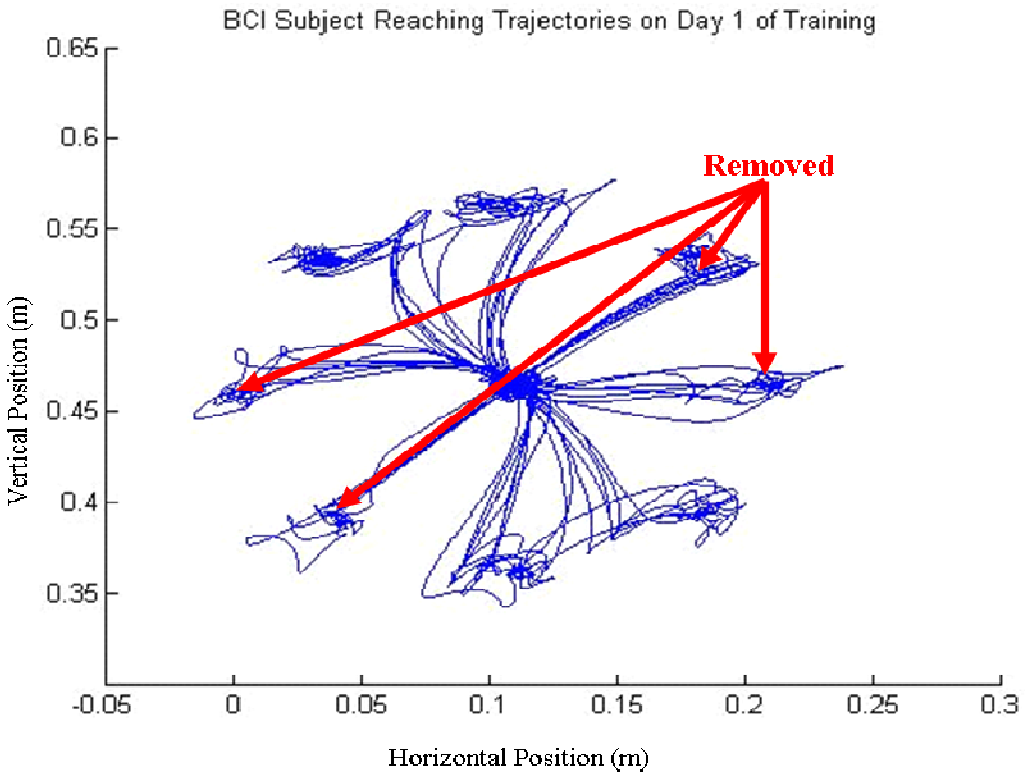

Figure 3.4-6. Sample reaching trajectories for BCI subject. Note that the data for the upper right diagonal, lower left diagonal and horizontal targets were removed before analysis due to bias.

Using non-linear regression, Equation (11) was fitted to each day of loaded reaching data; the rate of adaptation, b, was extracted for each subject on each individual day. Figure 3.4-7 shows the motor learning error data for a subset of the BCI group for all four days of training and the 4-week follow-up (Day 30). The solid colored lines correspond to the exponential fit, Equation (11).

Paired multiple-comparisons ANOVA with Bonferonni corrections determined the statistical significance of the within-group and between-group changes that occurred in the rate of adaptation after each day of training.

Estimated Total Error

To assess the subject's overall accuracy, a summed error was determined from the data using integration of the exponential fit. This calculation was analyzed for two phases of the loaded motor task. The first phase, the learning phase, produced the estimated *total learning error,* El_d, and occurred during the first 55 reaches of each day. The estimated location of the approximate half-life of the mean exponential decay of both the BCI group and the Non-BCI group error on the first day of training of all subjects was 55; therefore, the learning phase spanned the interval from one to 55 for all individual estimations of total learning error [115, 122]. The area under the exponential curve from the first reach to the 55^{th} reach estimated the total learning error for each day of training (Figure 3.4-8):

$$El_d = \int_1^{55} ae^{-bt}\,dt \qquad (12).$$

The calculation of the total learning error determined how quickly each subject predicted the task at the beginning of each day of loaded reaching by summing the estimated path deviations based on the exponential fit (Note that El_d and all other comparable measures were unit-less scalars because they estimated the summed total of *normalized* path deviations, i.e. meters/meters) [122]. To analyze the significance of total error, ANOVA multiple comparisons tests performed on the distribution of subjects within each group allowed for comparisons of the decrease in total learning error from Day 1 to Day 30.

The statistical analyses included paired tests to determine the significance of the daily change in learning error, El_d, $d \in [1,2,3,4,30]$, within each group (BCI and Non-BCI) and a between group test that determined the significance of the ratio of the difference between training Day One and all other days over training Day One:

$$D_{Eld} = \frac{El_1 - El_d}{El_1} \quad (13).$$

D_{Eld} gave an estimate of how the decrease in learning error related to where learning error started on Day One.

The second phase, the adapted phase, was calculated as the area under the estimated exponential fit from reaches 60 to 85:

$$Ea_d = \int_{60}^{85} ae^{-bt}\,dt \quad (14).$$

The *total adapted error,* Ea_d, measurement estimated the summed error after the subject had adapted to the task (exceeded the exponential decay half-life) on a particular day (Figure 3.4-9); the measurement gave an estimate of each subject's final (asymptotic) error on a given day [115]. ANOVA multiple comparisons performed between Day 1 and days two through 30 for each the within-group distribution determined whether there were significant reductions during each day of training. The between-group comparison of adapted learning used the same method described in Equation (13), to determine the ratio of adapted error reduction, D_{Ead}. Section 4.1 outlines the statistically significant changes that occurred within the BCI group.

Degree of Adaptation

The motor catch trial data can determine the degree to which a subject adapts to a task. As mentioned in Section 3.3.2, each MLA contained three sets of eight reaches during which the perpendicular force applied consistently from reaches one to reach 176 was removed. Once that force was removed all subjects produced reaches with offsets that overcompensated for the removed force (Figure 3.3-5E). Measuring the difference between the average value of the

adapted error and the average value of the catch trials determined the degree to which the subject learned the task. The measurement was taken as follows:

$$Ec_d = \frac{1}{4}\sum_{i=86}^{89} yn_i - \frac{1}{15} Ea_d \qquad (15)$$

where Ec_d was the degree of learning attained on a given day; this was measured as the difference between the *first* catch trial overshoot and the mean adapted error. *yn* represented the actual normalized path deviations of the first catch trial extracted from each subject's data. To reduce variability between subjects, Ec_d was normalized by the mean adapted error ($Ea_d/15$).

Multiple comparisons ANOVA tests assessed whether significant changes occurred during each day of training within each study group and between each study group.

Demographic Analyses

In addition to the four-target analysis, the measures described above were calculated for the front target and the back target separately. Because training only involved the front and back target, changes unique to these targets were given separate analyses with the techniques describes above.

The mean outcome of the statistical tests performed on the BCI group was compared to those in the in Non-BCI group. In addition, two age groups were selected and grouped as listed in Table 3.4-2.

Subjects' levels of physical activity varied less than age. Only two Non-BCI subjects and three BCI subjects reported that they engaged in hand-eye coordination activities for more than three hours per week. Individuals with three or more hours of hand-eye coordination activities (i.e. playing instruments or video games) were classified as "Gamers", and statistically analyzed for the measures described above. None of the subjects in this study were considered athletes or

participated in more than five hours of exercise per week; therefore, no separate consideration was made for athleticism.

Table 3.4-2. Groupings for Demographic Statistical Analysis

Group	BCI (#Subjects)	Non-BCI (#Subjects)
All	12	12
Ages 18-40	8	8
Ages 40+	4	4
"Gamers"	3	2
"Non-Gamers"	9	10

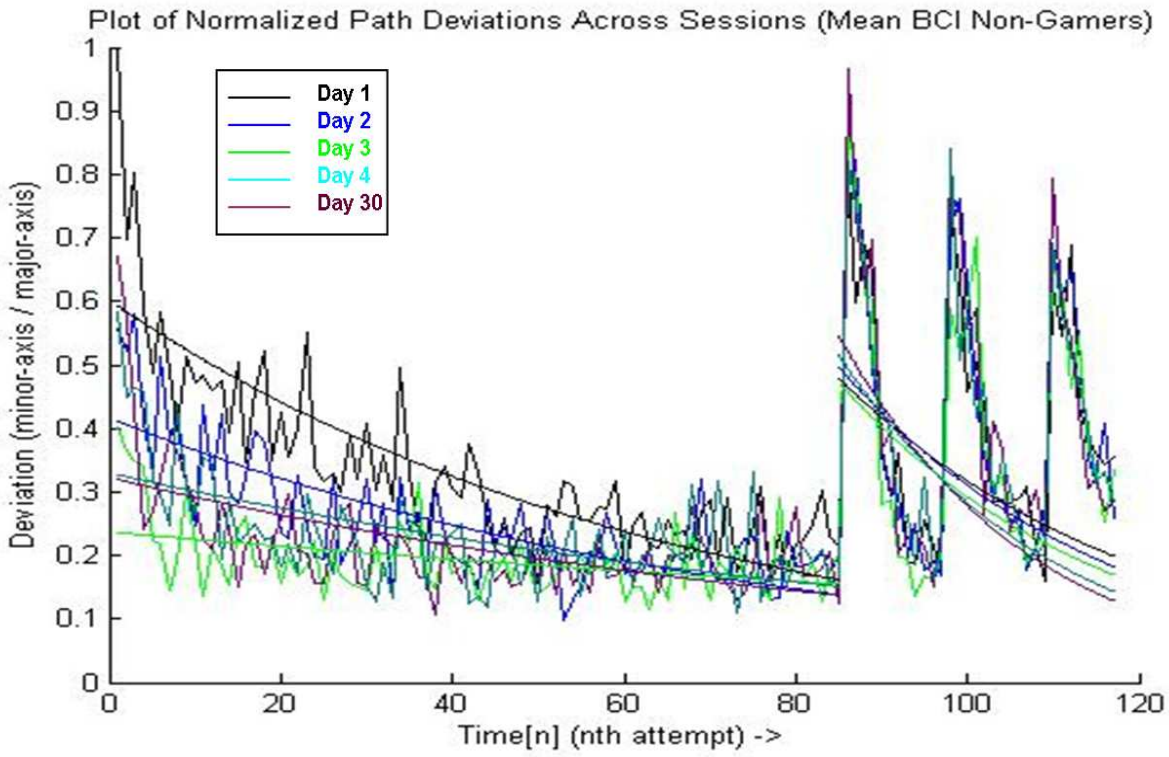

Figure 3.4-7. Motor learning data for four days of training and one 4-week follow-up day. The three peaks on the right of the graph show the locations of the catch trials.

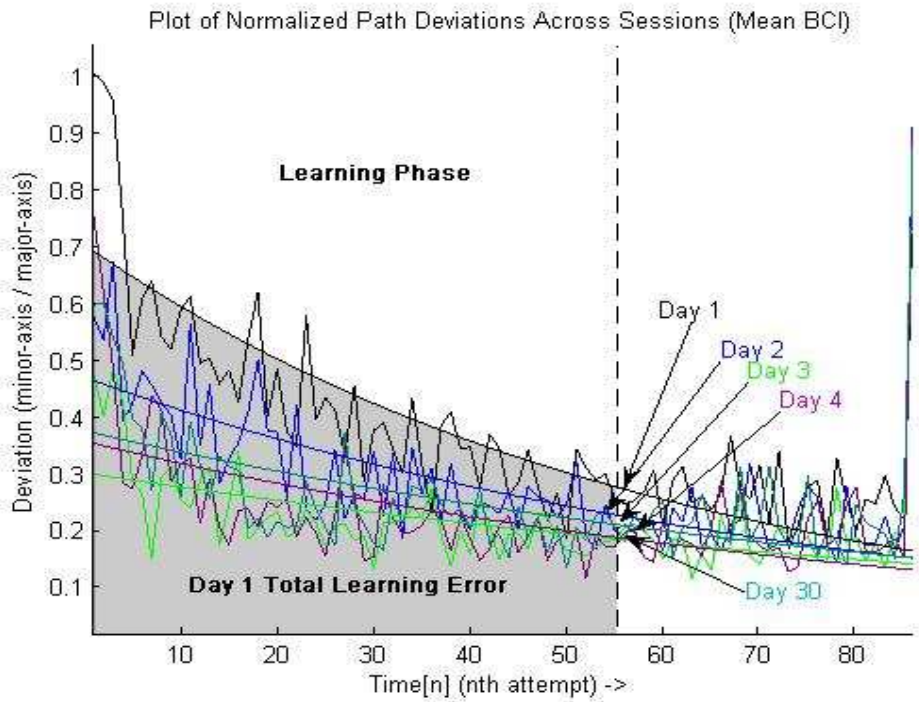

Figure 3.4-8. Estimated total learning error for the first day of training (mean non-BCI subjects).

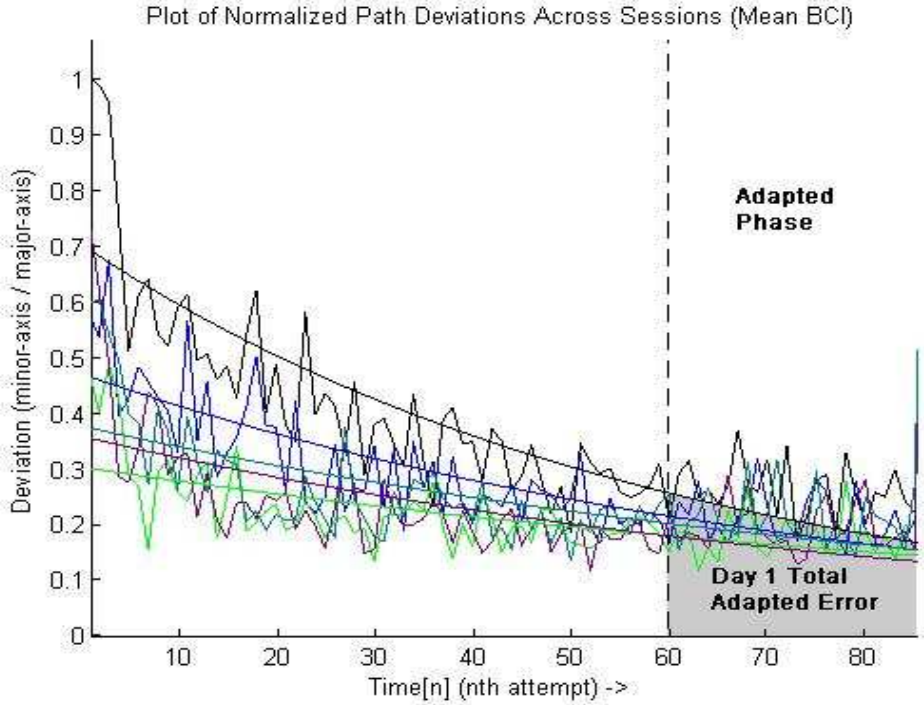

Figure 3.4-9. Estimated total learning error for the first day of training (mean non-BCI subjects).

3.4.3. Aim III: Detecting Forward and Backward Reaching in Guided-Imagery EEG

The guided-imagery task performed during the Follow-up portion of Training introduced a novel approach to invoking motor imagery. This aim sought to determine whether the EEG data extracted while subjects performed that task contained information on reaching directionality.

Figure 3.4-10 illustrates the task that subjects performed. Subjects kept their hands in their laps while they watched the KINARM robot move forward or backward towards randomly displayed targets. Subjects were told to imagine that their arm was in the robot performing the movements that they were observing. The EEG data extracted during this task was processed using the methods described in section 3.4.1; the extracted data represented the most significant channel-frequencies that contributed to two seconds of EEG activity during each guided-imagery reach (one second before the target appeared to the subject and one second after the target appeared when the robot moved and prompted the subject to imagine reaching).

The discussion below outlines the non-comprehensive analysis performed in this investigation. Further studies of this data are encouraged; therefore, the unprocessed data collected during this study will be available for researchers interested in performing other types of machine learning on this novel guided-imagery task. The link to this data is provided in Appendix C.

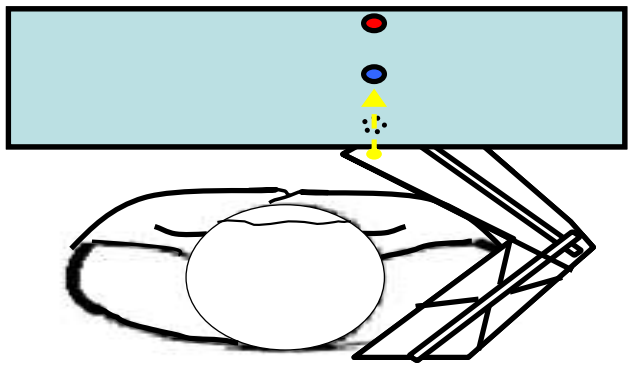

Figure 3.4-10. Guided-imagery task performed by subjects during follow-up sessions.

Data Decomposition

The EEG feature extraction methods in Aim I decomposed the data for each reach into multidimensional triplets consisting of channels with corresponding frequencies (channel-frequencies) and r^2 values. Table 3.4-3 gives an example of the feature components of two sample reaches. The feature space consisted of any combination of triplets in the 16-by-31 dimension space. To program the different classifiers employed in this aim, the multidimensional triplets were expanded into 496-dimensional variables, x_k; any unassigned channel-frequencies in the triplet space were given r^2 values of 0 in the 496-dimensional space. This approach, therefore, converted the reaches in the table below to the vectors outlined underneath the table. Each subject had 295 reaches available for classifier training and testing.

Table 3.4-3. Two Sample Single-Trial 3-Dimensional Reaching Feature Sets with Corresponding 496-Component Vectors (below).

	EEG Channel [1,2,..,16]	Frequency [5,6,…,35]	R^2 [0,1]
x_1 (Reach 1, Forward)	1	30	0.3466
	3	13	0.2068
	3	25	0.2142
	5	11	0.3402
	5	12	0.2175
	8	8	0.2636
x_2 (Reach 2,Backward)	7	19	0.2326
	9	6	0.2742

$x_1 = \langle 0,..., \ 0.3466, \ 0,..., \ 0.2068, \ 0,..., \ 0.2142, \ 0,..., \ 0.3402, \ 0.2175, \ 0,..., \ 0.2636 \ ...,0 \rangle$

$x_2 = \langle 0,..., \ 0.2324, \ 0,..., \ 0.2742 \ 0,..., \ 0,..., \ 0,..., \ 0,..., \ 0,..., \ 0,..., \ 0,..., \ 0,...,0 \rangle$

Classifiers Comparisons

This analysis employed three different types of classifiers for comparison, a support vector machine (SVM) with a Gaussian radial basis function kernel (GRBF), a Fishers Linear Discriminant analysis (FLD), and an FLD with an initial principle components analysis feature reduction step (FLDPCA). All methods were implemented using the Statistical Pattern Recognition Toolbox in *MATLAB*®.

Each subject's training set consisted of 236 reaches, x_k, with corresponding directional classifications, y_k (i.e. $[x_k,y_k]$). For forward reaches, y_k was '1', and for backward reaches, y_k was '-1'. The SVM estimated a decision function using the following equation:

$$h(x) = sign(\langle w \cdot x \rangle + b) \tag{16}$$

where $w = \sum_{i=1}^{236} \alpha_i y_i x_i$, with $\alpha_i \geq 0$. The Gaussian radial basis function kernel was calculated as

$$k(x_i, x) = e^{-||x_i - x|| / 2\sigma^2} \tag{17}$$

such that $k(x_i, x) = \varphi(x_i) \cdot \varphi(x)$, and input into Equation (16) to produce the decision equation:

$$h(x) = sign(\sum_{i=1}^{236} \alpha_i y_i k(x_i, x) + b) \quad (18)$$

The SVM was programmed to chose the best GRBF kernel machine out of every combination of arguments including σ (σ ϵ [0.1, 0.5, 1, 5, 10, 100]) and regularization constants C (C ϵ [1, 10, 100]) that minimized the quadratic programming problem:

$$C\sum_{i=1}^{236} \xi_i + \frac{1}{2}\|w\|^2 \quad (19)$$

where ξ_i is a misclassification estimate (for each training vector) greater than zero [123-126].

The FLD projected the data onto a one-dimensional subspace and use the means, within-group and between-group variances to maximize the separation of the data and attempt to classify forward versus backward reaching data. The FLDwPCA classifier performed an FLD training with a prior PCA step that reduced the 496-dimensional space to a projection that minimized the PCA reconstruction error [124].

Each subjects training set comprised 236 (first 4 out of 5 runs) reaches; test sets contained 59 total reaches. The results of this analysis are outline in Section 4.3.

Chapter 4: Experimental Results

Through the specific aim outlined in Chapter 1, this investigation sought to determine whether BCI training had quantifiable effects on brain plasticity and motor learning. Additionally, this investigation sought to determine whether EEG extracted during novel guided-imagery task introduced in this study contained features that could classify reaching direction.

The discussion below outlines the quantitative results of each specific aim. The brain plasticity analysis (Section 4.1) and the motor learning analysis (Section 4.2) were decomposed into several subcategories to highlight different relatable aspects of the data and to approach the analysis from several different perspectives. The classifier analysis in Section 4.3 outlines the results of the three classifiers discussed in Section 3.4.3. This chapter presents conclusions on how the data should be interpreted in each analysis; Chapter 5, however, discusses comprehensive conclusions of this investigation.

4.1. Brain Plasticity Analysis

The brain plasticity analysis employed statistical analyses of EEG data to determine whether there were discernable trends occurring in the BCI group that implied plasticity was influenced by BCI training. This investigation focused on two aspects of EEG data, frequency (spectral) content and the motor area of the brain (spatial) content. Additionally, two different comparisons were made. One comparison looked at the short-term changes that occurred between the first day (Training Day One) and the last day (Training Day Four) of training; the

other comparison looked at the persistent changes that occurred between the Screening session and Follow-up session.

4.1.1. Spectral Analysis

The analysis of spectral content considered the changes in mu and beta content of imagined reaches performed during short-term and long-term stages of the study protocol. Statistical tests paired EEG data extracted from individual subjects. Spectral content was characterized by two different measures. The first measure was the proportion of the entire feature space that comprised mu and beta frequencies (separately). The second measure was the mean power (r^2) of the mu and beta frequencies.

The statistical tests performed in this investigation looked for statistically significant changes with 95% confidence for individual subject spectral and spatial data.

Training Day One versus Training Day Four

The first analysis contrasted the spectral content produced during the beginning of training with that produced at the end. This analysis extracted mu (8-14Hz) and beta (18-26Hz) content from each subject's feature set for Training Day One and Training Day Four. Each frequency within the mu and beta bands received a proportion value to represent how often each frequency appeared in each feature set; similarly each frequency was also assigned its average r^2 in lieu of the proportion for the r^2 power analysis (recall the minimum r^2 was 0.2). The entire band of frequencies (i.e. mu or beta) comprised the distribution used for the Wilcoxon signed rank tests. The results of the statistical tests are outlined in Table 4.1-1, which shows the p-values of each test for each subject; significant p-values are bolded.

The results of the statistical tests showed that both groups contained subjects who experienced statistically significant changes in overall mu and beta activity. Four subjects in the BCI groups had significant changes in mu proportion (Total μ Proportion) from Training Day One to Training Day Four, whereas only two non-BCI subjects had significant changes in mu proportion. Figure 4.1-1 illustrates a chart of the proportions of each frequency feature during Training Day One (blue) and Training Day Four (red) for the two non-BCI subjects; Figure 4.1-2 illustrates the same for the four BCI subjects. All subjects showed a short-term increase in the presence of significant mu features.

Conversely, two subjects in the Non-BCI group experienced significant changes in the mean mu mean power (Total μ power), whereas only one of the BCI subjects showed statistically significant changes. While Non-BCI Subject 3 also showed significant changes in mu and beta proportion, as illustrated in Figure 4.1-1, his/her power increases were not substantial in relation to other frequencies. Opposed to the mu proportion results, the statistical changes in mu power were varied; the one Non-BCI subject had an increase in mu power, while the other subject had a decrease (Figure 4.1-3). The change in mu power experienced by the BCI subject was accompanied by increase in mean beta power; that BCI subject had an increase in mu power.

Two BCI subjects had significant changes in beta power; one subject experienced an increase and the other experienced a decrease (Figure 4.1-4). The one Non-BC subject who had significant changes in beta power had an overall decrease.

Table 4.1-1. Wilcoxon p-values for Training Day One vs. Training Day Four

BCI Subjects											
	Subject 1	Subject 2	Subject 3	Subject 4	Subject 5	Subject 6	Subject 7	Subject 8	Subject 9	Subject 10	Subject 11
Total μ Proportion	0.091	0.398	0.999	**0.018**	0.128	**0.018**	0.128	**0.018**	**0.043**	0.612	0.237
Total μ power	0.499	0.176	0.063	**0.028**	0.999	0.398	0.063	0.091	0.237	0.398	0.176
Total β Proportion	0.953	**0.008**	0.139	0.173	0.086	0.214	0.260	0.110	0.066	0.260	0.859
Total β power	0.374	0.678	0.515	**0.038**	0.110	0.953	0.374	0.515	**0.038**	0.139	0.066
Non-BCI Subjects											
	Subject 1	Subject 2	Subject 3	Subject 4	Subject 5	Subject 6	Subject 7	Subject 8	Subject 9	Subject 10	
Total μ Proportion	0.237	0.176	**0.018**	**0.028**	0.999	0.612	0.091	0.176	0.128	0.735	
Total μ power	0.063	0.063	**0.028**	0.091	**0.043**	0.237	0.310	0.866	0.128	0.237	
Total β Proportion	0.066	0.441	**0.051**	0.110	0.173	0.594	0.110	0.678	0.110	0.767	
Total β power	0.374	0.678	0.441	0.214	0.953	**0.051**	0.515	0.767	0.441	0.214	

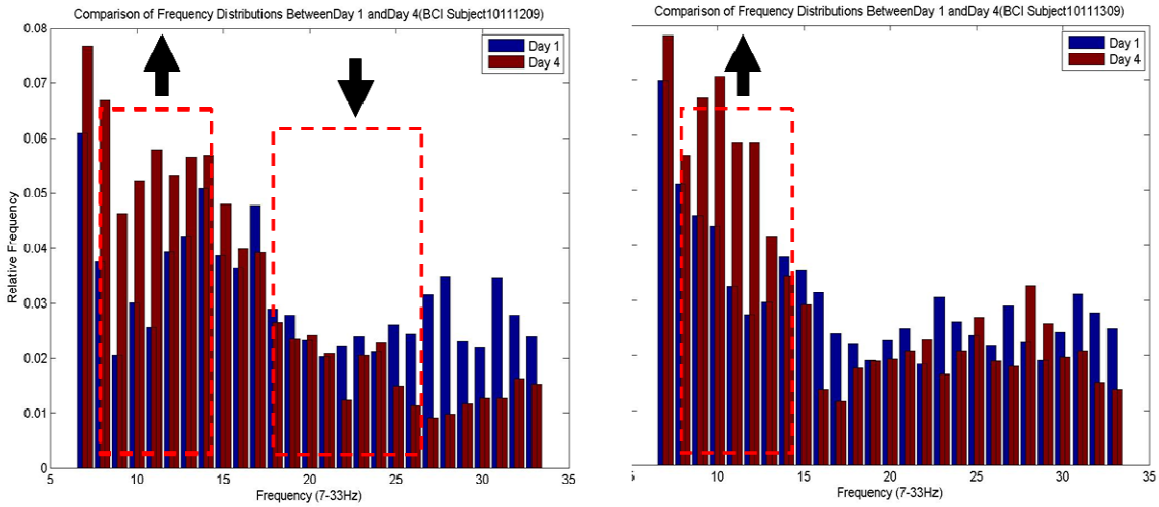

Figure 4.1-1. Chart of frequency proportions for Non-BCI subjects with significant mu proportion increases. The subject on the left also demonstrated a significant decrease in beta proportion.

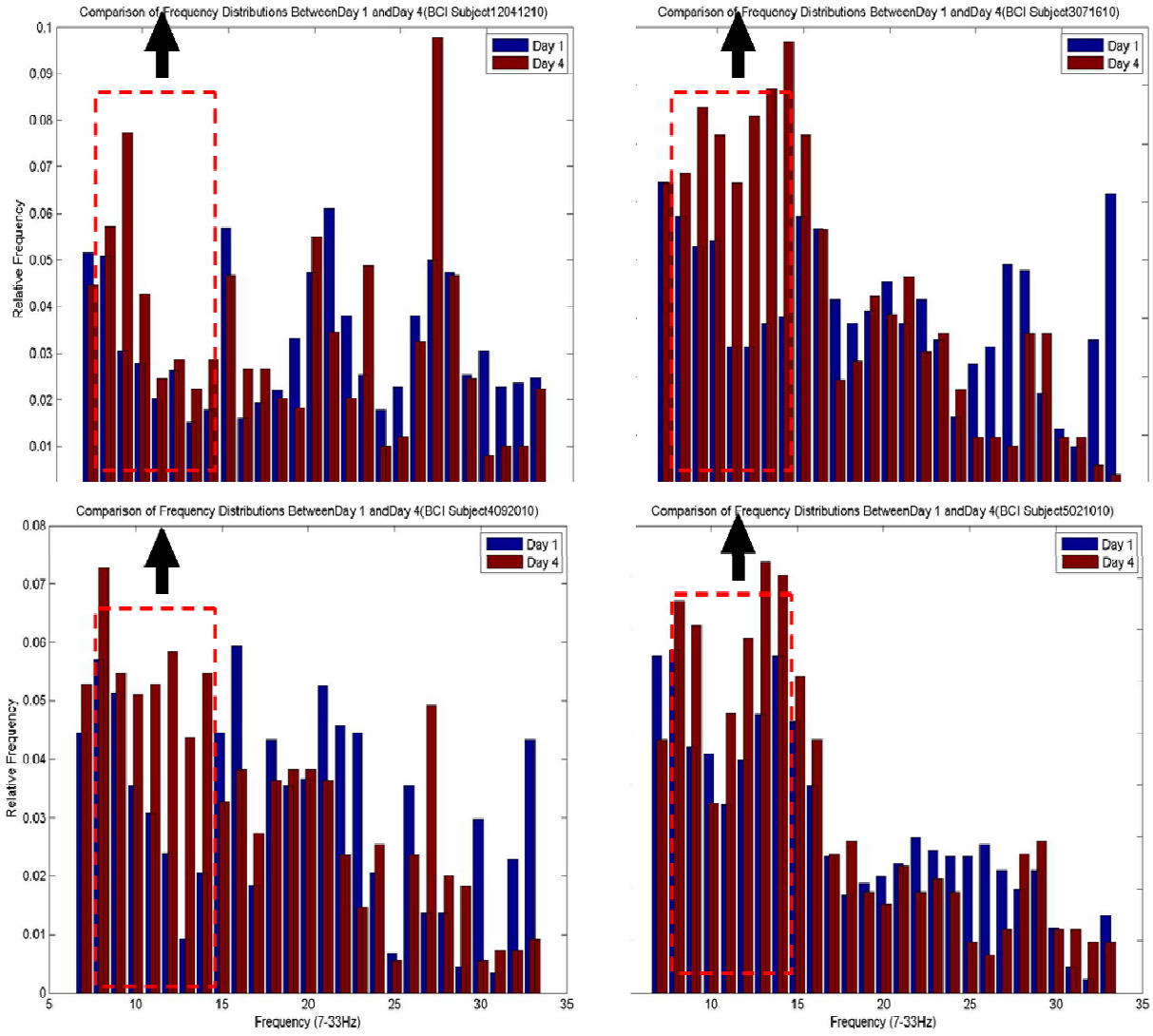

Figure 4.1-2. Chart of frequency proportions for BCI subjects with significant mu proportion increases.

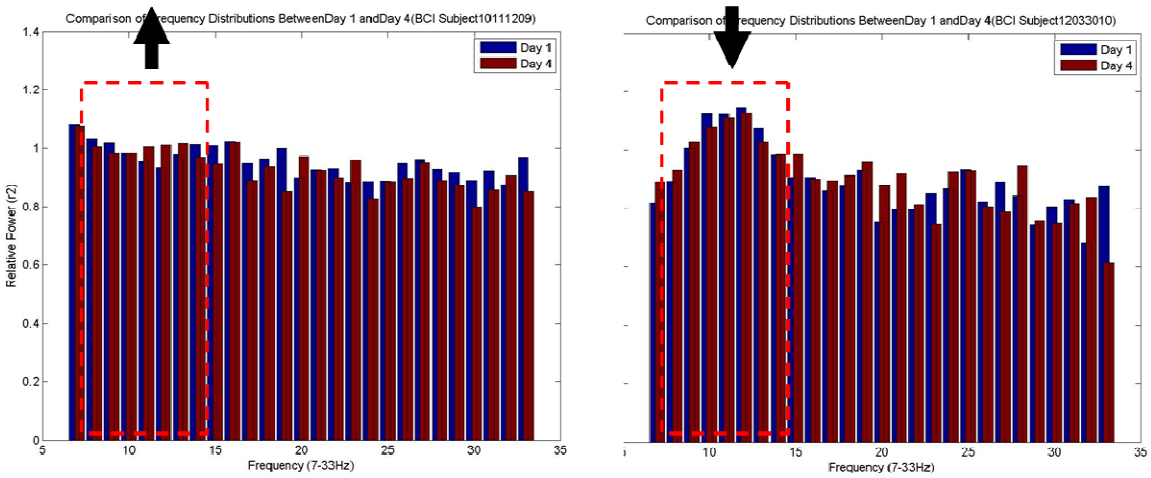

Figure 4.1-3. Chart of frequency powers for Non-BCI subjects with significant mu power changes.

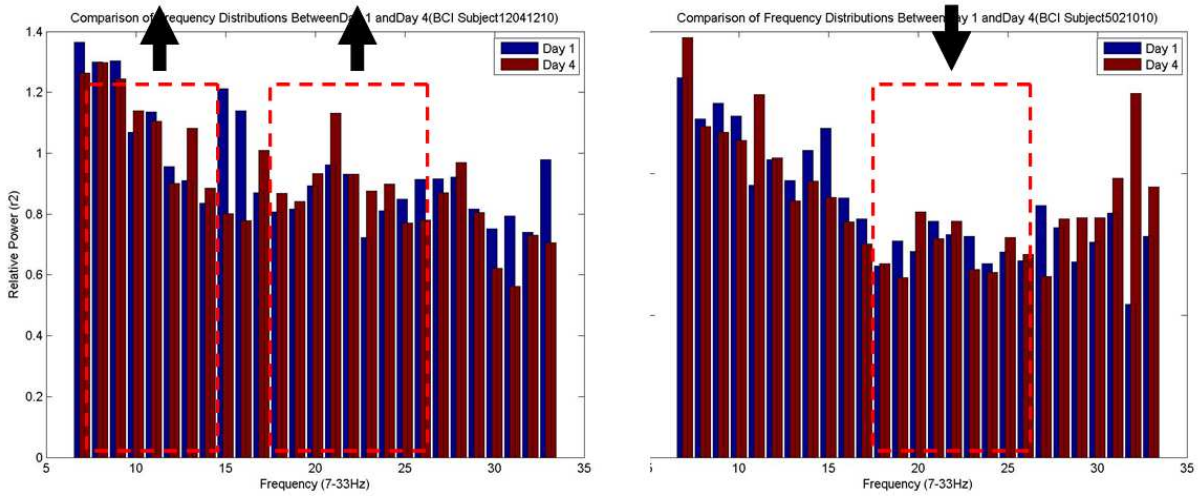

Figure 4.1-4. Chart of frequency powers for BCI subjects with significant mu and beta power changes.

Screening versus Follow-up

The second analysis examined the persistent effects of training on EEG content. The mu and beta signals that comprised the data set in this statistical analysis were extracted from EEG data collected while subjects in both groups performed motor imagery tasks during the Screening and Follow-up sessions. Once again, each frequency within the mu and beta bands received a proportion value and mean power value to form the distributions used for the Wilcoxon signed rank tests. The results of the statistical tests are outlined in Table 4.1-2, which shows the p-values of each test for each subject. Significant results are bold.

Table 4.1-2. Wilcoxon p-values for Screening vs. Follow-up

BCI Subjects											
	Subject 1	Subject 2	Subject 3	Subject 4	Subject 5	Subject 6	Subject 7	Subject 8	Subject 9	Subject 10	Subject 11
Total μ Proportion	0.866	0.612	0.499	0.176	0.866	0.310	0.176	0.176	0.063	**0.043**	0.063
Total μ Power	0.612	**0.018**	0.999	0.866	0.091	0.063	0.499	0.866	0.310	0.612	0.735
Total β Proportion	**0.028**	0.374	0.767	0.214	**0.050**	0.066	0.214	0.110	0.110	0.260	0.953
Total β Power	0.214	0.110	0.139	0.086	0.859	0.515	0.038	0.139	0.314	**0.051**	0.953
Non-BCI Subjects											
	Subject 1	Subject 2	Subject 3	Subject 4	Subject 5	Subject 6	Subject 7	Subject 8	Subject 9	Subject 10	
Total μ Proportion	**0.018**	0.178	**0.018**	**0.018**	**0.018**	0.398	0.398	0.735	0.237	0.866	
Total μ Power	**0.018**	**0.043**	**0.018**	**0.018**	0.499	**0.028**	0.735	0.612	**0.043**	0.866	
Total β Proportion	0.441	0.314	**0.038**	0.110	0.110	0.374	0.110	0.953	0.110	**0.021**	
Total β Power	0.086	0.139	0.173	**0.008**	0.953	0.767	0.594	0.767	**0.038**	0.767	

Significant changes in the BCI group were dispersed. Only one BCI subject had significant changes in more than one measure, an increase in both mu proportion and beta power (Figure 4.1-5). The other subjects only experienced significant changes in one measure each. Two BCI subjects showed significant short-term reductions in beta proportion (Figure 4.1-6).

Within the Non-BCI group, short-term changes were noticeably present in the mu band with several subjects having significant changes. Four Non-BCI subjects had significant changes in the mu proportion, three of which had significant changes in mu power. Five Non-BCI subjects overall had changes in mu power.

Figure 4.1-7 illustrates the four Non-BCI subjects' frequency proportions for Screening and Follow-up. Three of the four subjects had an decrease in mu proportion between Screening and Follow-up; these are the same three subjects who also had changes in mu power, which were also decreases (Figure 4.1-8).

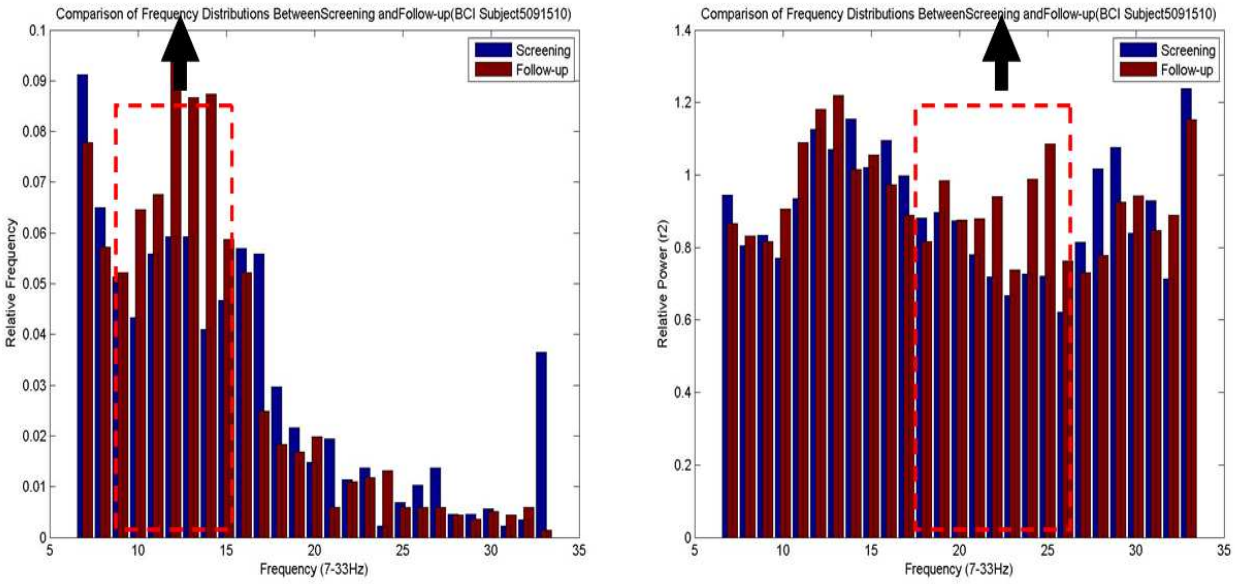

Figure 4.1-5. Frequency proportions and powers for BCI Subject 10 with significant increases in mu proportion and beta power.

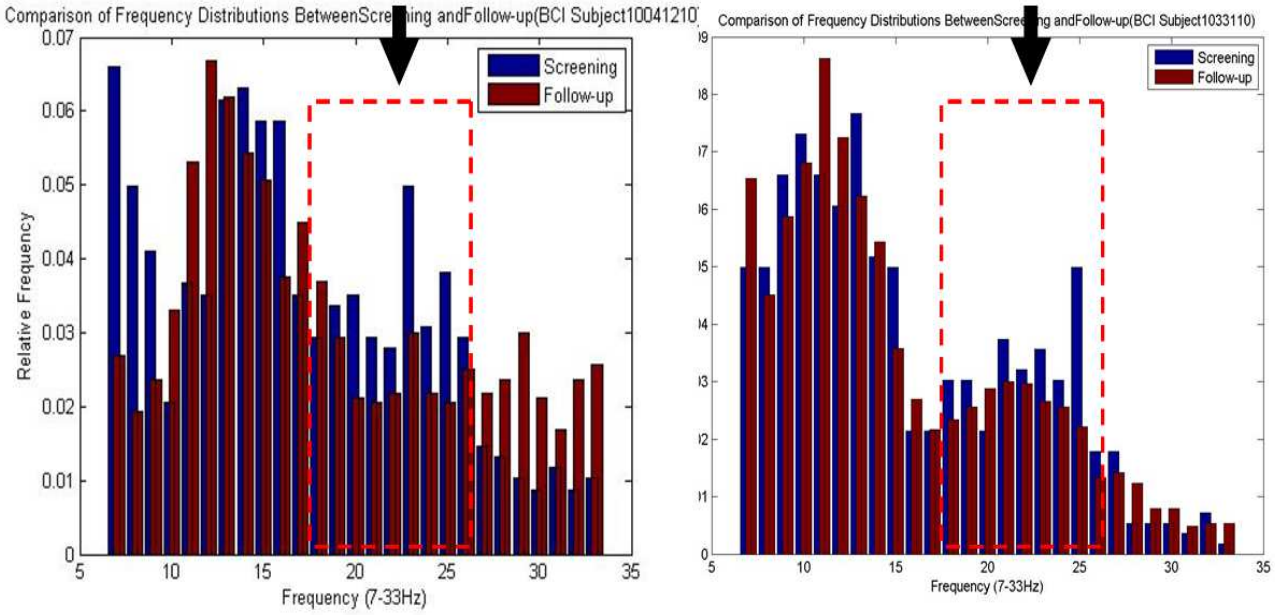

Figure 4.1-6. Chart of frequency proportions for BCI subjects with significant changes in beta proportion.

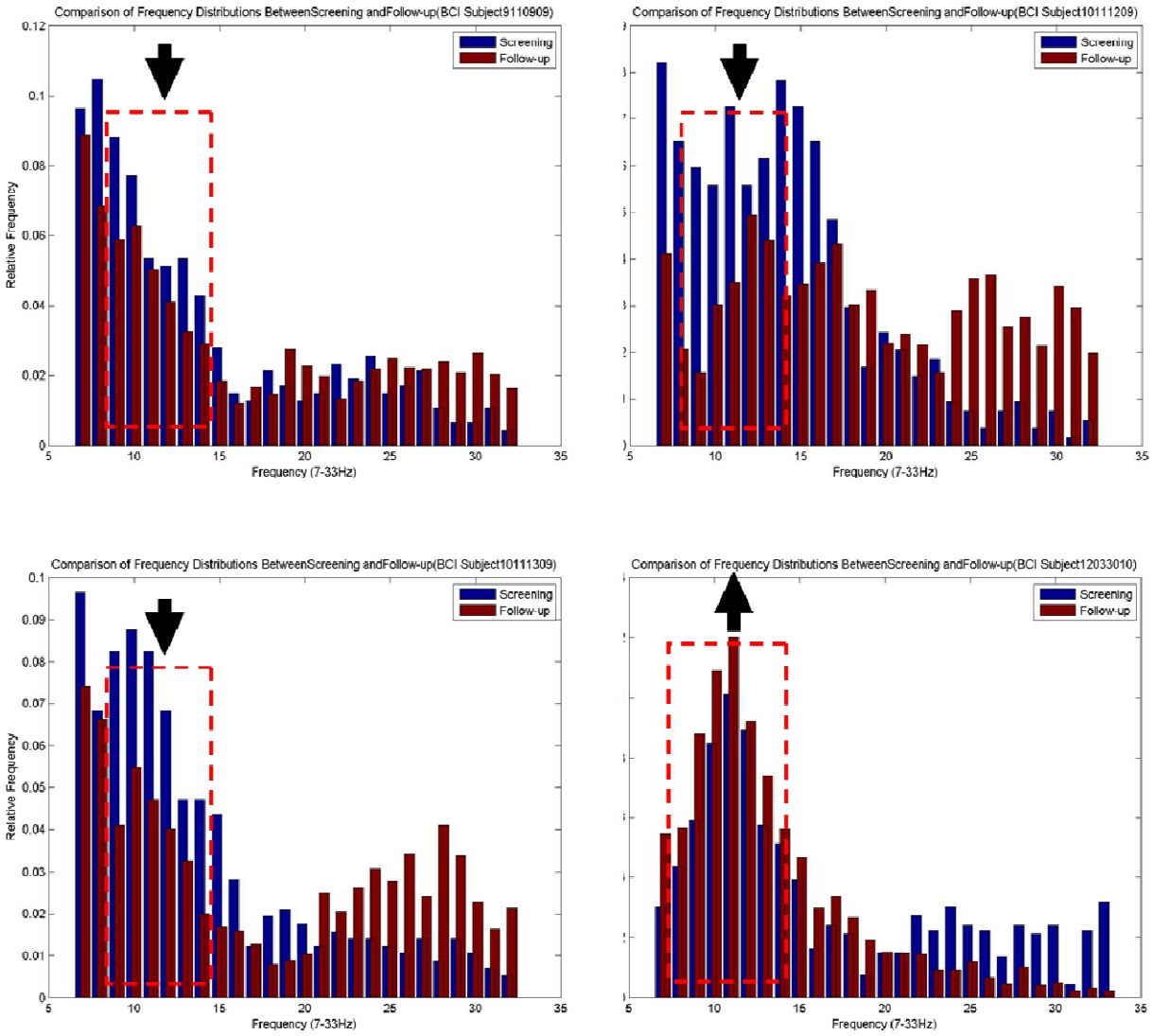

Figure 4.1- 7. Frequency proportions for Non-BCI subejcts with significant changes in mu proportions.

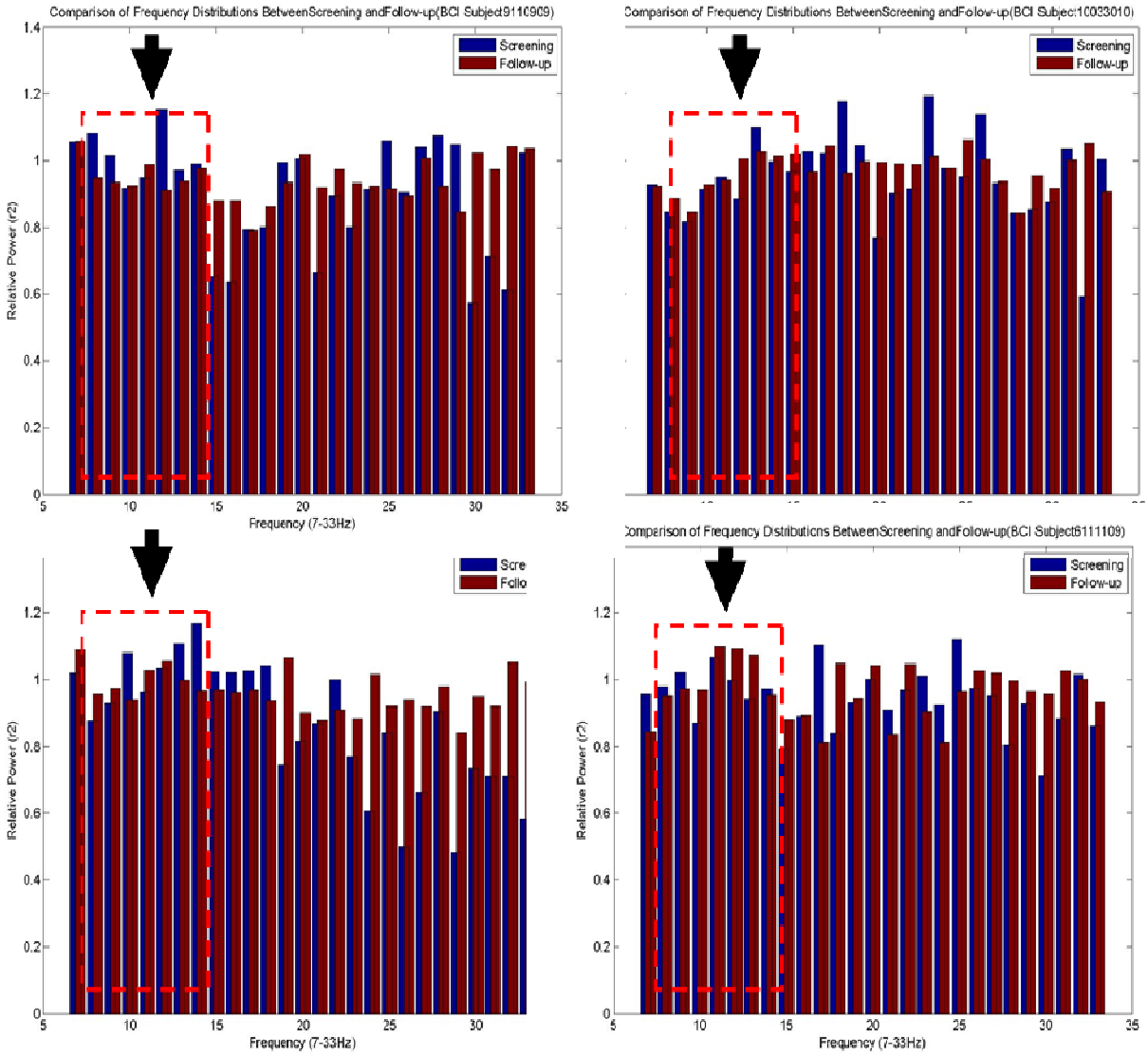

Figure 4.1-8. Frequency powers for Non-BCI subjects with significant changes in mu power.

4.1.2. Spatial Analysis

The spatial analysis performed comparisons of each subjects features sets for each stage of the study as was done in the spectral analysis. In this section, however, the mu and beta activities of only certain channels were tested and compared with the rest of the channel space. Proportion and power of mu and beta comprised the test distributions for Wilcoxon signed rank tests.

The scalp topographies illustrated in this section show difference measures between each stage of the study similar to Figure 3.4-4C. The color scales are unique for each topographic mapping; the scales are relative to the maximum and minimum differences present over the entire scalp.

Training Day One versus Training Day Four

Each subject was tested for short-term changes that occurred between Training Day One and Training Day Four. The p-values of the Wilcoxon tests are outlined in Table 4.1-3.

Changes in the BCI group were dispersed among several different subjects. Four of the 11 BCI Subjects had significant changes in mu proportion between Training Day One and Training Day Four over the *left-brain*; two of these four had increased mu proportions whereas one subject experienced a decrease (Figures 4.1-9 to 4.1-12). In addition, all subjects who had changes in mu power experienced an increase over the *left-brain* or *motor strip*.

Three BCI subjects experienced changes in beta proportion over the *motor strip*; all of these were decreases (Figures 4.1-13 to 4.1-15). One of the subjects who had a decrease in beta was also included in the group of subjects who had an increase in mu power (Figure 4.1-16); the other two subjects who had beta proportion decreases experienced no other short-term changes.

Within the Non-BCI group, only three subjects experienced significant changes. Almost all changes involved an increase in mu activity with the exception of a decrease in beta proportion over the *left-brain* for subject 3. Figures 4.1.2-17 to 4.1.2-22 illustrate all short-term spatial changes that occurred in the Non-BCI group.

Table 4.1- 3. Wilcoxon p-Values for Training Day One vs. Training Day Four Tests

BCI Subjects											
	Subject 1	Subject 2	Subject 3	Subject 4	Subject 5	Subject 6	Subject 7	Subject 8	Subject 9	Subject 10	Subject 11
Left-brain μ Proportion	**0.028**	0.398	0.398	0.063	0.237	**0.028**	0.237	**0.018**	0.128	0.398	**0.043**
Left-brain μ Power	0.091	0.176	0.063	**0.043**	0.310	0.499	0.128	0.374	0.237	0.237	0.128
Motor strip μ Proportion	0.116	0.612	0.612	0.345	0.091	0.091	0.176	**0.018**	0.237	0.497	0.999
Motor strip μ Power	**0.046**	0.735	0.499	0.249	0.237	0.735	0.091	0.398	0.866	0.237	**0.028**
Left-brain β Proportion	0.374	0.441	0.214	0.110	0.173	0.594	0.109	0.176	0.109	0.673	0.594
Left-brain β Power	0.678	0.953	0.594	0.441	0.374	0.594	0.173	0.515	0.086	0.779	0.767
Motor strip β Proportion	0.917	0.139	0.441	0.859	0.063	0.499	0.092	**0.015**	**0.028**	**0.042**	0.498
Motor strip β Power	0.600	0.767	0.594	0.594	0.999	0.128	**0.012**	0.110	0.063	0.500	0.686
Non-BCI Subjects											
Left-brain μ Proportion	0.499	0.499	**0.018**	**0.028**	0.999	0.091	0.398	0.612	0.999	0.128	
Left-brain μ Power	0.310	0.063	**0.028**	0.091	**0.018**	0.398	0.398	0.735	0.091	0.866	
Motor strip μ Proportion	0.866	0.398	**0.018**	**0.018**	0.735	0.063	0.176	0.091	0.735	0.735	
Motor strip μ Power	0.398	0.310	**0.018**	**0.028**	0.128	0.237	0.091	0.735	0.237	0.735	
Left-brain β Proportion	0.086	0.515	**0.050**	0.260	0.953	0.139	0.441	0.594	0.110	0.173	
Left-brain β Power	0.678	0.678	0.953	0.066	0.515	0.678	0.594	0.515	0.260	0.859	
Motor strip β Proportion	0.678	0.314	0.109	0.173	0.173	0.085	0.953	0.953	0.674	0.139	
Motor strip β Power	0.859	0.767	0.515	0.678	0.859	0.139	0.594	0.139	0.208	0.086	

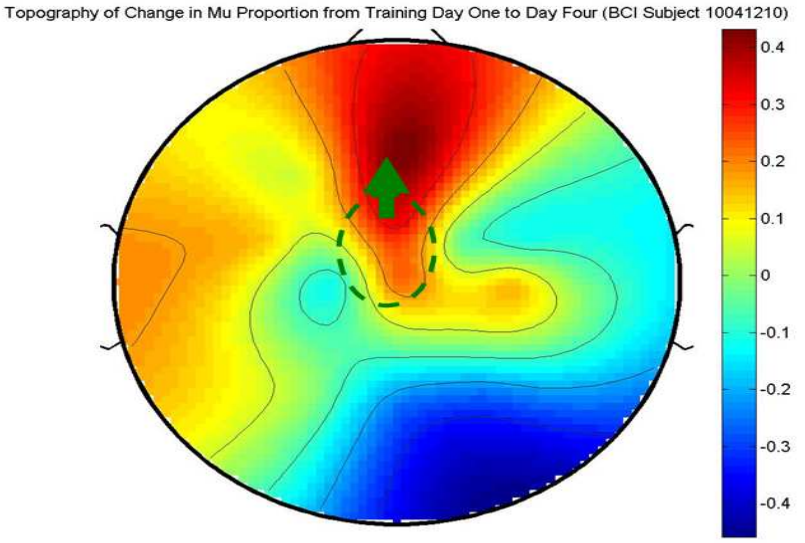

Figure 4.1-9. Topographical map of short-term changes in mu proportion for BCI Subject 1. Color scale interprets the relative spatial proportional change from Training Day One to Training Day Four; the green arrow implies a quantitative increase in the designated area of the scalp.

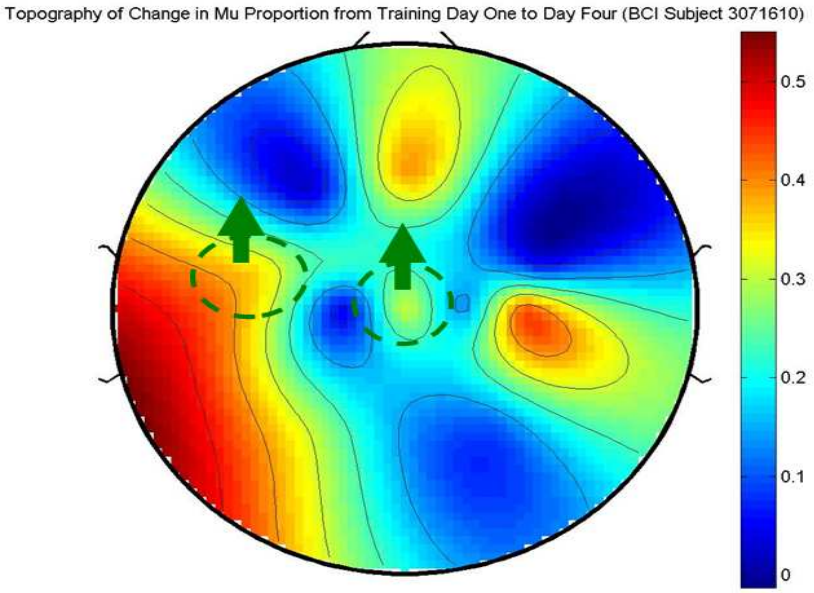

Figure 4.1-10. Topographical map of short-term changes in mu proportion for BCI Subject 6. Color scale interprets the relative spatial proportional change from Training Day One to Training Day Four; the green arrows imply a quantitative increase in the designated area of the scalp.

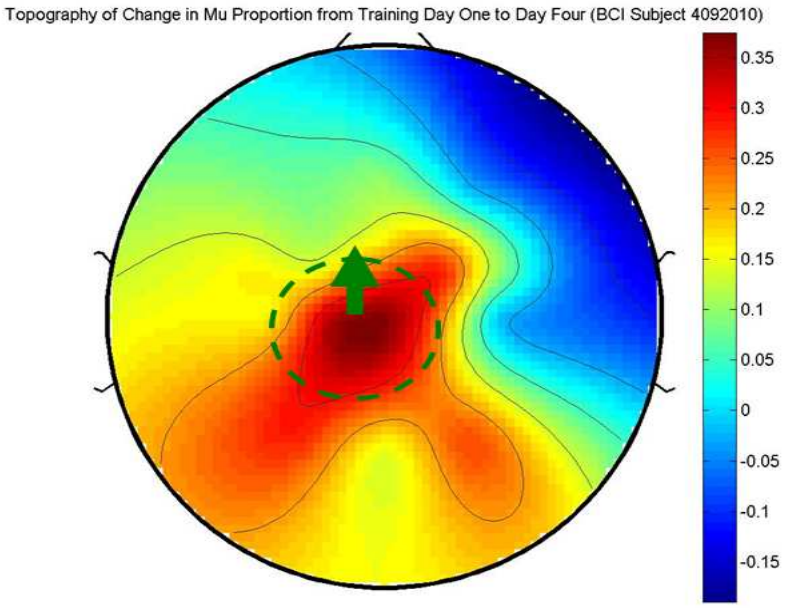

Figure 4.1-11. Topographical map of short-term changes in mu proportion for BCI Subject 8. Color scale interprets the relative spatial proportional change from Training Day One to Training Day Four; the green arrow implies a quantitative increase in the designated area of the scalp.

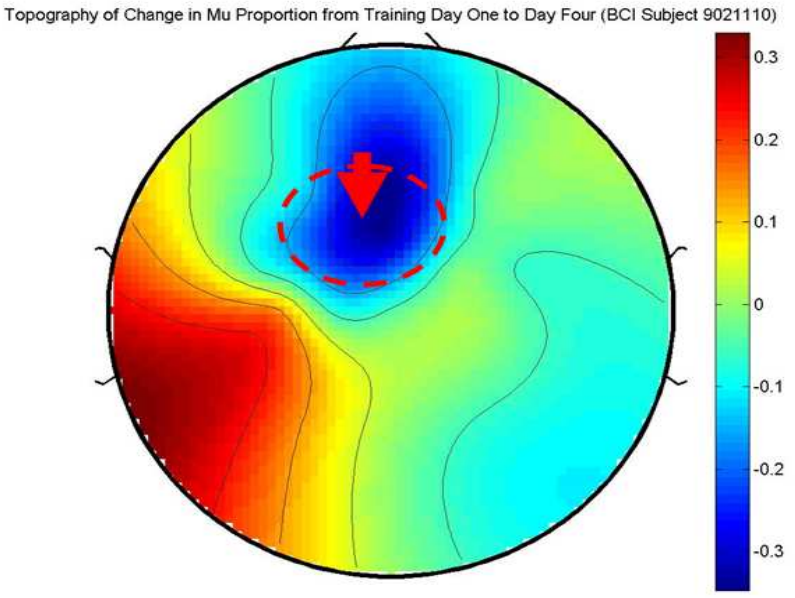

Figure 4.1-12. Topographical map of short-term changes in mu proportion for BCI Subject 11. Color scale interprets the relative spatial proportional change from Training Day One to Training Day Four; the red arrow implies a quantitative decrease in the designated area of the scalp.

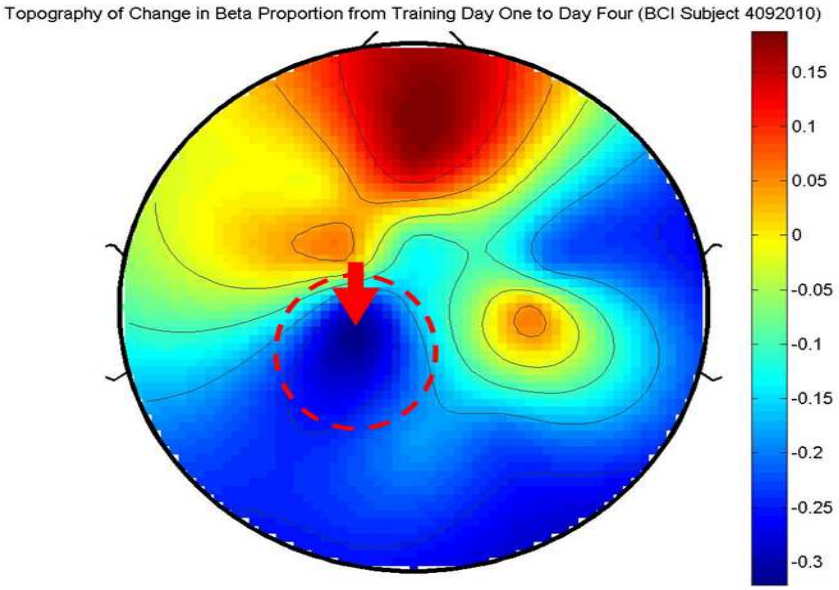

Figure 4.1-13. Topographical map of short-term changes in beta proportion for BCI Subject 8. Color scale interprets the relative spatial proportional change from Training Day One to Training Day Four; the red arrow implies a quantitative decrease in the designated area of the scalp.

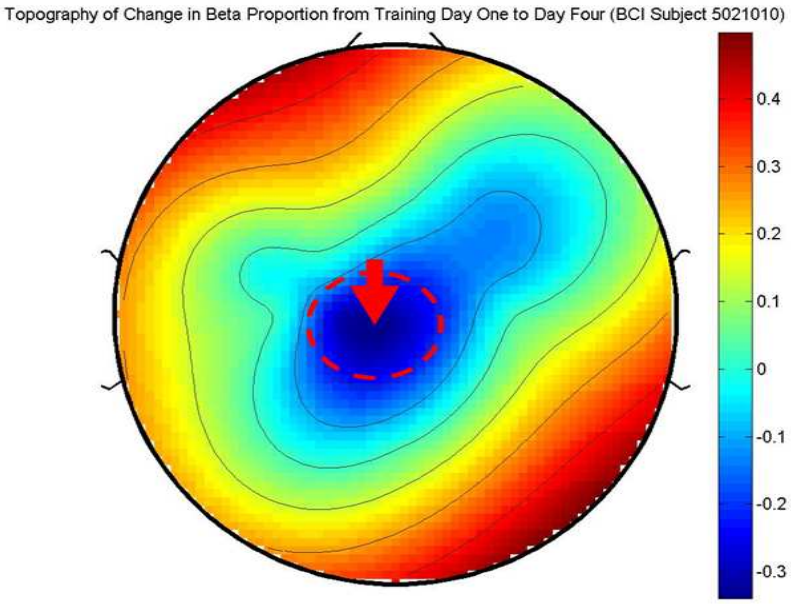

Figure 4.1-14. Topographical map of short-term changes in beta proportion for BCI Subject 9. Color scale interprets the relative spatial proportional change from Training Day One to Training Day Four; the red arrow implies a quantitative decrease in the designated area of the scalp.

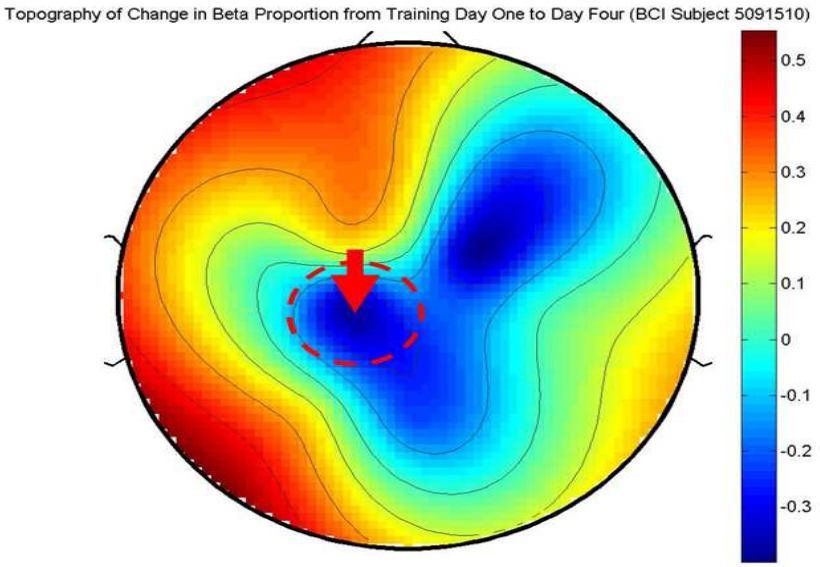

Figure 4.1-15. Topographical map of short-term changes in beta proportion for BCI Subject 10. Color scale interprets the relative spatial proportional change from Training Day One to Training Day Four; the red arrow implies a quantitative decrease in the designated area of the scalp.

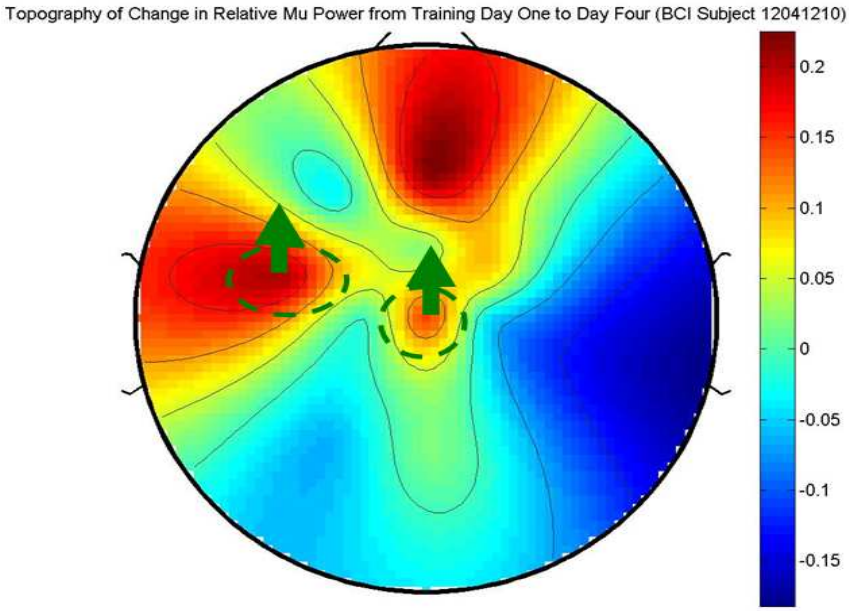

Figure 4.1-16. Topographical map of short-term changes in mu power for BCI Subject 4. Color scale interprets the relative spatial power changes from Training Day One to Training Day Four; the green arrows imply a quantitative increase in the designated area of the scalp.

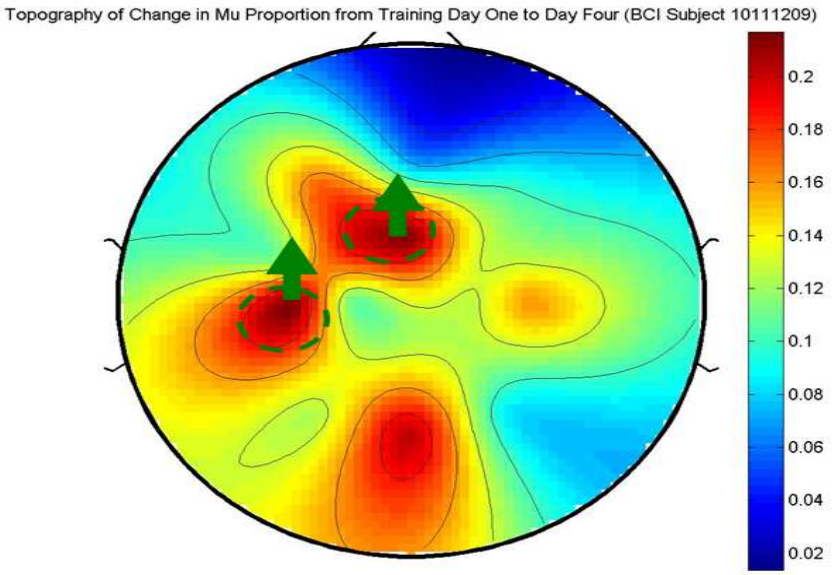

Figure 4.1-17. Topographical map of short-term changes in mu proportion for Non-BCI Subject 3. Color scale interprets the relative spatial proportional change from Training Day One to Training Day Four; the green arrows imply a quantitative increase in the designated area of the scalp.

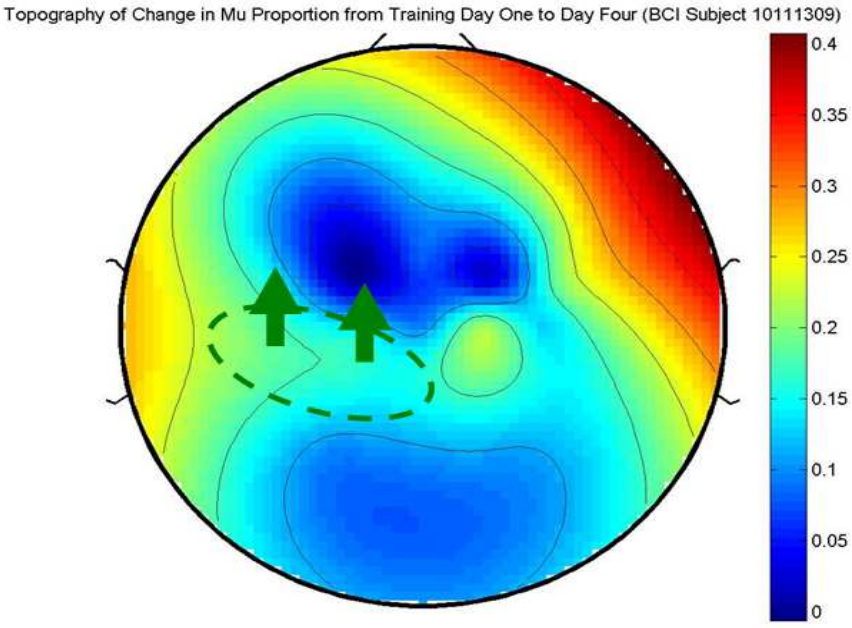

Figure 4.1-18. Topographical map of short-term changes in mu proportion for Non-BCI Subject 4. Color scale interprets the relative spatial proportional change from Training Day One to Training Day Four; the green arrow imply a quantitative increase in the designated area of the scalp.

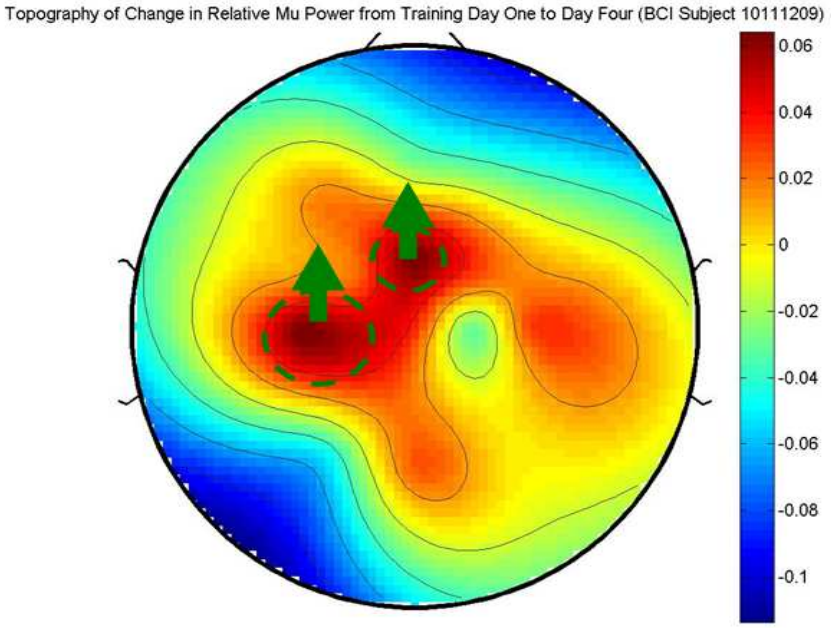

Figure 4.1-19. Topographical map of short-term changes in mu power for Non-BCI Subject 3. Color scale interprets the relative spatial power changes from Training Day One to Training Day Four; the green arrows imply a quantitative increase in the designated area of the scalp.

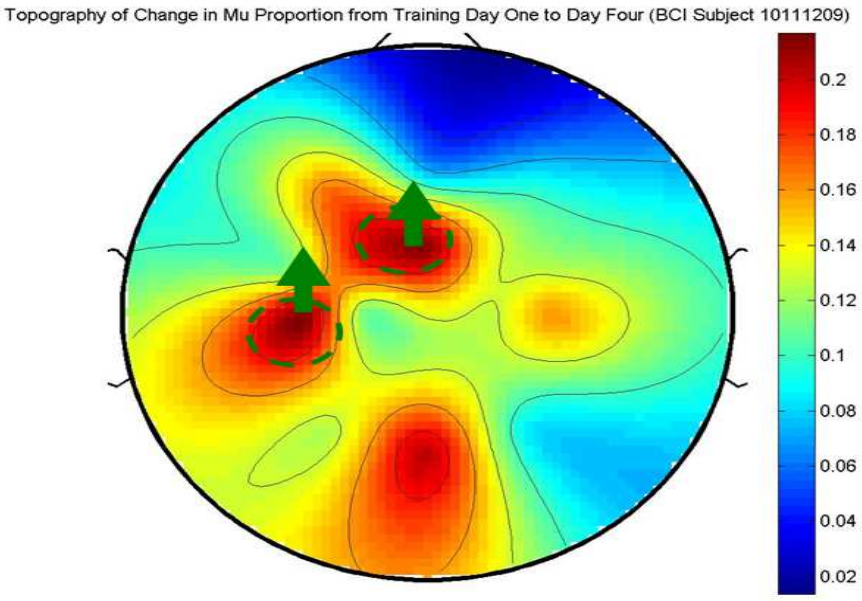

Figure 4.1-20. Topographical map of short-term changes in mu proportion for Non-BCI Subject 3. Color scale interprets the relative spatial proportional change from Training Day One to Training Day Four; the green arrow imply a quantitative increase in the designated area of the scalp.

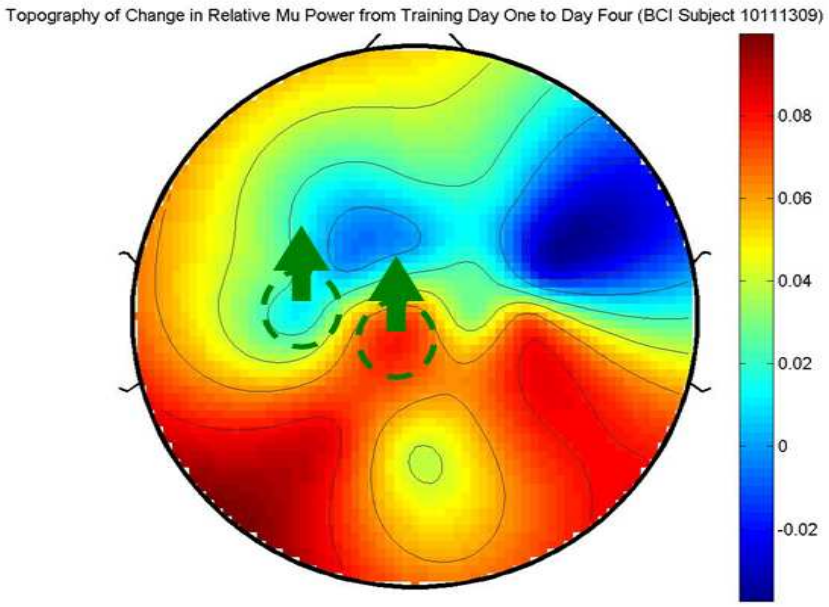

Figure 4.1-21. Topographical map of short-term changes in mu power for Non-BCI Subject 4. Color scale interprets the relative spatial power changes from Training Day One to Training Day Four; the green arrows imply a quantitative increase in the designated area of the scalp.

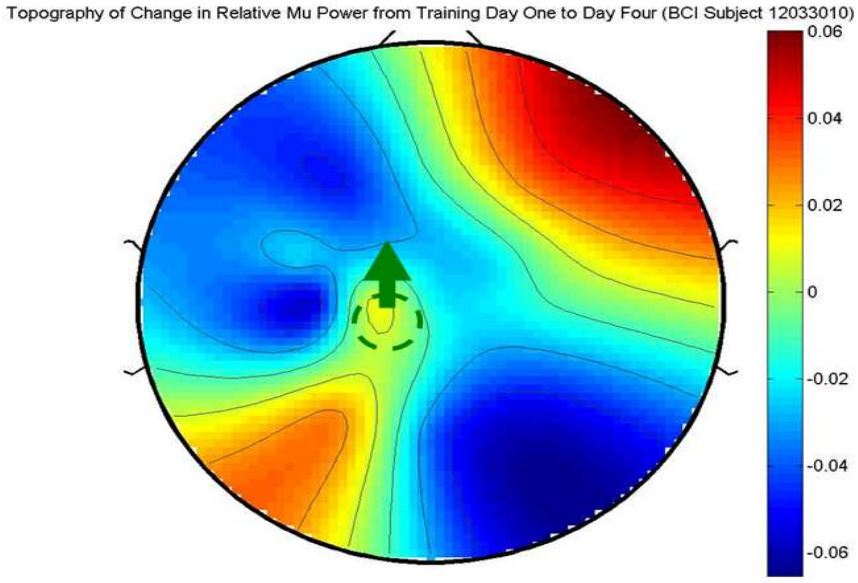

Figure 4.1-22. Topographical map of short-term changes in mu power for Non-BCI Subject 5. Color scale interprets the relative spatial power changes from Training Day One to Training Day Four; the green arrow implies a quantitative increase in the designated area of the scalp.

Screening versus Follow-up

The outcome of the Screening versus Follow-up spatial analysis had very clear distinguishing trends. When looking at the changes in the BCI group, only four subjects showed statistically significant changes between the two stages, Subjects 5, 7, 8 and 10. All subjects had changes in the beta band. Only one, Subject 10, showed a significant change in the mu band, which was an increase in mu proportion. Subjects 5, 7 and 8 had significant decreases in beta proportion in the *motor strip*; Subjects 5 and 8 also experienced significant decreases in beta power over *motor strip*. Conversely, Subject 10, the only BCI subject that had a change in mu activity, experienced an increase in beta proportion over the *left-brain*.

The Non-BCI group had almost the opposite effect. Similar to the BCI group, only four subjects experienced statistically significant changes. However, unlike the BCI group, most subjects experienced changes in mu activity, whereas only one subject had a change in beta activity. Subjects 8 and 10 showed significant increases in mu power over *left-brain* and *motor strip* while Subject 4 had an overall decrease in mu power. The single subject who experienced a change in beta activity, Subject 6, experienced a reduction in beta proportion over *motor strip*.

Table 4.1-4. Wilcoxon p-Values for Screening vs. Follow-up Tests

BCI Subjects											
	Subject 1	Subject 2	Subject 3	Subject 4	Subject 5	Subject 6	Subject 7	Subject 8	Subject 9	Subject 10	Subject 11
Left-brain μ Proportion	0.499	0.866	0.735	0.735	0.735	0.128	0.237	0.310	0.398	0.063	**0.028**
Left-brain μ Power	0.499	0.176	0.735	0.999	0.128	0.735	0.176	0.866	0.063	0.237	0.767
Motor strip μ Proportion	0.612	0.735	0.612	0.735	0.176	0.999	0.735	0.612	0.398	**0.043**	0.237
Motor strip μ Power	0.499	0.237	0.063	0.310	0.499	0.176	0.866	0.612	0.866	0.237	0.176
Left-brain β Proportion	0.086	0.441	0.767	0.314	**0.021**	0.173	**0.051**	**0.051**	0.110	0.594	0.066
Left-brain β Power	0.314	0.314	0.066	0.441	0.3742	0.678	0.110	0.110	0.859	**0.021**	0.866
Motor strip β Proportion	0.674	0.374	0.767	0.635	**0.011**	0.059	**0.046**	**0.017**	0.176	0.074	0.463
Motor strip β Power	0.674	0.314	0.314	0.767	**0.015**	0.144	0.753	**0.025**	0.735	0.116	0.345
Non-BCI Subjects											
	Subject 1	Subject 2	Subject 3	Subject 4	Subject 5	Subject 6	Subject 7	Subject 8	Subject 9	Subject 10	
Left-brain μ Proportion	0.345	0.176	0.176	0.063	0.091	0.345	0.999	0.917	0.237	0.345	
Left-brain μ Power	0.249	0.128	0.735	**0.018**	0.866	0.249	0.310	**0.028**	0.735	**0.028**	
Motor strip μ Proportion	0.249	0.176	0.063	0.128	0.091	0.345	0.866	0.344	0.600	0.735	
Motor strip μ Power	0.249	0.237	0.176	**0.018**	0.499	0.686	0.237	**0.046**	0.753	**0.028**	
Left-brain β Proportion	0.715	0.214	0.180	0.999	0.515	0.116	0.314	0.779	0.674	0.344	
Left-brain β Power	0.068	0.086	0.655	0.465	0.767	0.753	0.859	0.123	0.327	0.463	
Motor strip β Proportion	0.999	0.575		0.461	0.093	**0.044**	0.263	0.128	0.074	0.285	
Motor strip β Power	0.068	0.401		0.465	0.999	0.753	0.779	0.999	0.600	0.999	

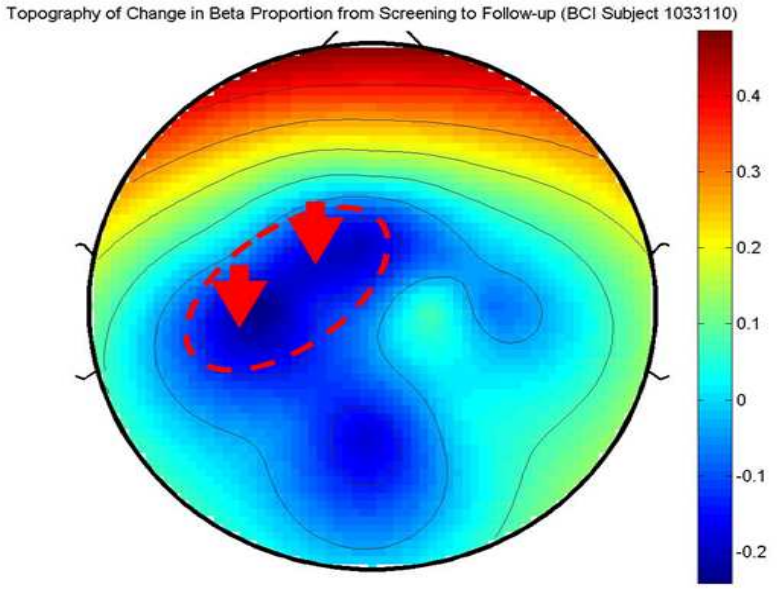

Figure 4.1-23. Topographical map of persistent changes in beta proportion for BCI Subject 5. Color scale interprets the relative spatial proportional changes from Training Day One to Training Day Four; the red arrows imply quantitative decreases in the designated areas of the scalp.

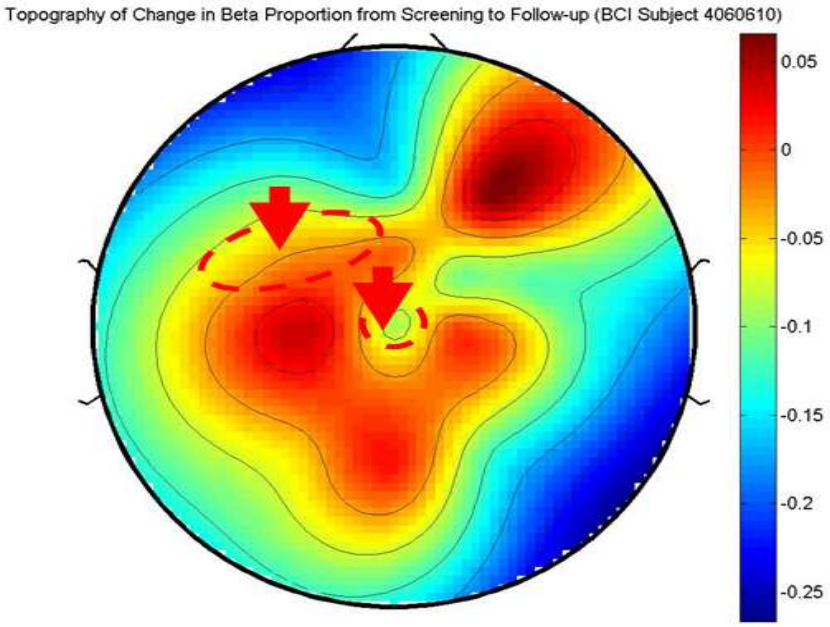

Figure 4.1-24. Topographical map of persistent changes in beta proportion for BCI Subject 7. Color scale interprets the relative spatial proportional changes from Training Day One to Training Day Four; the red arrows imply quantitative decreases in the designated areas of the scalp.

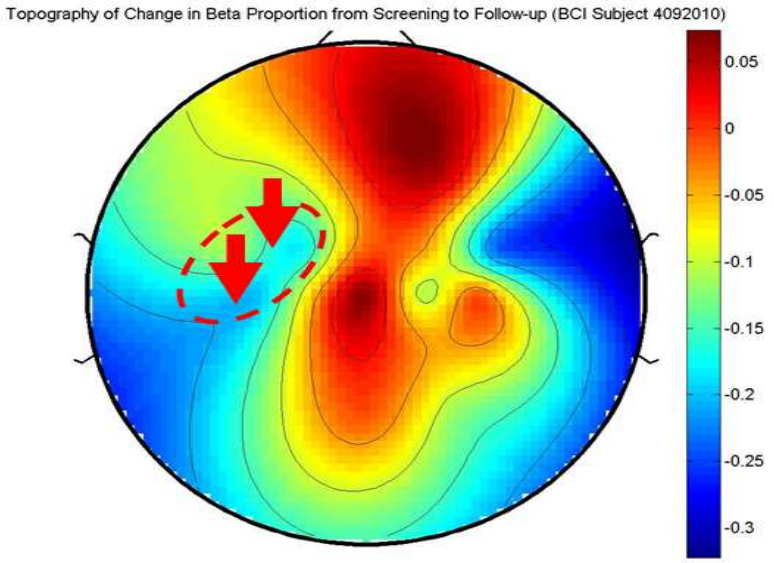

Figure 4.1-25. Topographical map of persistent changes in beta proportion for BCI Subject 8. Color scale interprets the relative spatial proportional changes from Training Day One to Training Day Four; the red arrows imply quantitative decreases in the designated areas of the scalp.

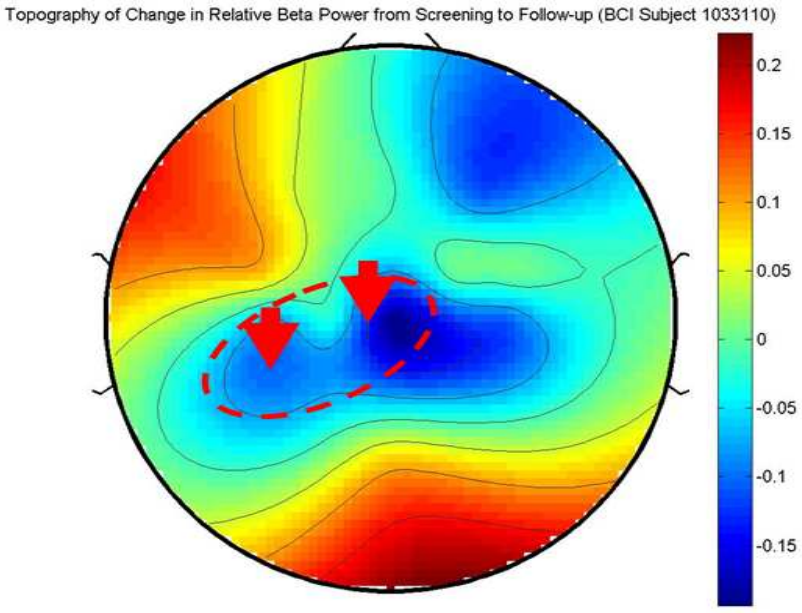

Figure 4.1-26. Topographical map of persistent changes in beta power for BCI Subject 5. Color scale interprets the relative spatial power changes from Training Day One to Training Day Four; the red arrows imply quantitative decreases in the designated areas of the scalp.

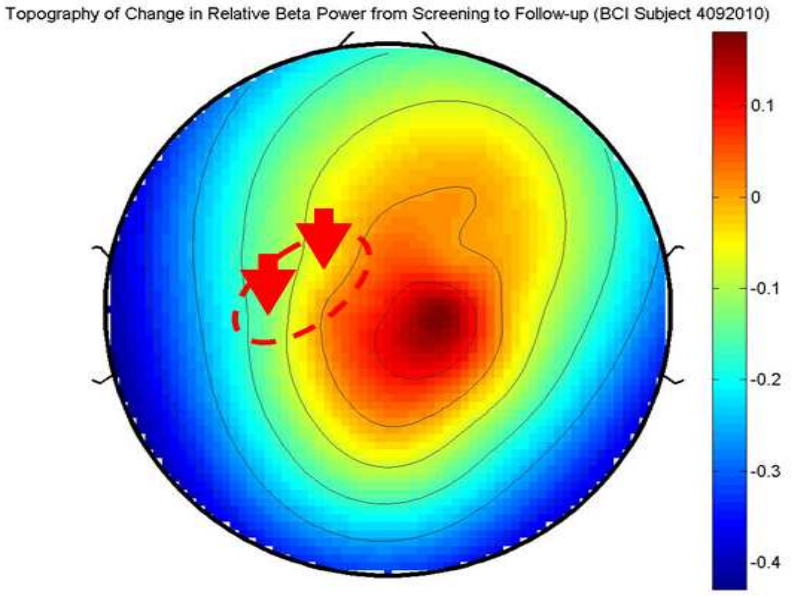

Figure 4.1- 27. Topographical map of persistent changes in beta power for BCI Subject 8. Color scale interprets the relative spatial power changes from Training Day One to Training Day Four; the red arrows imply quantitative decreases in the designated areas of the scalp.

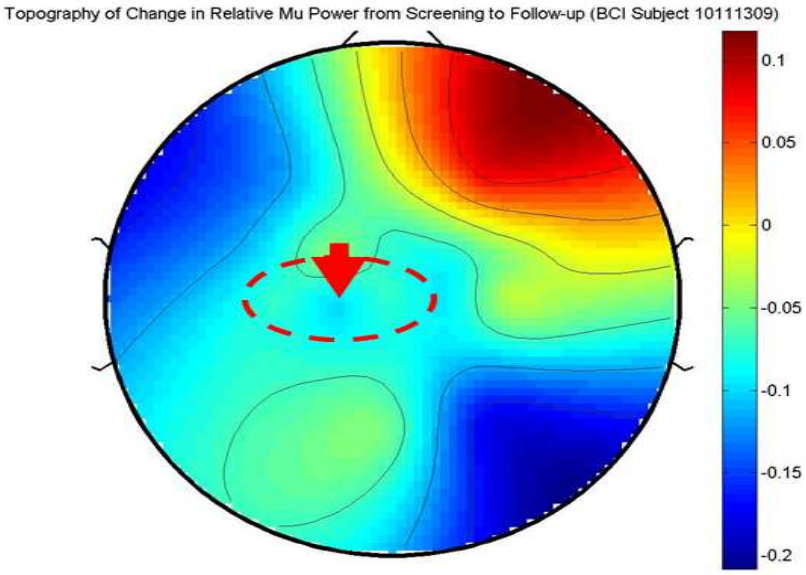

Figure 4.1-28. Topographical map of persistent changes in mu power for Non-BCI Subject 4. Color scale interprets the relative spatial power changes from Training Day One to Training Day Four; the red arrow implies a quantitative decrease in the designated area of the scalp.

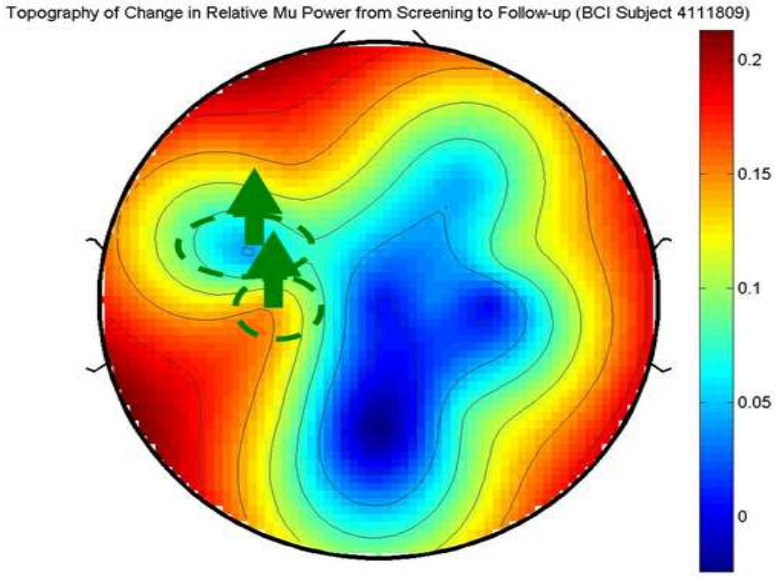

Figure 4.1-29. Topographical map of persistent changes in mu power for Non-BCI Subject 8. Color scale interprets the relative spatial power changes from Training Day One to Training Day Four; the green arrows imply quantitative increases in the designated areas of the scalp.

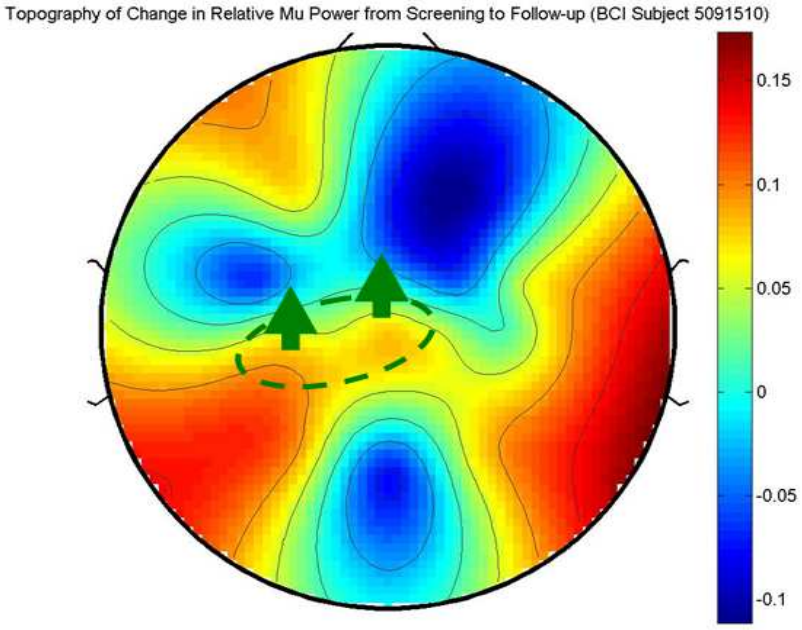

Figure 4.1-30. Topographical map of persistent changes in mu power for Non-BCI Subject 10. Color scale interprets the relative spatial power changes from Training Day One to Training Day Four; the green arrows imply quantitative increases in the designated areas of the scalp.

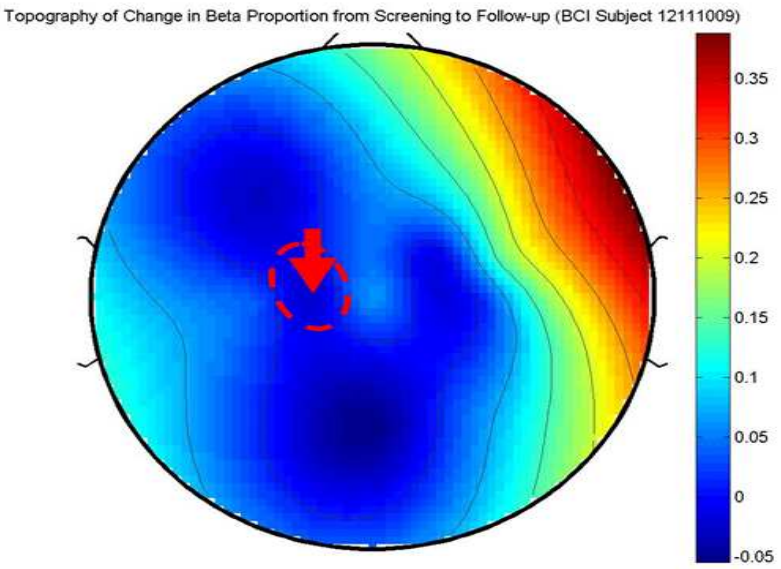

Figure 4.1-31. Topographical map of persistent changes in beta proportion for Non-BCI Subject 6. Color scale interprets the relative spatial proportional changes from Training Day One to Training Day Four; the red arrow implies a quantitative decrease in the designated area of the scalp.

4.1.3. Summary

The results of the plasticity analysis have shown distinctions between the two study groups that might imply some trends particular to each study group in addition to some differences based on different study conditions. Chapter 5 details the results of this analysis and draws conclusions on how this training may have influenced brain plasticity.

4.2. Motor Learning Analysis

To determine whether BCI-robot training had an affect on motor learning, the data extracted during motor learning tasks was divided into three subcategories.

1. Rate of adaptation
2. Total error.
3. Degree of adaptation.

To analyze data for the first two categories, exponential curves modeled all motor learning data to represent each day of assessment either for each individual or for a group mean. Each day of MLA was fitted using non-linear regression with the curve represented in Equation (11). The goodness-of-fit measures for this analysis are outlined in Appendix B.

4.2.1. Rate of Adaptation

As described in Section 3.4.2, the rate of adaptation is the exponent, *b*, extracted from the estimate of Equation (11) for each day of each subject's MLA. Every subject performed five MLAs during the course of this study, four during the week of training and one during the 30-day follow-up session. The distributions of rates of adaptation were separated into each group for each day of assessment (Figures 4.2-1 and 4.2-2). The means of the distributions of the rates of adaptation for the BCI and non-BCI groups were calculated for each day and are plotted in Figure 4.2-3.

Figure 4.2-3 illustrates a significant difference between the BCI group and the Non-BCI group. The rate of adaptation for the Non-BCI group quickly reached its minimum value after the first day of assessment, whereas the rate of adaptation for the BCI group descended less rapidly. Additionally, once the minimum rate of adaptation for the BCI group was reached, the

subsequent increase in the rate of adaptation on Day 30 was much less profound than that of the Non-BCI group.

Figures 4.2-4 and 4.2-5 illustrate the results of the statistical analyses. Multiple-comparisons ANOVA tests showed that when contrasting consecutive days of the distribution of *b* for the BCI group, the means of the distributions decreased significantly (with 95% confidence) from Day One to Days Three and Four; the mean rate of adaptation remains significantly lower at Day 30. The Non-BCI group had an early decrease from Day One to Day Two and that decrease remained consistent through Days Three and Four; however; the decrease in *b* lost significance on Day 30. These results suggest that the reduction in rate of adaptation, *b*, remained consistent in the BCI group and not in the Non-BCI group. Table 4.2-1 lists the results of the statistical comparisons of each day of MLA for each group. All measures were significant with 95% confidence (Bonferroni corrected).

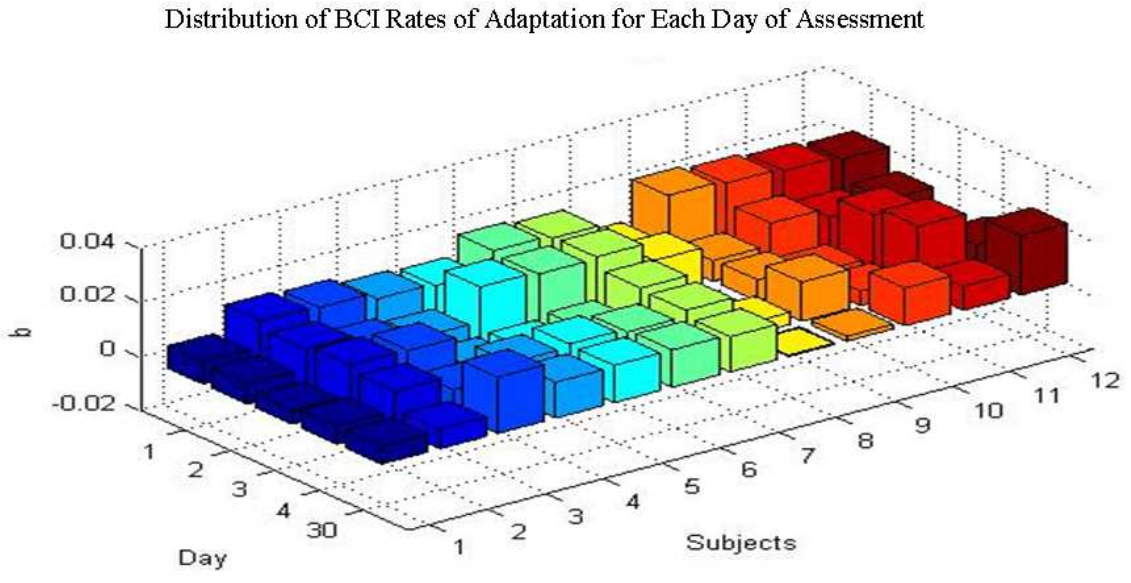

Figure 4.2-1. Distribution of BCI group rates of adaptation, *b*, from Days 1-4 and 30.

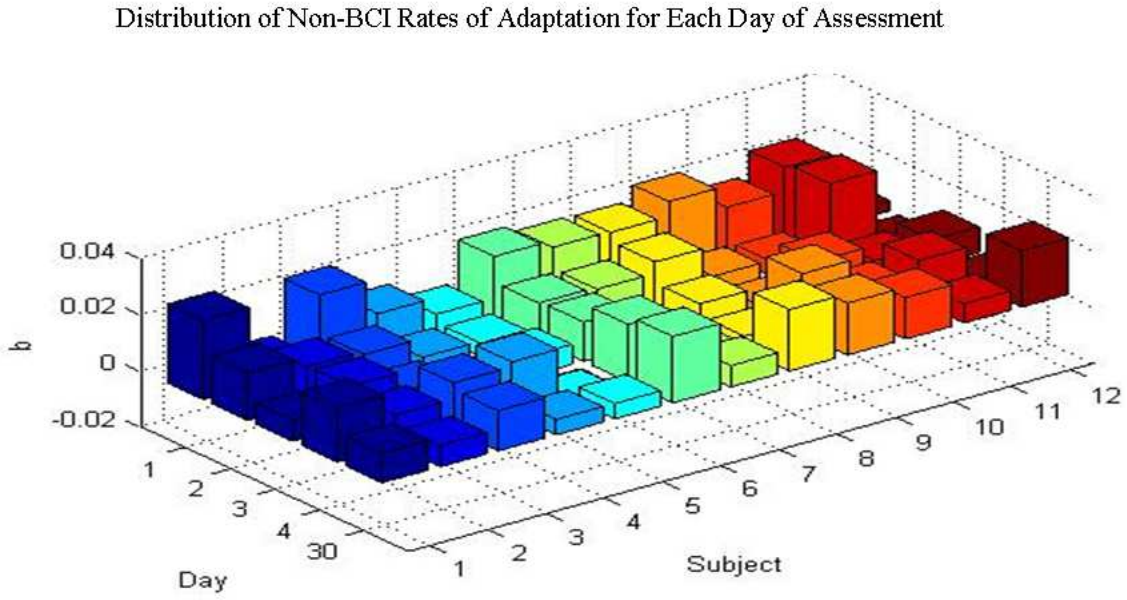

Figure 4.2-2. . Distribution of Non-BCI group rates of adaptation, *b*, from Days 1-4 and 30

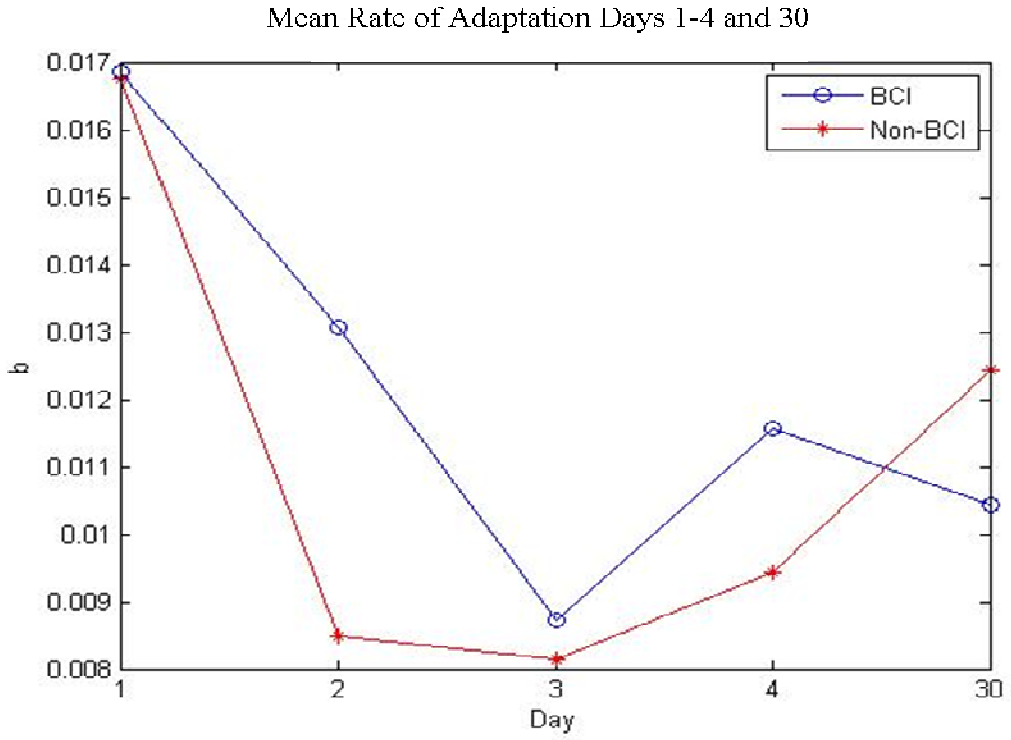

Figure 4.2-3. Mean Rate of Adaptation vs. Day for the BCI group (blue) and the Non-BCI group (red).

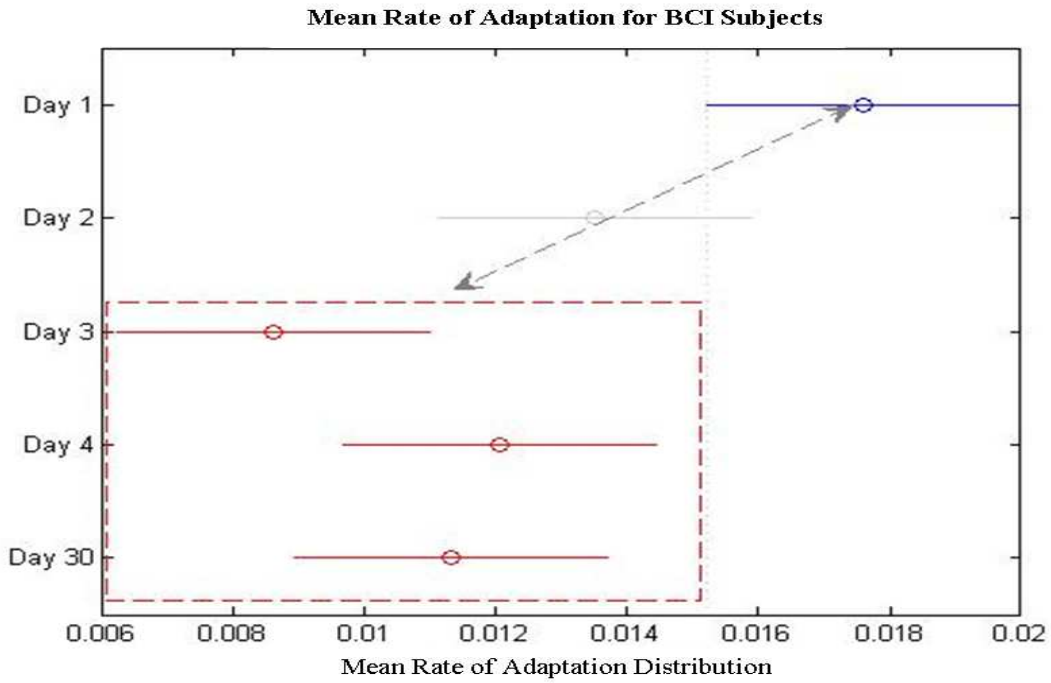

Figure 4.2-4. Comparisons of mean rate of adaptation distributions for the BCI group. Day One is highlighted in blue; significant changes from Day One are highlighted in red (circles represent the mean and lines represent 95% confidence intervals of the mean estimates).

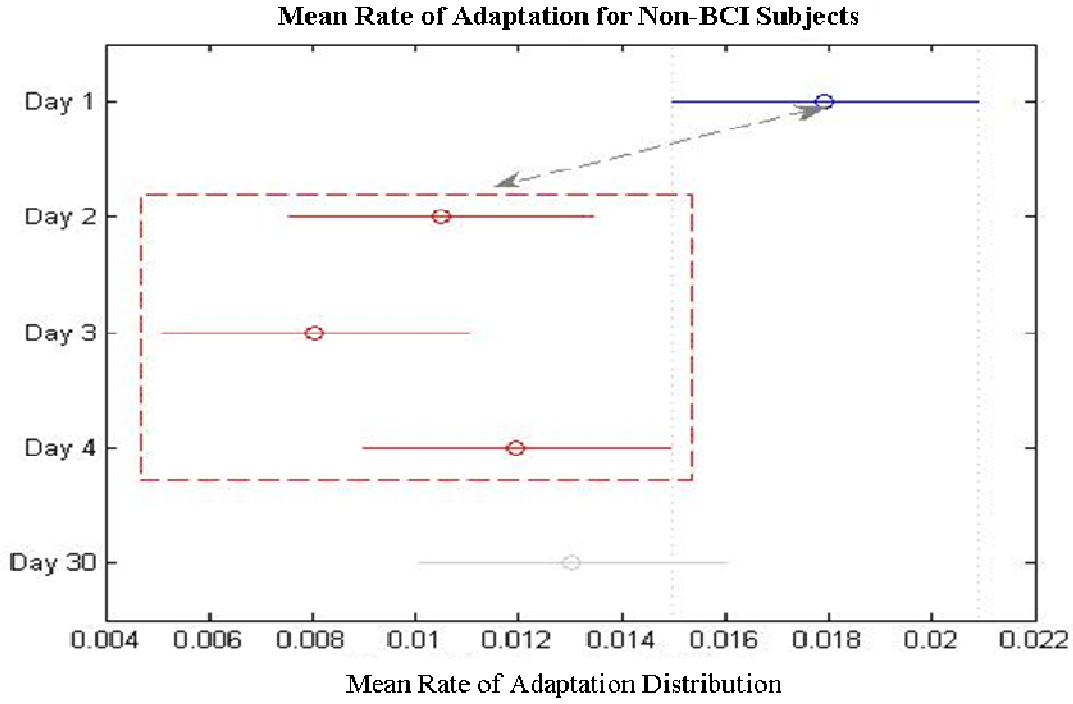

Figure 4.2- 5. Comparisons of mean rate of adaptation distributions for the Non-BCI group. Day One is highlighted in blue; significant changes from Day One are highlighted in red (circles represent the mean and lines represent 95% confidence intervals of the mean estimates).

Table 4.2-1. Confidence Intervals (95%) for ANOVA of Change in Daily Rate of Adaptation (*b*)

Rate of Adaptation (*b*) Comparisons (ANOVA, with Bonferroni Corrections)	BCI		Non-BCI	
	P = 0.0076		P = 0.0239	
	CI		CI	
Day 1 vs. Day 2	-0.007	0.0089	**0.0015**	**0.0134**
Day 1 vs. Day3	**0.0042**	**0.0138**	**0.0039**	**0.0158**
Day 1 vs. Day 4	**0.0008**	**0.0103**	**0.0000**	**0.0119**
Day 1 vs. Day 30	**0.0015**	**0.0111**	-0.0010	0.0108

In most motor learning protocols, the rate of adaptation generally reduces over time because of plateau effects [114, 127]. Humans have physiological limitations; therefore, practice will become less influenced by the rate of adaptation over time. This results in a reduction of rate of adaptation as a subject practices more. In this investigation, the BCI group demonstrated a slower decrease in rate of adaptation and a significant residual effect of that decrease after several weeks. These results might suggest that BCI training slowed the loss of influence of practice on the rate of adaptation. BCI training, therefore, increased the amount of time in which a subject benefited from practice. The next section presents data that furthers supports these findings.

4.2.2. Total Error

Estimated Learning Error

Total Error was calculated for two separate phases of each day MLA. The first phase, the learning phase, was calculated as an estimation of how subjects performed at the beginning of the daily MLA. These measures, which gave an estimate of how well subjects predicted the task, were calculated as the integration of the estimated exponential curve during the first 55 reaches

(the approximate half life of the exponential curve). Figures 4.2-6 and 4.2-7 illustrate the mean exponential curves for Day One through Day 30 for the BCI group and Non-BCI group respectively. The highlighted areas of each illustration show the location of where estimate of total learning error was calculated for Day One (top) and Day 30 (bottom).

The estimations of each day of total learning error were calculated for each subject within each group. ANOVA multiple comparison tests contrasted the within-group changes in total learning error for each day of assessment. Figures 4.2-10 nd 4.2-11 illustrate the comparisons of the within-group estimated total learning errors for the BCI and Non-BCI groups respectively.

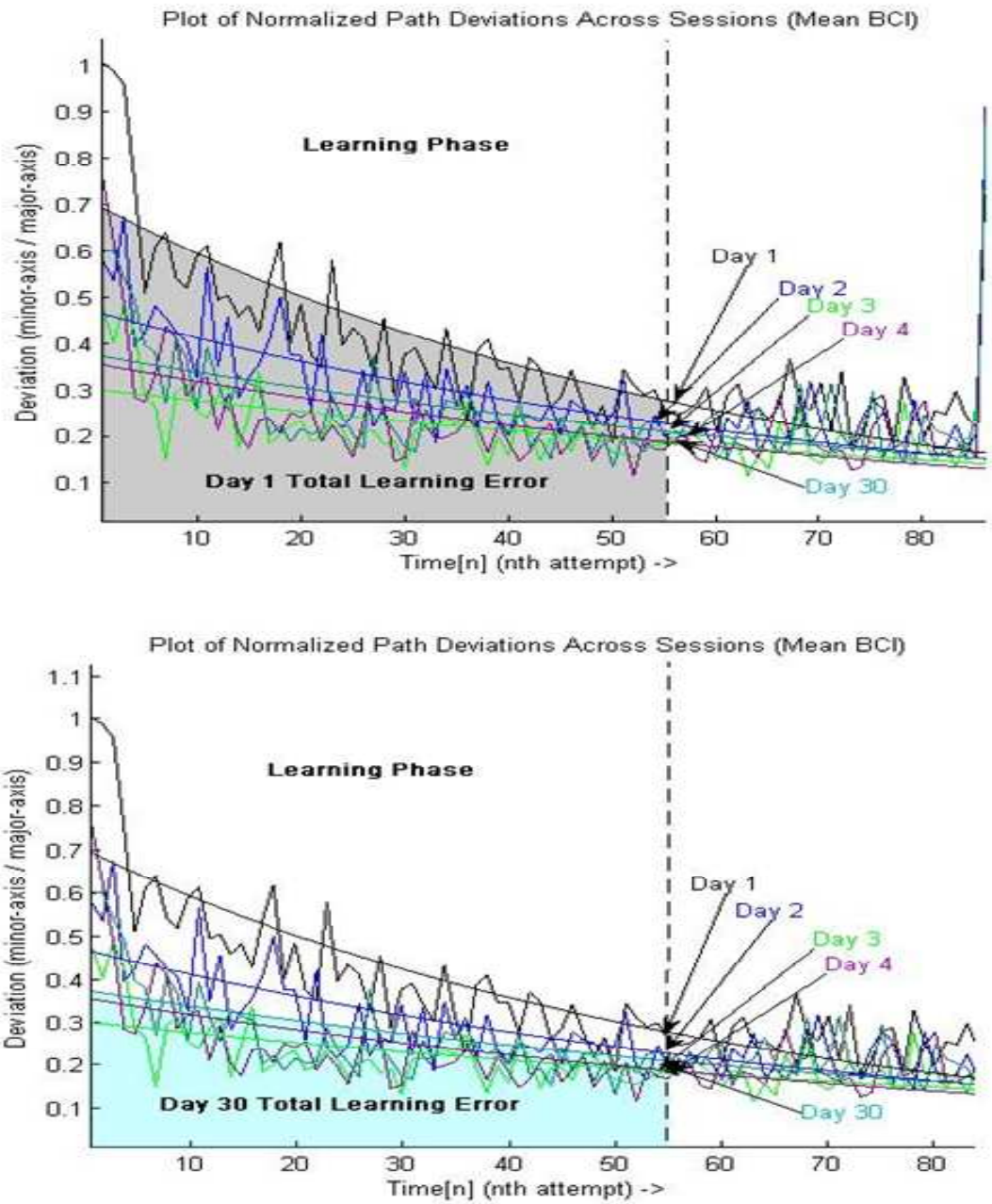

Figure 4.2-6. Mean BCI group path deviations. Shaded areas show location of estimated total learning errors (integral) for Day One (top) and Day 30 (bottom).

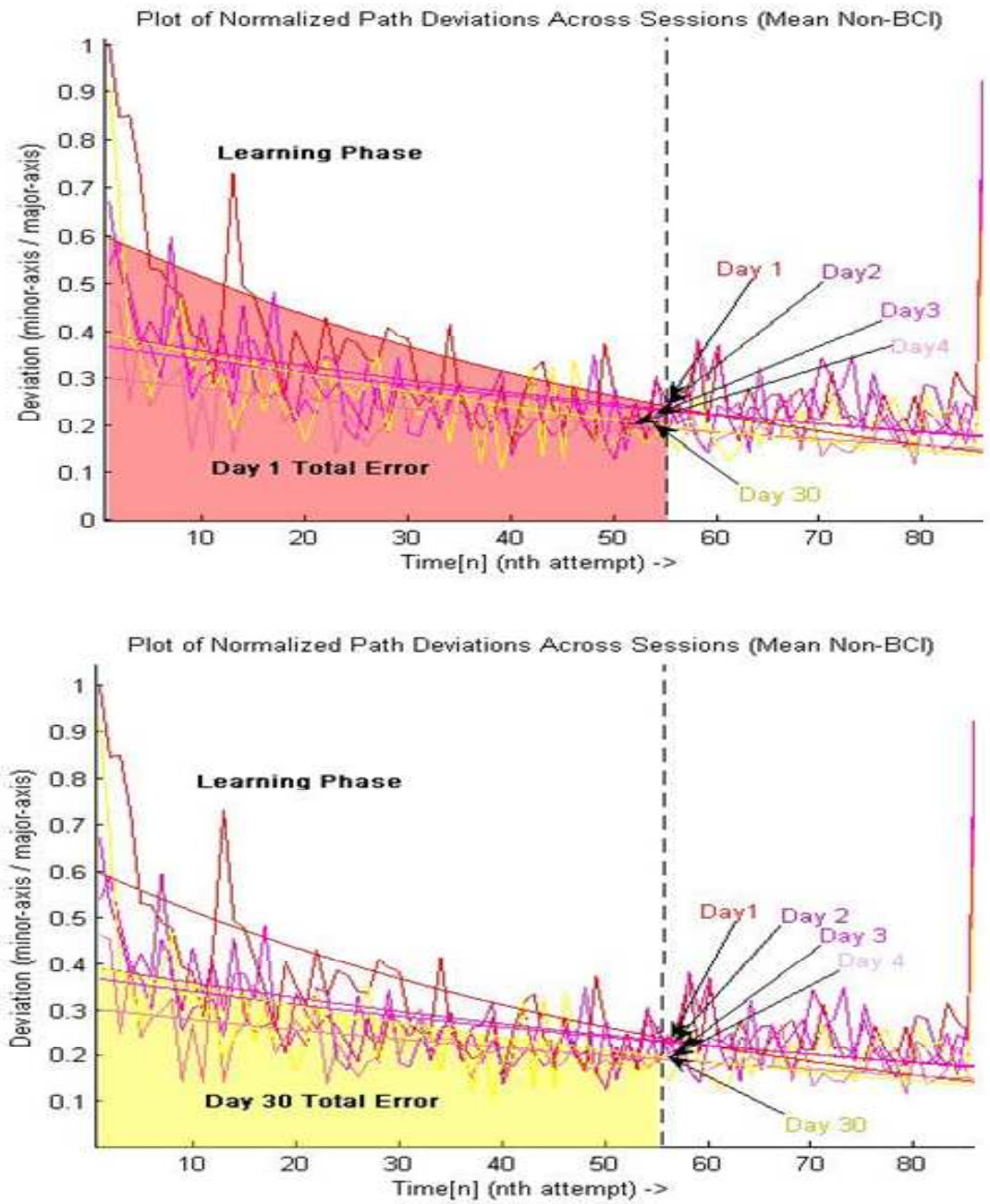

Figure 4.2-7. Mean Non-BCI group path deviations. Shaded areas show location of estimated total learning errors (integral) for Day One (top) and Day 30 (bottom).

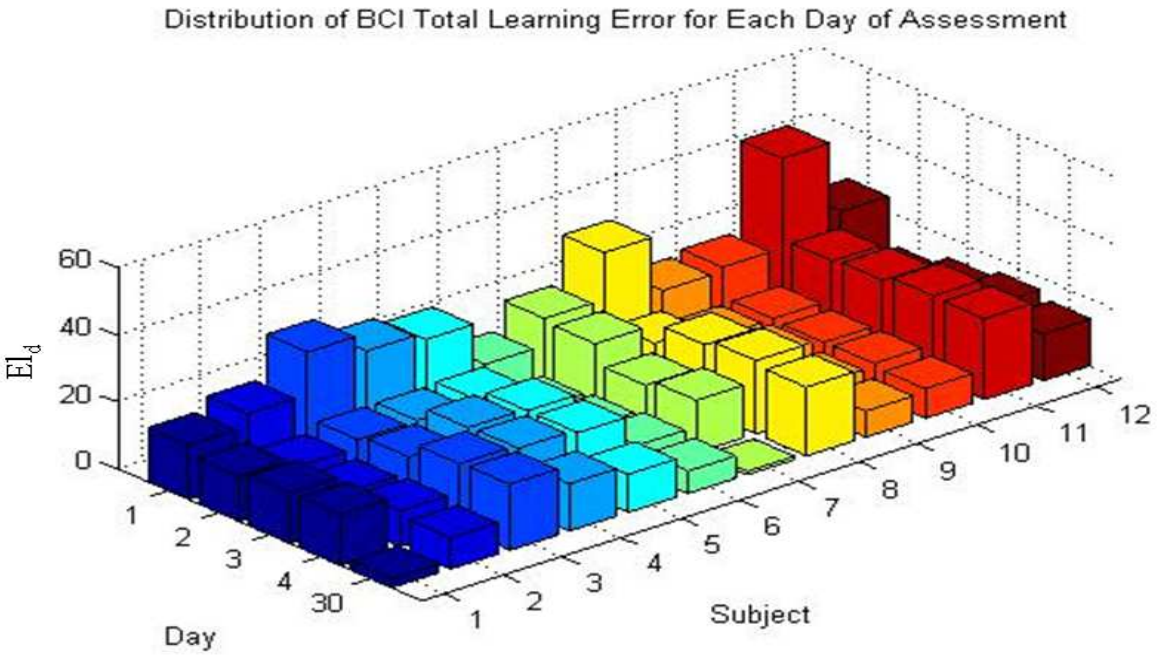

Figure 4.2-8. Distribution of BCI group total learning error, El_d, from Days 1-4 and 30.

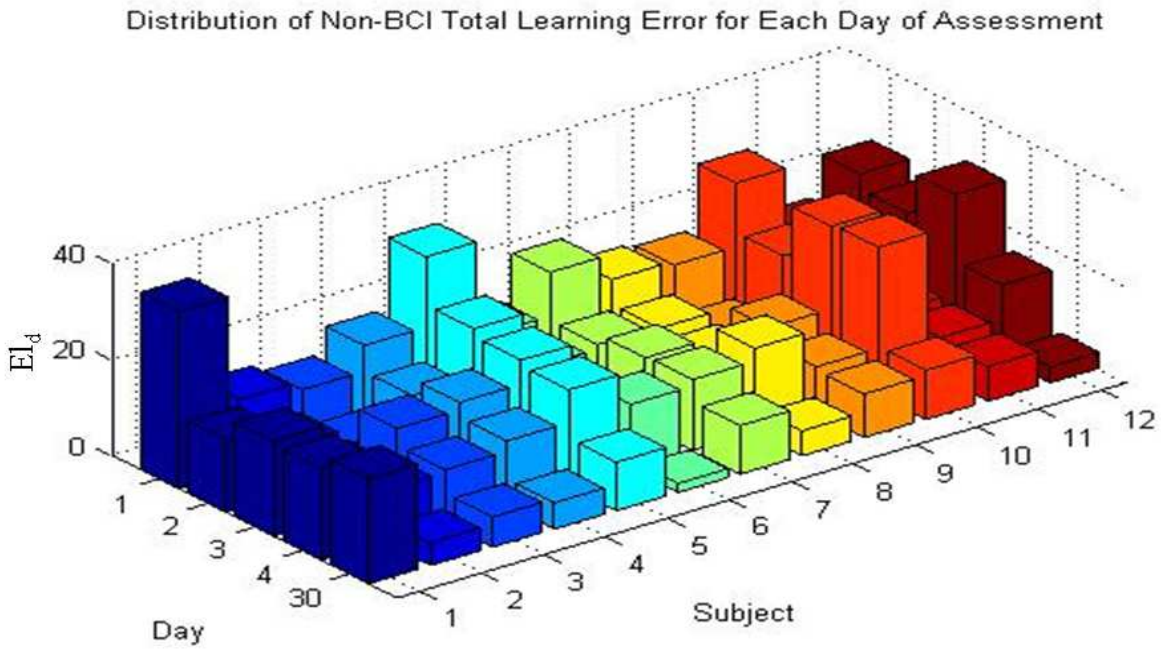

Figure 4.2-9. Distribution of Non-BCI group total learning error, El_d, from Days 1-4 and 30.

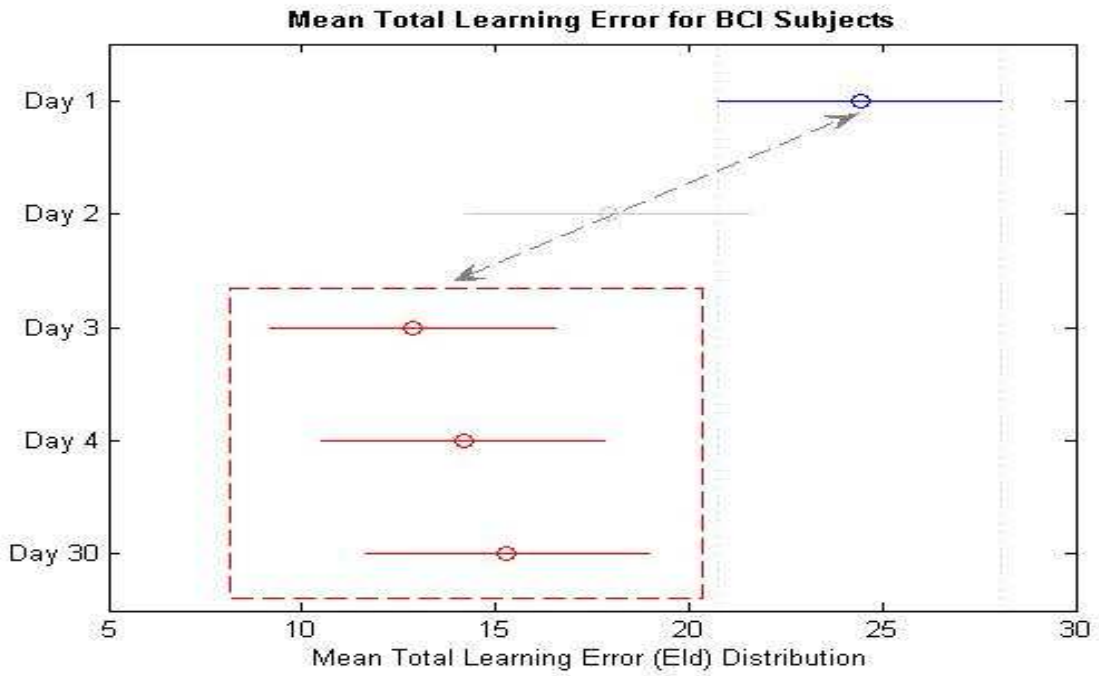

Figure 4.2-10. Multiple-comparisons ANOVA test of mean estimated total learning error distribution of the BCI group. Day One is highlighted blue; days with significant decreases in total learning error are highlight red (Days Three, Four and 30). Note: Circles represent the mean and lines represent 95% confidence intervals of the mean estimates.

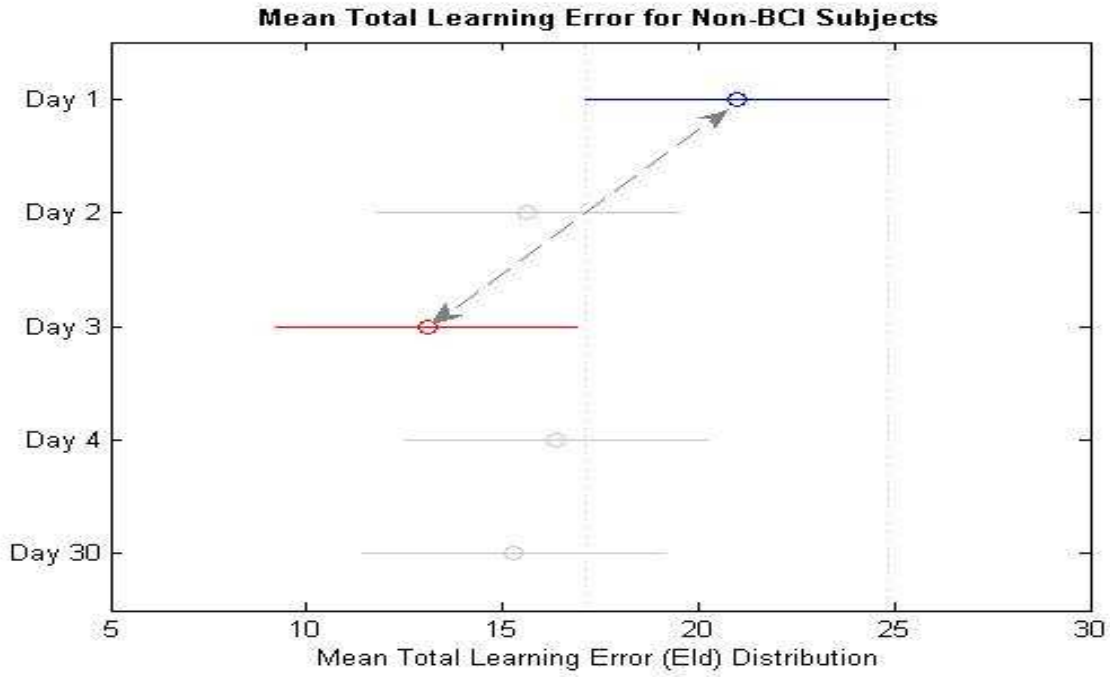

Figure 4.2-11. Muliple-comparisons ANOVA test of mean estimated total learning error distribution of the Non-BCI group. Day One is highlighted blue; Day three (the only day of significant decrease in total error) is highlighted red. Note: Circles represent the mean and lines represent 95% confidence intervals of the mean estimates.

As is illustrated above, the BCI group clearly achieved and sustained significant decreases in total learning error during training and on the 30-day follow-up. The Non-BCI group, on the other hand, only achieved a significant reduction in error on Day Three of assessment and afterward began to lose the overall learning effect. It should be noted that both groups followed the same trend of achieving the greatest reduction in error on Day Three of assessment. The increase in total error on Day Four was likely due to the workload of that day; there might have been a fatigue factor due to the fact that all subjects had an added EEG task on the last day of training. Table 4.2-2 lists the confidence intervals of the within-group statistical comparisons.

Table 4.2-2. Confidence Intervals (95%) for ANOVA of Change in Eld

Total Learning Error (El_d) Tests (ANOVA, with Bonferroni Corrections)	BCI		Non-BCI	
	P = 0.0002		P = 0.0585	
	CI		CI	
Day 1 vs. Day 2	-0.8166	13.8352	-2.3807	13.0249
Day 1 vs. Day3	**4.2503**	**18.9022**	**0.1937**	**15.5994**
Day 1 vs. Day 4	**2.9377**	**17.5896**	-3.1191	12.2865
Day 1 vs. Day 30	**1.8040**	**16.4559**	-2.9994	13.3962

Ratio of Reduction of Learning Error Between-group Comparison

When looking at the contrasts between the two study groups, the ratio of the decrease in total learning error and Day One of assessment had significant disparities. For each day of assessment, the BCI group had larger reductions in total error and, thus, greater increases in the reduction ratio, $D_{Eld,}$ in comparison to the Non-BCI group (Figure 4.2-12). Most notably, the ratio of the reduction in learning error for Day Four of the BCI group was statically significantly greater than that of the Non-BCI group (Table 4.2-3). This suggests that the reduction in

learning error experienced by the BCI group by the end of training was more significant in comparison to the Non-BCI group. The results of this comparison may suggest that the BCI group had a better ability to predict the resistance of the MLA task, thus preceding the Non-BCI group in adapting to the task [122].

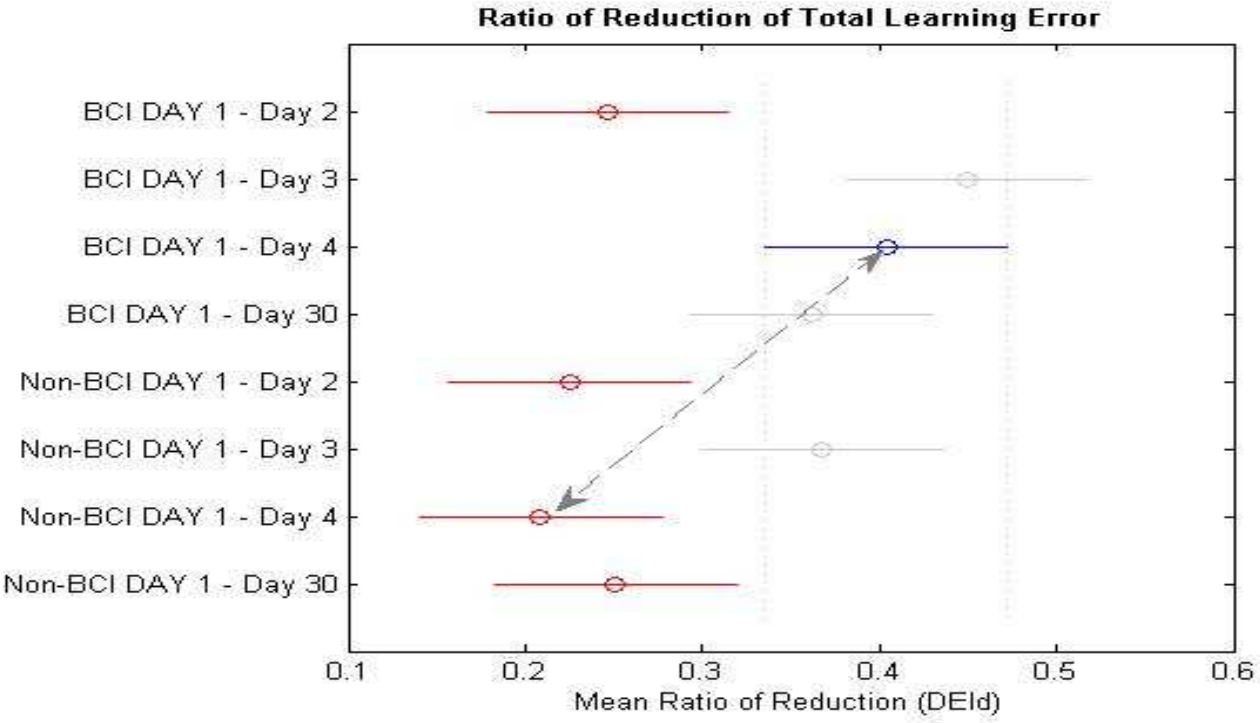

Figure 4.2-12. Multiple-comparisons ANOVA test of mean ratio of reduction of learning error (D_{Eld}) for BCI and Non-BCI groups. The grey line highlights a significant difference between Day 4 of BCI and Day 4 of Non-BCI.

Table 4.2-3. Confidence Intervals (95%) for ANOVA of D_{Eld}

Ratio of Reduction in Learning Error (D_{Eld}) Tests (ANOVA with Bonferroni Correction)	BCI vs. Non-BCI	
	P = 0.0041, F = 8.78	
	CI	
BCI Day 2 vs. Non-BCI Day 2	-0.1145	0.1577
BCI Day 3vs. Non-BCI Day 3	-0.0546	0.2176
BCI Day 4 vs. Non-BCI Day 4	**0.0592**	**0.3314**
BCI Day 5 vs. Non-BCI Day 5	-0.0254	0.2468

Estimated Adapted Error

The total adapted error estimated the amount of error produced by each subject during the latter part of each daily MLA (reaches 60 through 85). Figures 4.2-13 and 4.2-14 illustrate the mean exponential curves for Day One through Day 30 for the BCI group and Non-BCI group respectively. The highlighted areas of each illustration show the location of where estimate of total adapted error was calculated for Day One (top) and Day 30 (bottom).

The estimations of each day of total adapted error were calculated for each subject within each group (Figures 4.2-15 and 4.2-16). Multiple-comparisons ANOVA tests contrasted the within-group changes in total adapted error for each day of assessment. Figures 4.2-17 and 4.2-18 illustrate the comparisons of the within-group estimated total adapted errors for the BCI and Non-BCI groups respectively.

As is illustrated in Figures 4.2-17and 4.2-18 the changes in total adapted error are much less profound than in the total learning error; however, there is still a noticeably larger reduction of the adapted error in the BCI group than in the Non-BCI group.

Ratio of Reduction of Adapted Error Between-group Comparison

The between-group comparison of the ratio of reduction of total adapted error, D_{Ead}, follows a similar trend as that of the total learning error, D_{Eld}. Figure 4.2.2-14 demonstrates, once again, that the BCI group has greater relative reductions in D_{Ead} from Day 2 to Day 30. While not demonstrating statistical significance, Figure 4.2-19illustrates a Bonferroni corrected multiple comparisons ANOVA with 95% confidence interval. Bonferroni corrections tend to make conservative adjustments to the α level when determining the confidence intervals for statistical tests, therefore, α may be overcorrected in this case considering the F-tests produced a relatively

large F-statistic (9.01) [128-130]. Figure 4.2-20 shows a multiple-comparisons ANOVA test with a least significant difference calculation of confidence intervals. The analysis illustrated in Figure 4.2-20 shows that the BCI group has more significant reductions in total adapted error at the end of training just as was demonstrated for total learning error.

Overall, the BCI group had more significant changes in total error during the learning phase and adapted phase of motor learning error assessment. The pronounced differences between the BCI group and the Non-BCI provide support to the analysis in Section 4.2.1 that suggests that the BCI group had benefitted from a higher rate of adaptation for a longer period of time. The next section further demonstrates the distinctions between the BCI and Non-BCI groups.

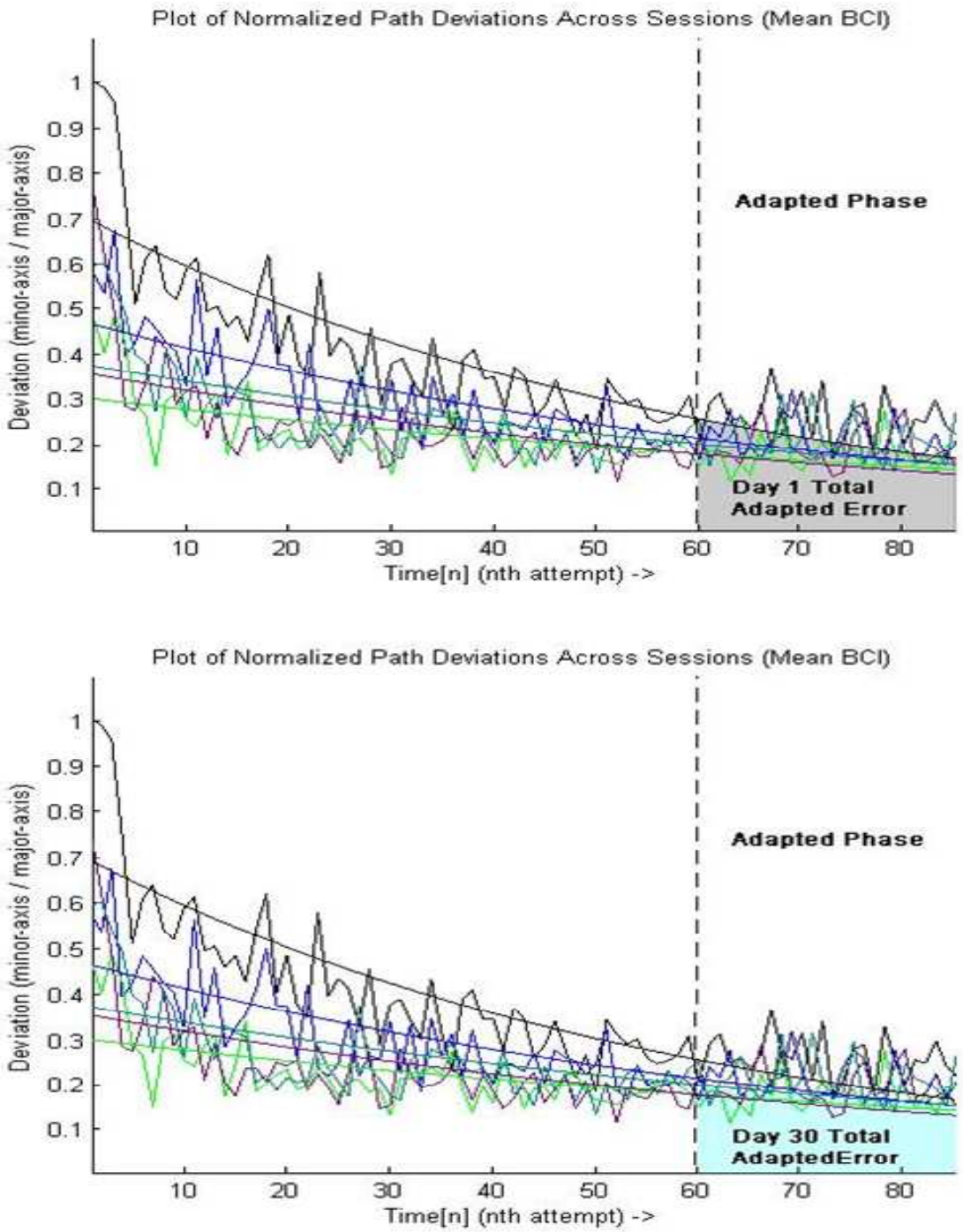

Figure 4.2-13. Mean BCI group path deviations. Shaded areas show location of estimated total adapted errors for Day One (top) and Day 30 (bottom).

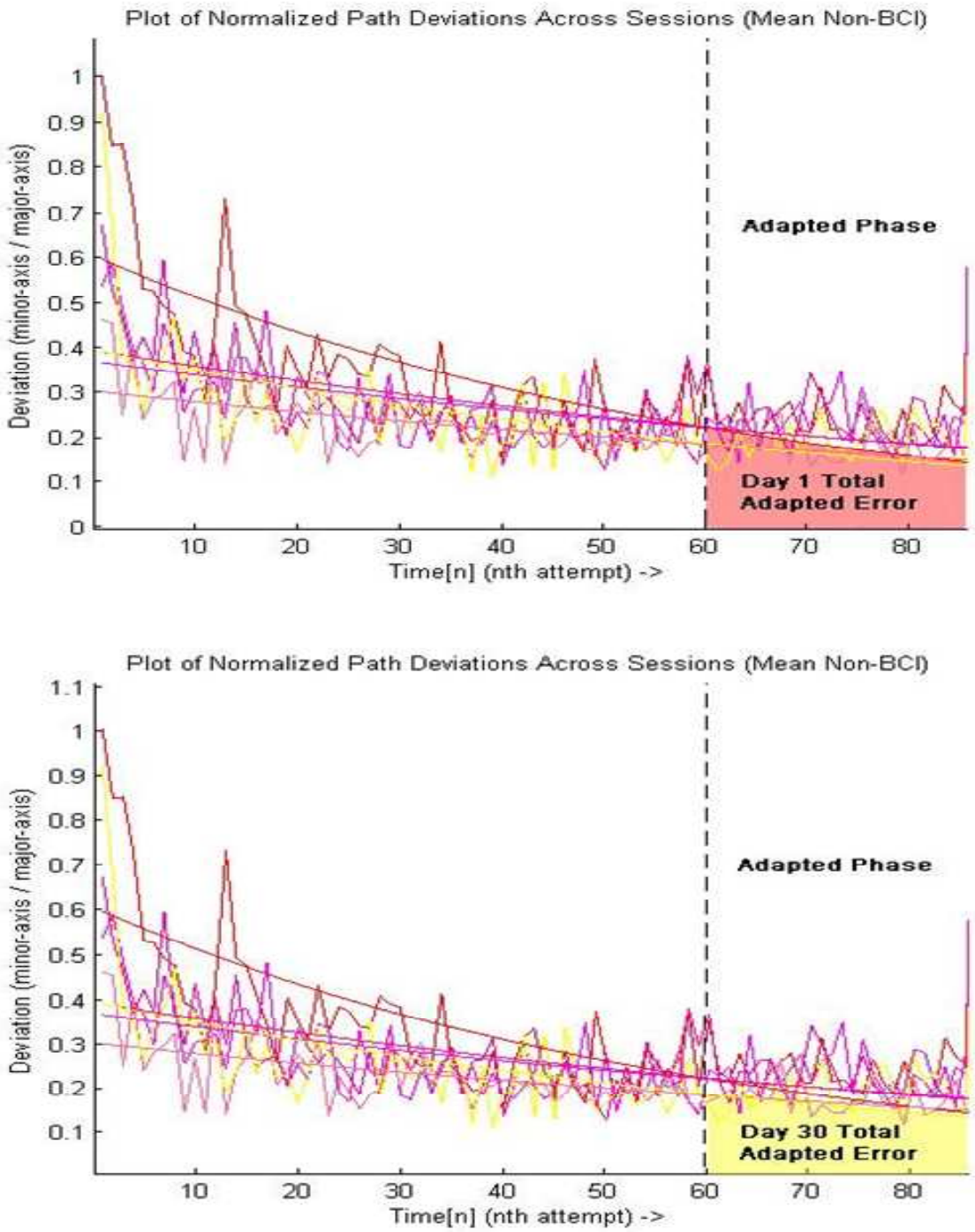

Figure 4.2-14. Mean Non-BCI group path deviations. Shaded areas show location of estimated total learning errors for Day One (top) and Day 30 (bottom).

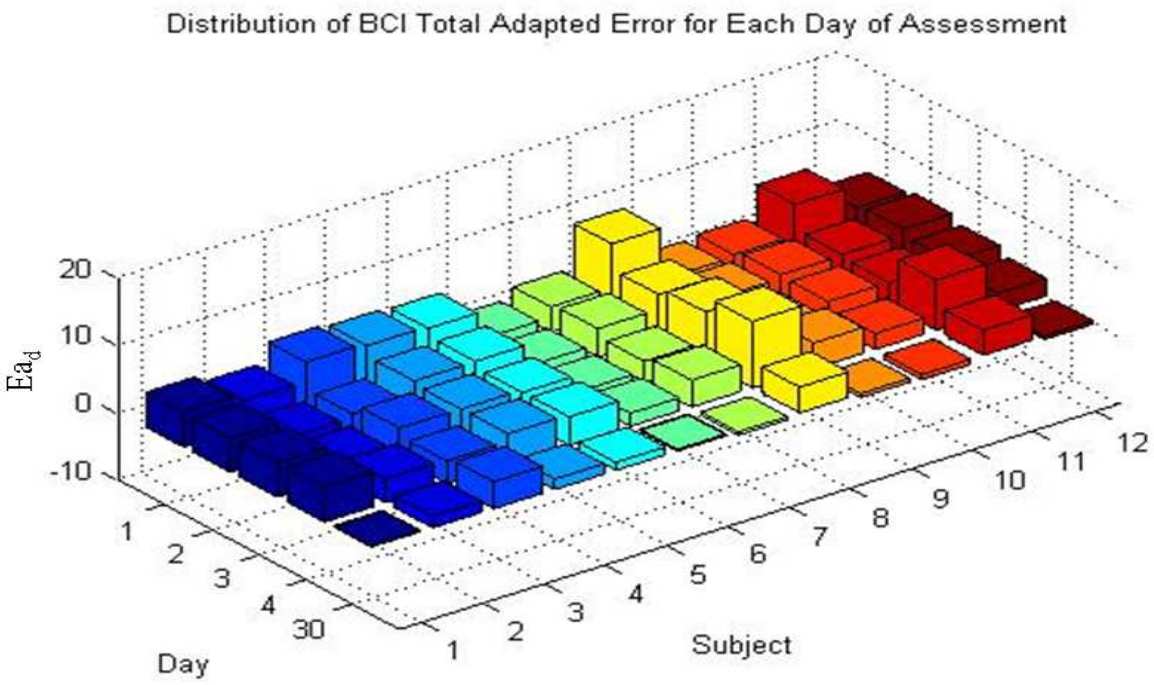

Figure 4.2-15. Distribution of BCI group total adapted error, Ea_d, from Days 1-4 and 30.

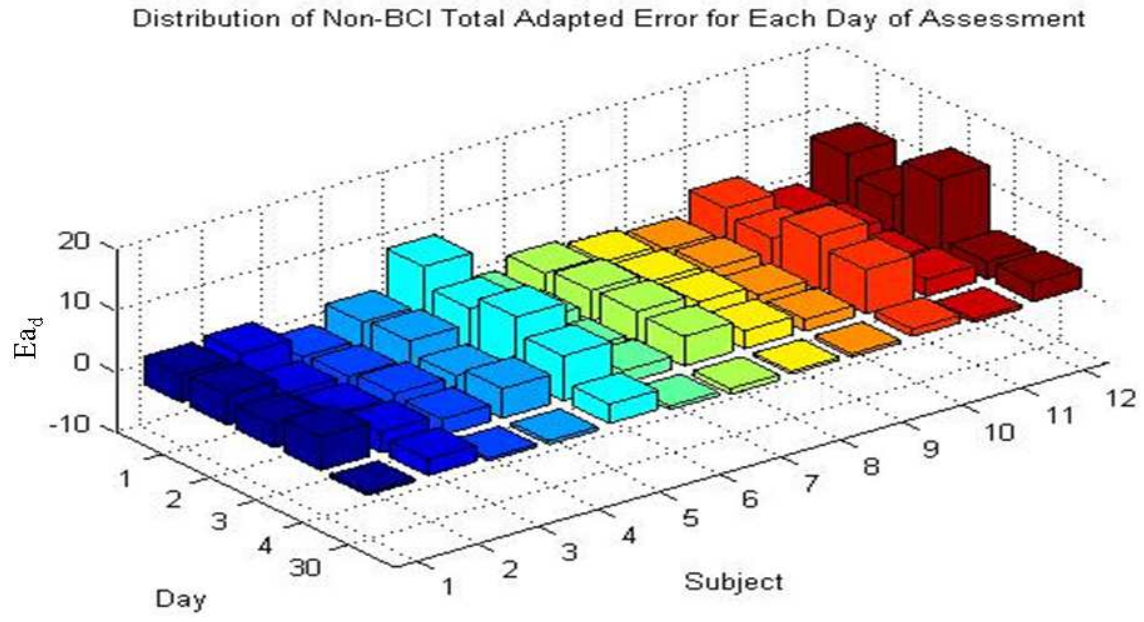

Figure 4.2-16. Distribution of Non-BCI group total adapted error, Ea_d, from Days 1-4 and 30.

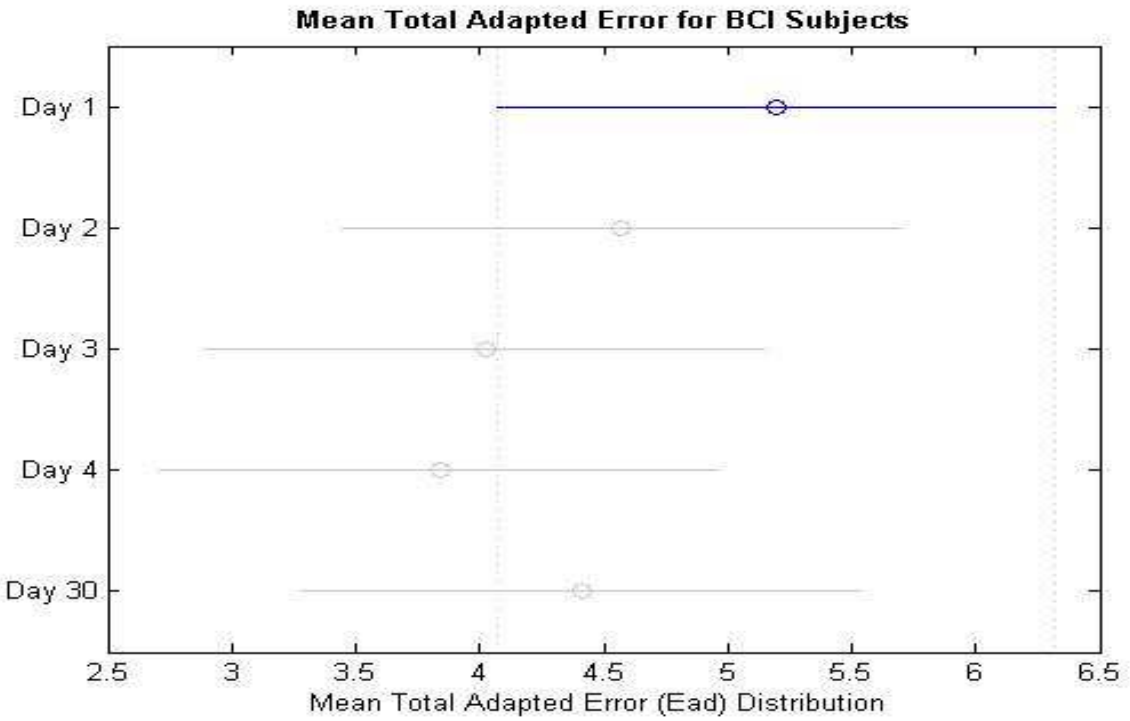

Figure 4.2-17. Multiple-comparisons ANOVA test of mean estimated total adapted error distributions for the BCI group (circles represent the mean and lines represent 95% confidence intervals of the mean estimates).

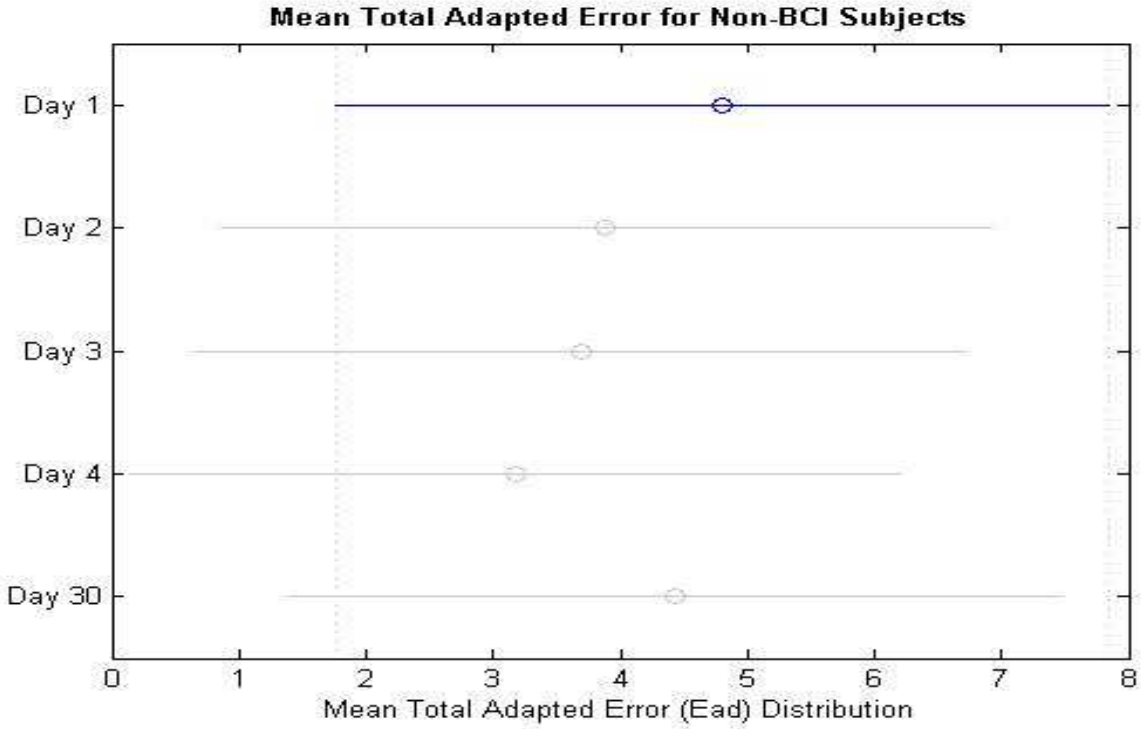

Figure 4.2-18. Multiple-comparisons ANOVA test of mean estimated total adapted error distributions for the Non-BCI group (circles represent the mean and lines represent 95% confidence intervals of the mean estimates).

Table 4.2-4. Confidence Intervals (95%) for ANOVA of Change in Ead

Total Adapted Error (Ea_d) Tests (ANOVA, with Bonferroni Corrections)	BCI		Non-BCI	
	P = 0.4412		P = 0.0585	
	CI		CI	
Day 1 vs. Day 2	-0.9221	2.1699	-5.1601	6.9924
Day 1 vs. Day3	-0.3713	2.7206	-4.9604	7.1921
Day 1 vs. Day 4	-0.1890	2.9029	-4.4438	7.7088
Day 1 vs. Day 30	-0.7577	2.3343	-5.7004	6.4521

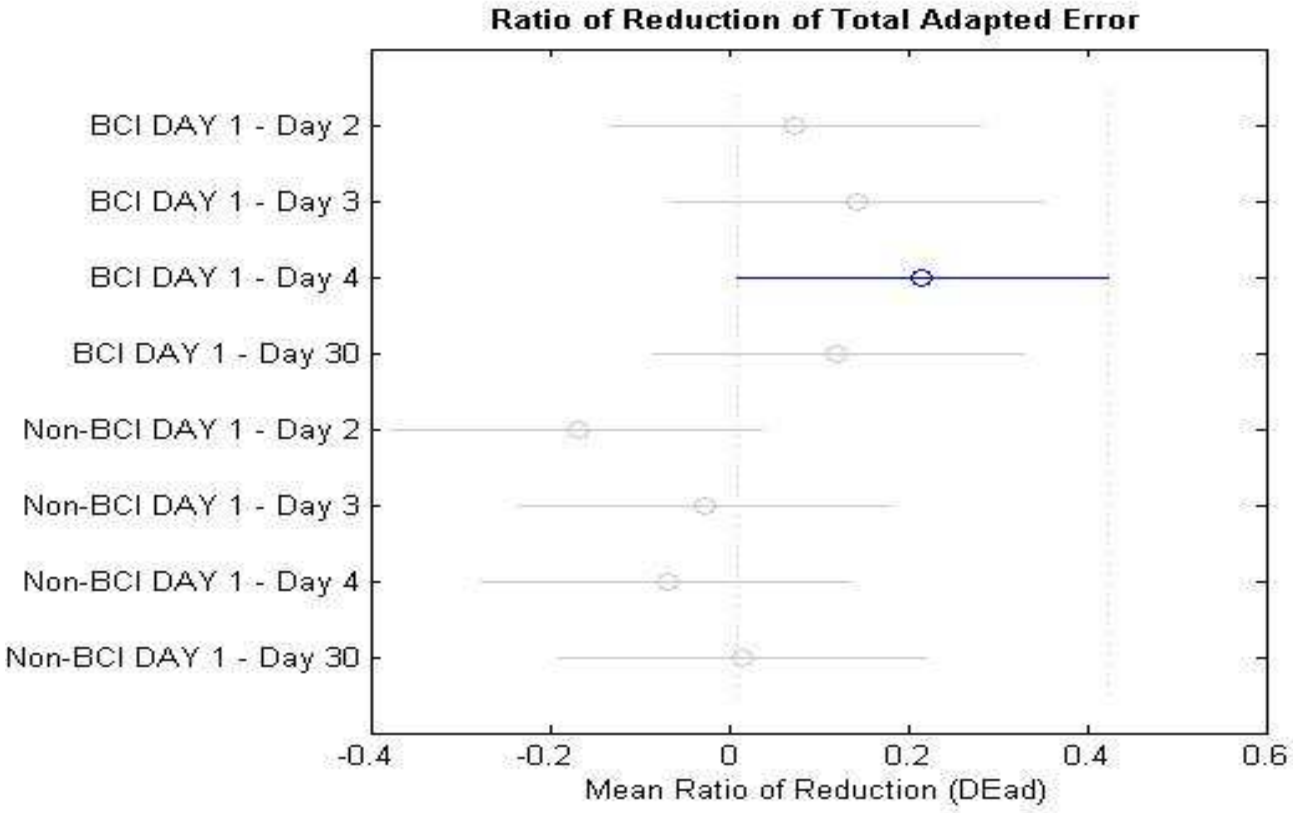

Figure 4.2-19. Multiple-comparisons ANOVA test of mean ratio of reduction of adapted error (D_{Ead}) for BCI and Non-BCI groups with Bonferroni correction.

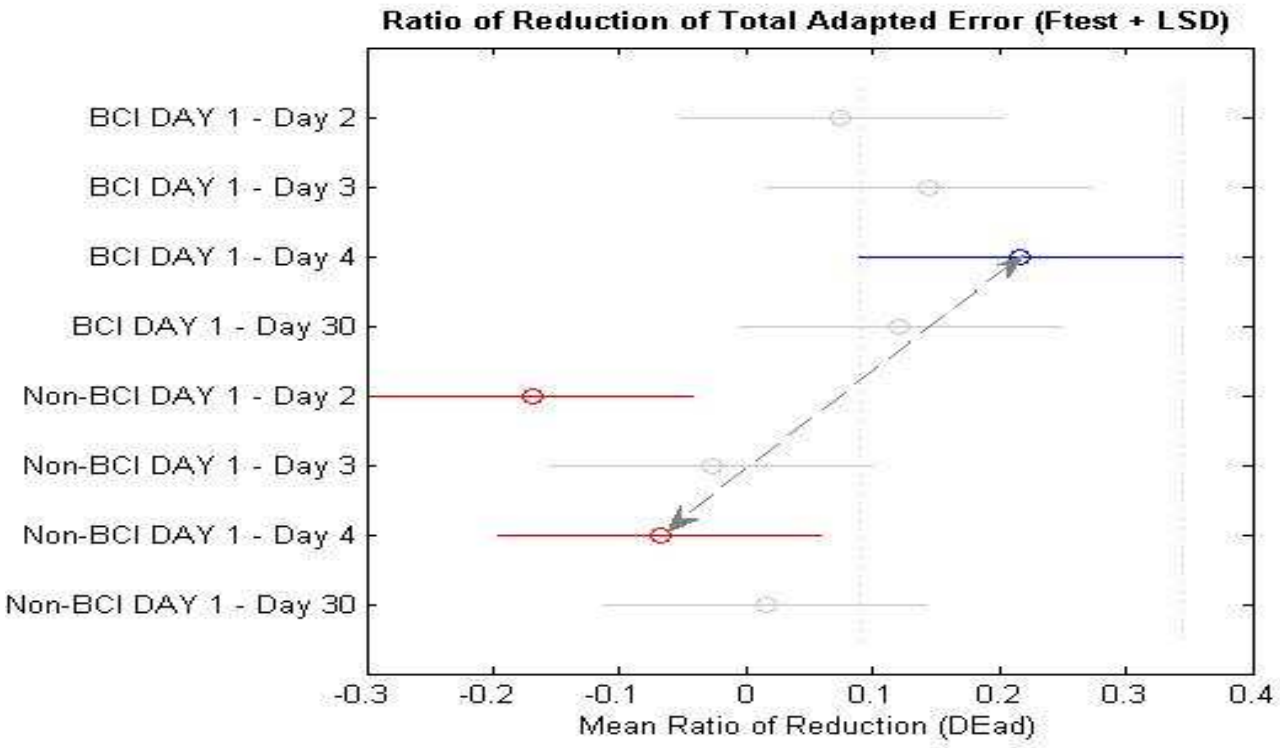

Figure 4.2-20. Multiple-comparisons ANOVA of mean ratio of reduction of adapted error (D_{Ead}) for BCI and Non-BCI groups F-test and least significant differences comparisons. The grey line highlights a significant difference between Day 4 of BCI and Day 4 of Non-BCI.

Table 4.2-5. Confidence Intervals (95%) for ANOVA of D_{Ead}

Ratio of Reduction in Adapted Error (D_{Ead}) Tests (ANOVA F-Test with LSD)	BCI vs. Non-BCI	
	P = 0.0037 , F = 9.01	
	CI	
BCI Day 2 vs. Non-BCI Day 2	-0.0110	0.4987
BCI Day 3vs. Non-BCI Day 3	-0.0833	0.4264
BCI Day 4 vs. Non-BCI Day 4	**0.0302**	**0.5399**
BCI Day 5 vs. Non-BCI Day 5	-0.1487	0.3610

4.2.3. Degree of Adaptation (Catch Trial Analysis)

The degree of adaptation estimated how well subjects conformed to the task. This measure incorporated the motor catch trials, a common motor learning test. As mentioned in Section **3.4.2**, after performing several loaded reaching tasks, subjects are expected to overcompensate significantly when the load is removed. The amount of overcompensation estimates the degree to which a subject has adapted.

The degree of adaptation, Ec_d, measured the normalized difference between the average path deviation produced during the first catch trial and the average value of the total adapted error (Equation (15)) on each day. The distribution of the degrees of adaptation for each group are illustrated in Figures 4.2-21 and 4.2-22. Figure 4.2-23 illustrates the mean degree of adaptation for each group to show the group trends.

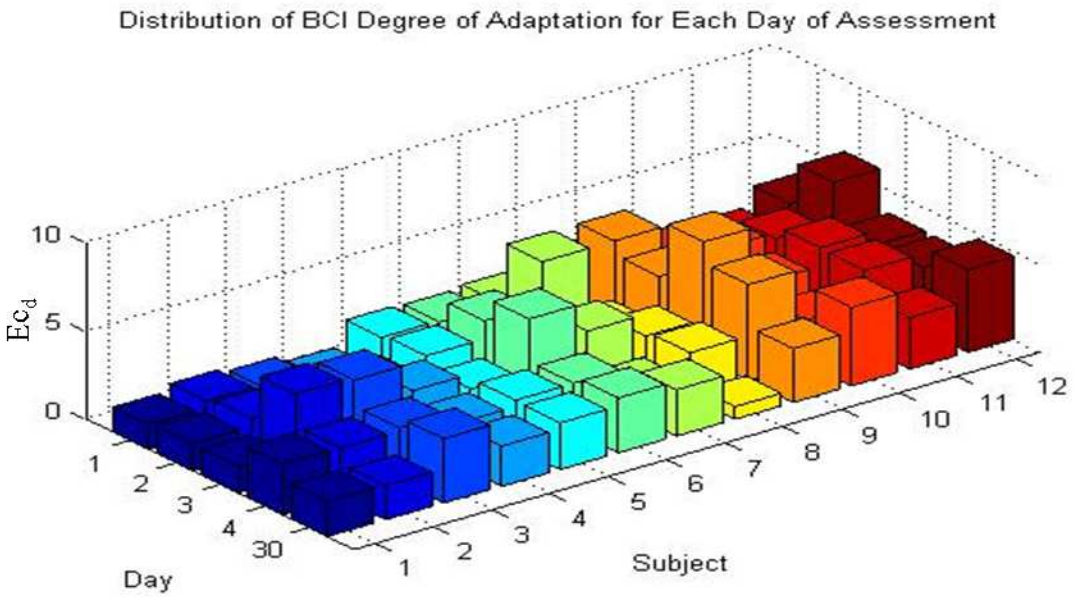

Figure 4.2-21. Distribution of BCI group degree of adaptation, Ec_d, from Days 1-4 and 30.

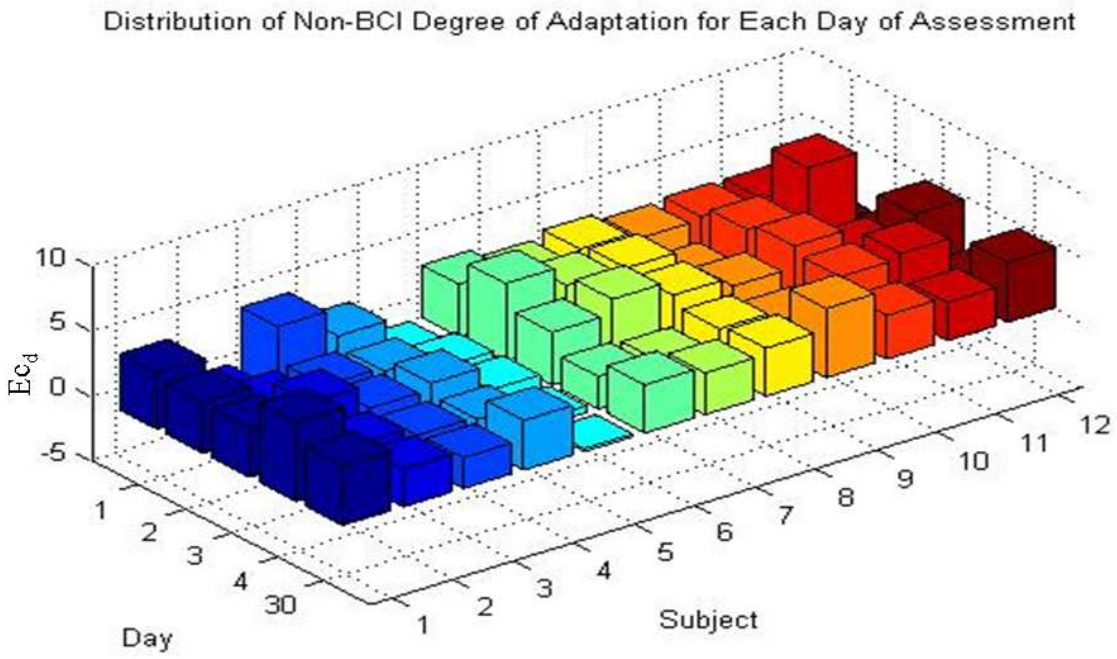

Figure 4.2-22. Distribution of Non-BCI group degree of adaptation, Ec_d, from Days 1-4 and 30.

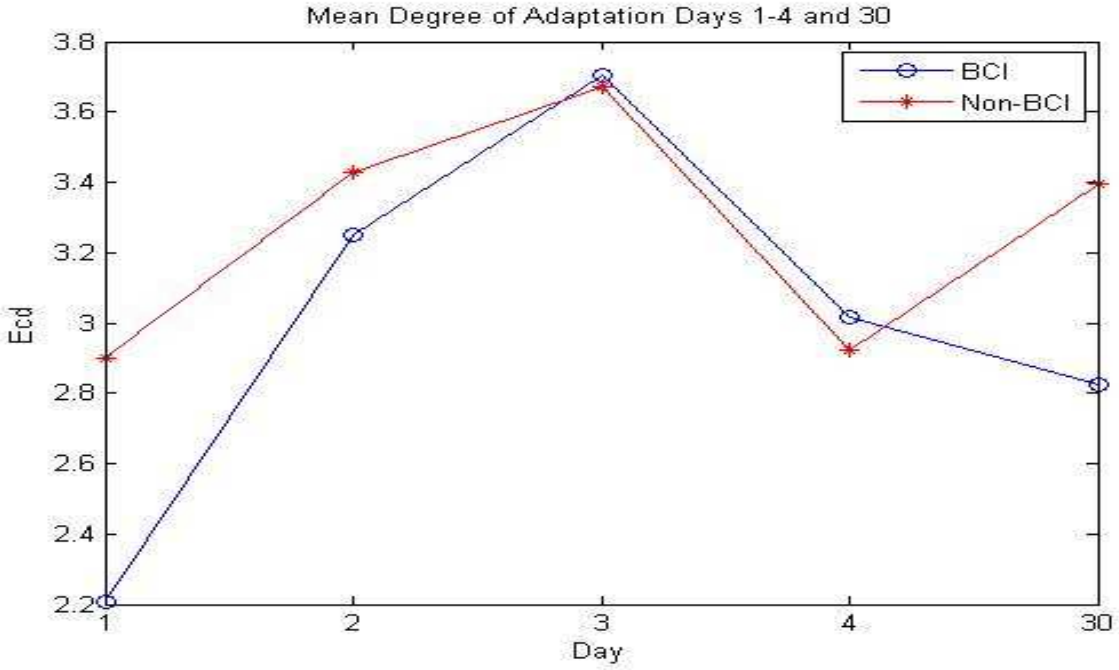

Figure 4.2-23. Contrast of mean degree of adaptation per day of the BCI group and the Non-BCI group.

Multiple-comparisons ANOVA determined whether statistically significant changes of the degree of adaptation, Ec_d, occurred within each study group. Figures 4.2-24 and 4.2-25 illustrate the distributions of the ANOVA tests for the BCI group and the Non-BCI group respectively. Figures 4.2-23, 4.2-24 and 4.2-25 all illustrate that the BCI group, while starting at a lower degree of adaptation, increased its average degree of adaptation significantly on Day Two and Day Three. The Non-BCI group, on the other hand, showed no significant changes between Day One and any other day of assessment. Table 4.2-6 contains the 95% confidence intervals for each within-group test of the change in degree of adaptation. Between-group tests showed no significant differences and, therefore, are not illustrated.

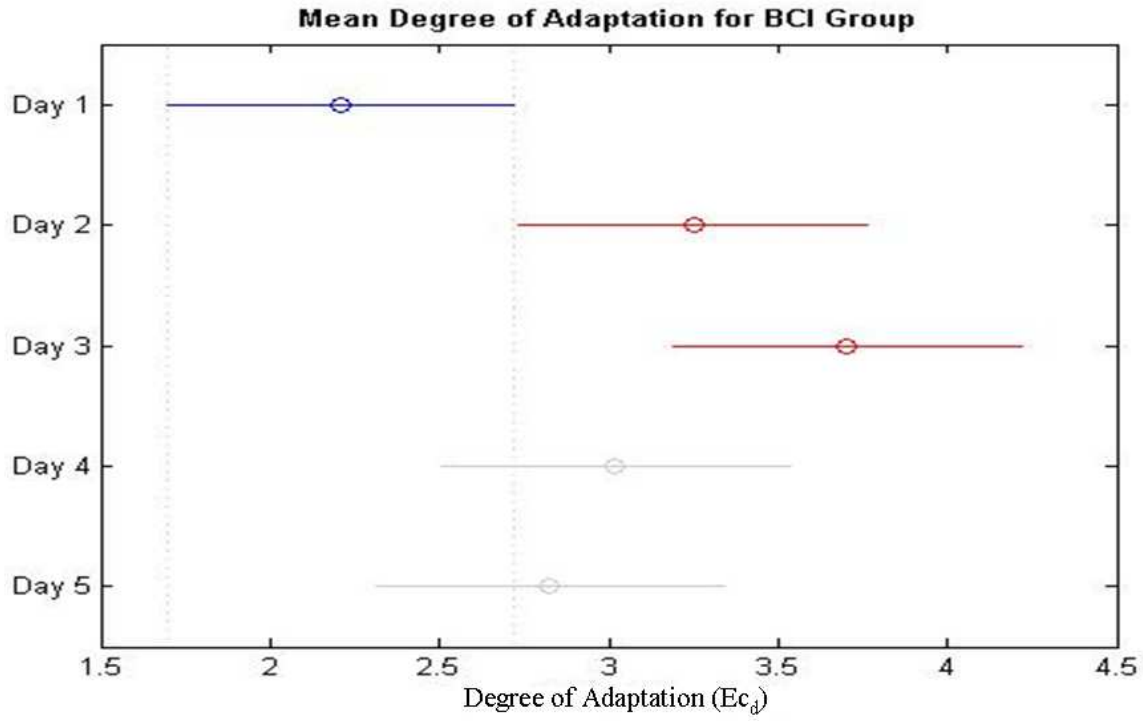

Figure 4.2-24. Multiple-comparisons ANOVA of mean degree of adaptation (Ec_d) for the BCI group. The grey line highlights a significant increase between Day 1 and Days 2 and 3.

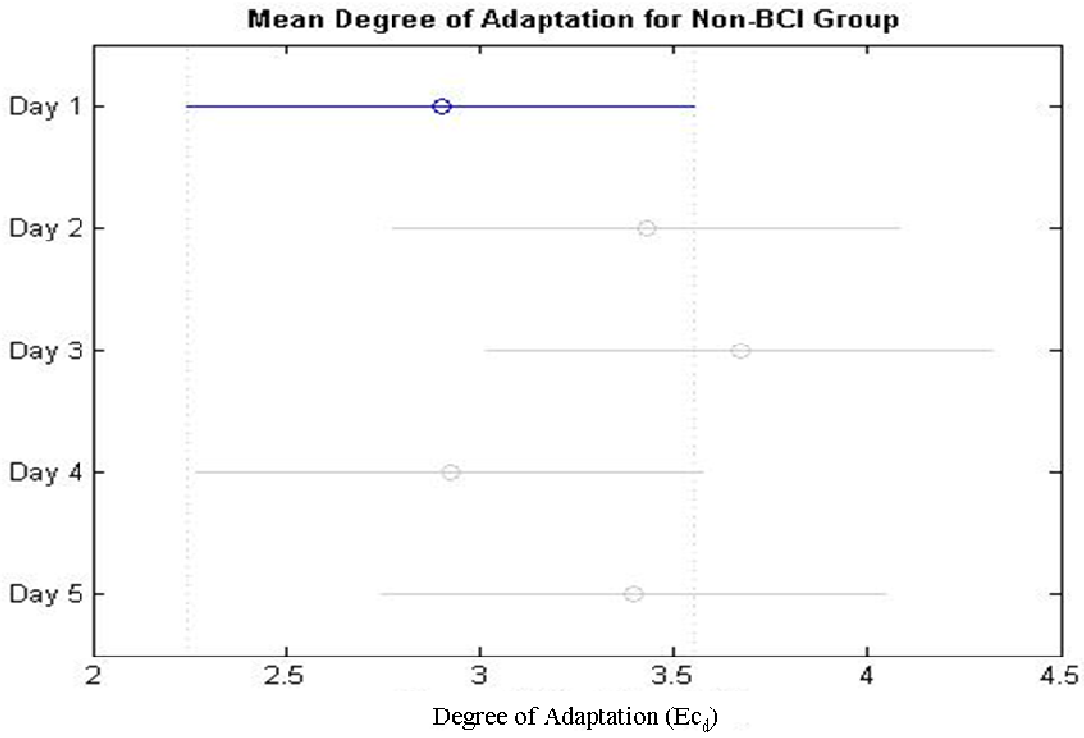

Figure 4.2-25. Multiple-comparisons ANOVA of mean degree of adaptation (Ec_d) for the Non-BCI group. The grey line highlights that there are no significant changes from Day 1.

Table 4.2-6. Confidence Intervals (95%) for ANOVA of Change in Ec_d

Mean Degree of Adaptation (Ec_d) Tests (ANOVA, with Bonferroni Corrections)	BCI		Non-BCI	
	P = 0.0695		P = 0.7064	
	CI		CI	
Day 1 vs. Day 2	**-2.0693**	**-0.0141**	-1.8367	0.7762
Day 1 vs. Day3	**-2.5216**	**-0.4664**	-2.0769	0.5359
Day 1 vs. Day 4	-1.8371	0.2182	-1.3288	1.2840
Day 1 vs. Day 30	-1.6448	0.4104	-1.8028	0.8100

4.2.4. Summary

The results of the motor learning analysis showed clear distinctions between the data distributions of the BCI group and the Non-BCI group. The BCI group had significantly greater improvements in all motor learning measures. Section 5.2 will take a closer look at the way age contributed to the variability in the statistical analysis presented above. Section 5.2 will also outline the implications of these experimental results.

4.3. Guided-Imagery Classification Analysis

As outlined in Section 3.4.3, because the method employed in this investigation to prompt motor imagery was a novel approach (Figure 3.4-10), an additional aim was added. The goal of this aim was to explore whether the EEG data extracted while performing guided-imagery reaching tasks and determine whether reaching directionality could be decoded.

This analysis is not meant to be an exhaustive search for trainable data, but an inquisition into whether the data extracted and processed for BCI control and plasticity analysis be used in a more specified task. Positive results would suggest that the novel guided-imagery task presented in this investigation could aid in designing a BCI that effectively classifies motor imagery of real-time gross limb movement.

The addition of this analysis sought to initiate exploration by other investigators into using mirrored tasks as methods for producing motor imagery useful for BCI classification. The data collected during this aim will be available for further analysis by other investigators; Appendix C specifies the location and retrieval instructions for this data.

4.3.1. Classification Methods and Accuracies

The three classification methods implemented in this aim were chosen because of their relative success with other BCI studies and their relevance to the type of data [131-134]. As mentioned in Section 3.4.3, the three classification methods, SVM, FLD and FLDwPCA, were compared to determine which distinguished between forward versus backward reaching with the greatest accuracy.

A classification accuracy that was greater than chance would fall into the range of 55-67% because of the random distributions of the test sets. Table 4.3-1. outlines the results of the analyses.

Table 4.3-1. SVM, FLDwPCA and FLD Classification Accuracies (%) per Subject

Subject	SVM	FLD w/PCA	FLD
BCI Subjects			
1	67.7966	50.8475	32.2034
3	49.1525	52.5424	50.8475
4	**76.2712**	44.0678	23.7288
5	**76.2712**	44.0678	23.7288
6	49.1525	52.5424	50.8475
7	49.1525	52.5424	50.8475
8	49.1525	52.5424	50.8475
9	67.7966	54.2373	30.5085
10	**74.5763**	54.2373	25.4237
11	49.1525	50.8475	50.8475
Non-BCI Subjects			
1	49.1525	52.5424	50.8475
2	**77.9661**	44.0678	22.0339
3	55.9322	54.2373	50.8475
4	57.6271	30.5085	50.8475
5	66.1017	42.3729	28.8136
6	44.0678	61.0169	50.8475
7	49.1525	47.4576	50.8475
8	44.0678	49.1525	50.8475
9	47.4576	45.7627	50.8475
10	47.4576	45.7627	50.8475

The SVM achieved the greatest classification accuracies with five BCI subjects and one Non-BCI subject having classification accuracies greater than chance (the similarities in the quantities are due to similarities in the test distribution).

4.3.2. Guided-Imagery Classification Summary

The results of this analysis showed promise; however, the classification accuracies achieved are not great enough to develop a reliable real-time BCI. Section 5.3 will discuss the likely limitations that led to low classification rates and outline some other approaches to classification that may produce greater accuracies.

Chapter 5: Discussion of Data Trends

5.1. Brain Plasticity Trends

The brain plasticity analysis demonstrated that plasticity is highly variable among different subjects; however, certain changes appeared to be consistent among subjects within the same group. The discussion below highlights significant findings.

5.1.1. Short-Term Plasticity

The comparison of Training Day One to Training Day Four yielded insight into the short-term changes in EEG activity that occurred within each subject during the study. As illustrated in Section 4.1.1, several noticeable spatial changes occurred within subjects in each group; however, similarities between subjects within each group were less obvious.

Tables 5.1-1 and 5.1-2 chart the subjects who had significant changes in the spectral and spatial analyses within the BCI group and the Non-BCI group respectively. Highlighted columns correspond to subjects who had both spectral changes and spatial changes. Members of both the BCI group and the Non-BCI group experienced short-term changes in mu proportion over the whole head and within the *left-brain* and/or *motor strip*. All BCI subjects, with the exception of one, experienced an increase in mu proportion; similarly all Non-BCI subjects, with the exception of one, who experienced a change in mu power, experienced an increase.

The short-term increase in mu prevalence demonstrated in both groups relates to an occurrence that has been documented in past studies; these studies showed that acquired motor skill have been accompanied by an increase in EEG spectral activity in the 8-14Hz bandwidth [135, 136]. In most studies, however, the 8-14Hz bandwidth was referred to as *alpha*. While the

8-14Hz bandwidth is primarily referred to as mu in this investigation, there was mention of the alpha band earlier in this text that refers to a more documented, ever-present signal of which its dipoles have been recorded in multiple cortical locations, but carry the greatest power in the frontal and occipital lobes [137, 138]. Alpha and mu are inter-changeable to a degree; mu refers only to alpha signals whose dipoles are measured over the (pre)motor cortex. Past studies had reported increases in alpha activity when subjects learned or performed motor tasks; however, in those studies, the location of alpha was not localized over motor cortex [135]. In this study, the increases in mu were present over the whole head (in the spectral case) and in the motor cortex (in the spatial case); this was very similar to past studies, thus indicating that some motor learning occurred with subjects in both groups. However, there were no noticeable differences between the two groups.

Changes in beta activity were more dispersed; however, three out of 11 subjects in the BCI group experienced a decrease in beta proportion over *motor strip* (highlighted in green in Table 5.1-1). Only one out of ten subjects in the Non-BCI group experienced a significant change in beta proportion, which was also a decrease over the *motor strip*; however, this decrease was correlated a the whole head (spectral) decrease in beta proportion thus implying that the change in motor cortex could have likely been an artifact of the spectral change. The trend with beta proportion reduction in the BCI group was concentrated over the motor cortex and was also expressed in the analysis of persistent changes.

To add to the discussion, on average, the increases in mu and decreases in beta experienced by the Non-BCI group were considerably lower (in the cases of mu power and beta proportion, an order of 10 lower) than those of the BCI group. Figure 5.1-1 highlights these differences; the bars illustrate the mean topographical centers of mass difference for the *left-*

*brain*s of each subject. These significant differences could imply that the BCI training had a more profound quantitative effect on brain plasticity and, possibly, contributed to the persistent changes discussed in the next section.

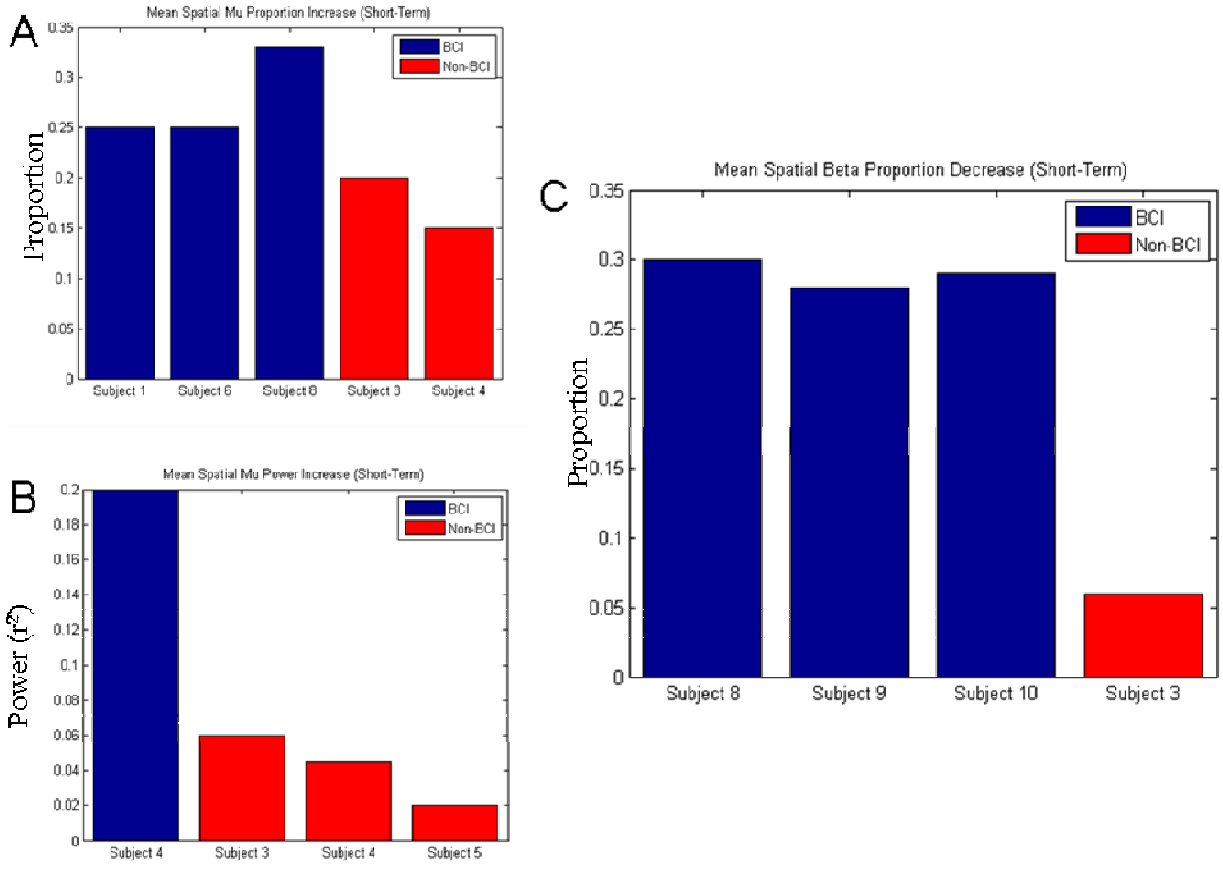

Figure 5.1-1. Mean subject *left-brain* topographical center of mass for (A) change in mu proportion, (B) change in mu power and (C) reduction in beta proportion.

Table 5.1-1. Comparison of Short-Term Spectral and Spatial Analyses of BCI Subjects

	Subject 1	Subject 2	Subject 4	Subject 6	Subject 8	Subject 9	Subject 10	Subject 11
Spectral								
Total μ Proportion	0.091	0.398	**0.018↑**	**0.018↑**	**0.018↑**	**0.043↑**	0.612	0.237
Total μ power	0.499	0.176	**0.028↑**	0.398	0.091	0.237	0.398	0.176
Total β Proportion	0.953	**0.008↑**	0.173	0.214	0.110	0.066	0.260	0.859
Total β power	0.374	0.678	**0.038↑**	0.953	0.515	**0.038↓**	0.139	0.066
Spatial								
Left-brain μ Proportion	**0.028↑**	0.398	0.063↑	**0.028↑**	**0.018↑**	0.128	0.398	**0.043↓**
Left-brain μ Power	0.091	0.176	**0.043↑**	0.499	0.374	0.237	0.237	0.128
Motor strip μ Proportion	0.116	0.612	0.345	0.091	**0.018↓**	0.237	0.497	0.999
Motor strip μ Power	**0.046↑**	0.735	0.249	0.735	0.398	0.866	0.237	**0.028↑**
Motor strip β Proportion	0.917	0.139	0.859	0.499	**0.015↓**	**0.028↓**	**0.042↓**	0.498

(Note: Mu changes are highlight in yellow, beta changes are highlighted in green)

Table 5.1-2. Comparison of Short-Term Spectral and Spatial Analyses of Non-BCI Subjects

	Subject 3	Subject 4	Subject 5	Subject 6
Spectral				
Total μ Proportion	**0.018↑**	**0.028↑**	0.999	0.612
Total μ power	**0.028↑**	0.091	**0.043↓**	0.237
Total β Proportion	**0.051**	0.110	0.173	0.594
Total β power	0.441	0.214	0.953	**0.051**
Spatial				
Left-brain μ Proportion	**0.018↑**	**0.028↑**	0.999	0.091
Left-brain μ Power	**0.028↑**	0.091	**0.018↑**	0.398
Motor strip μ Proportion	**0.018↑**	**0.018↑**	0.735	0.063
Motor strip μ Power	**0.018↑**	**0.028↑**	0.128	0.237
Left-brain β Proportion	**0.050↓**	0.260	0.953	0.139

(Note: Mu changes are highlight in yellow, beta changes are highlighted in green)

5.1.2. Persistent Plasticity

The analysis of the Screening data versus the Follow-up data gave insight into how BCI training might have contributed to changes in EEG activity. Section 4.1.2 showed that several changes occurred in both groups a clear occurrence stood out. There was an opposing trend between the groups where the BCI group had more subjects experiencing changes in beta activity and the Non-BCI group had more subjects experiencing changes in mu.

In Table 5.1-3, the BCI subjects who experienced significant changes in beta activity are highlighted in green. Theses subjects had significant decreases in beta proportion in the overall

frequency analysis and in the *left-brain* and *motor strip* (Subject 1's *left-brain* decrease not was statistically significant but was approaching significance). Only one subject, Subject 10 (highlighted in yellow in Table 5.1-3), had persistent changes in mu and beta spectral and spatial activities. Similar to the other BCI subjects, Subject 10 experienced a reduction in beta proportion (while beta proportion was not significant spatially, it was approaching significance) and an increase in mu proportion and power. All subjects showed greater significance in beta reduction as the area of the brain covered in the analysis decreased (i.e. p-value of *motor strip* was less than *left-brain* and p-value of *left-brain* was less than spectral), thus implying that the changes in beta for mostly concentrated over the motor cortex.

With these results, it appeared that BCI training may have had a unique influence on beta coherence with respect to reaching; it appeared that beta content in EEG may decreases as one acquires motor skills. The effect BCI training on beta power was inconsistent as some BCI subjects saw increases in power while others saw decreases. The analyses of mu activity in this investigation were inclusive, as only one subject had significant persistent changes in mu; however, this effect was consistent with literature assuming BCI training facilitated motor learning [135, 136].

The Non-BCI group showed inconsistent and fewer changes in beta activity; however, the changes in mu activity were considerable. Several subjects had either spectral decreases in mu power and proportion, others had spatial increases in mu power. The only subject who had both spectral and spatial changes was Subject 4 (highlighted in yellow in Table 5.1-4) who experienced spectral decreases in mu power and proportion and spatial decreases in mu power (Figure 5.1-2). The significance of the decreases were equal in all measures so it is likely that the spatial changes in mu were merely artifacts of alpha.

It should be noted that the subjects who experienced spectral decreases in mu proportion and power were Non-BCI subjects who performed the Screening tasks with the older EEG montage, whereas the single subject, Subject 5, who experienced mu proportion increases did not. It is likely that older EEG montage was more sensitive to alpha activity in the frontal and occipital lobe and, therefore, caused the significant changes highlighted in this analysis. This is further supported by the general lack of correlation between the spectral and spatial analysis of the Non-BCI group.

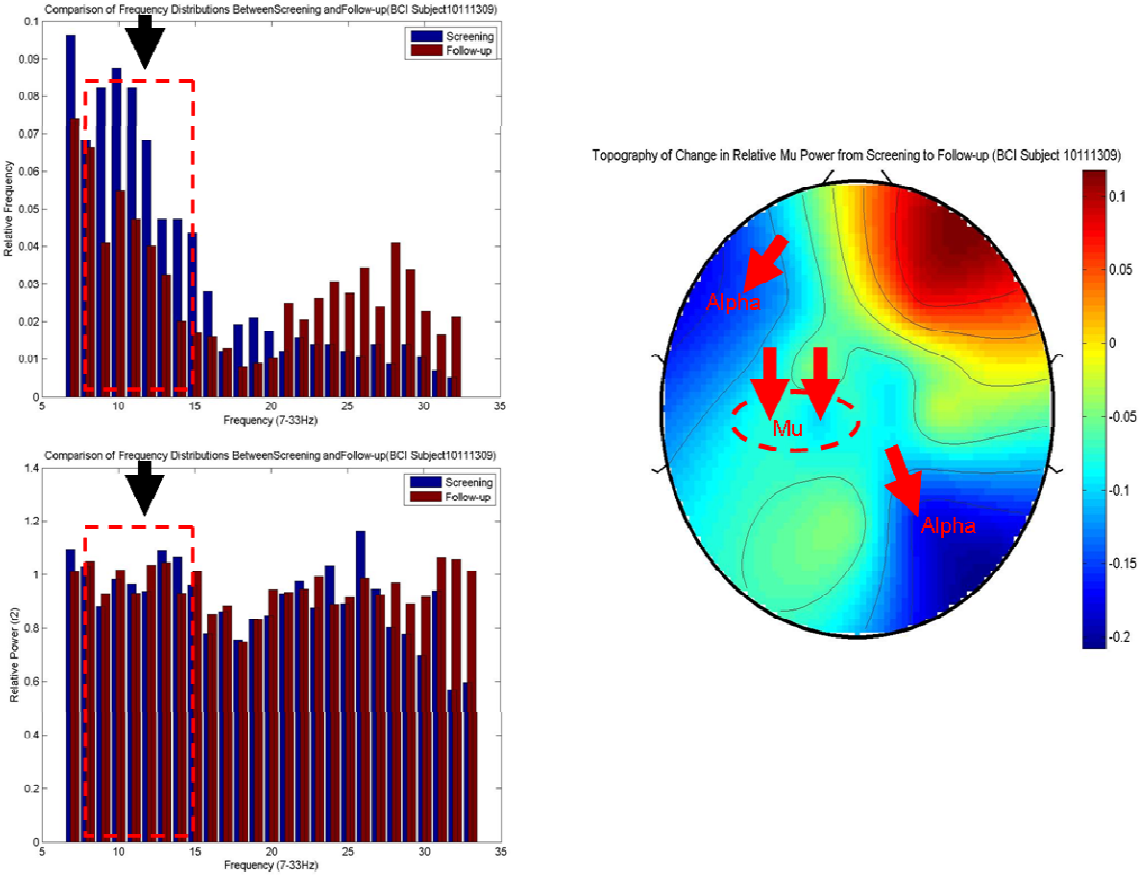

Figure 5.1-2. Spectral and spatial activity of Non-BCI Subject 4. The topography shows that, while significant reductions in mu occurred, the majority of the reduction were likely due to alphas content in the frontal and occipital lobes.

Table 5.1-3. Comparison of Persistent Spectral and Spatial Analyses of BCI Subjects

	Subject 1	Subject 2	Subject 5	Subject 7	Subject 8	Subject 10	Subject 11
Spectral							
Total μ Proportion	0.866	0.612	0.866	0.176	0.176	**0.043↑**	0.063
Total μ Power	0.612	**0.018**	0.091	0.499	0.866	0.612	0.735
Total β Proportion	**0.028↓**	0.374	**0.050↓**	0.214	0.110	0.260	0.953
Total β Power	0.214	0.110	0.859	**0.038↓**	0.139	**0.051**	0.953
Spatial							
Left-brain μ Proportion	0.499	0.866	0.735	0.237	0.310	0.063↑	**0.028**
Motor strip μ Proportion	0.612	0.735	0.176	0.735	0.612	**0.043↑**	0.237
Left-brain β Proportion	0.086↓	0.441	**0.021↓**	**0.051↓**	**0.051↓**	0.594	0.066
Left-brain β Power	0.314	0.314	0.374	0.110	0.110	**0.021↓**	0.866
Motor strip β Proportion	0.674	0.374	**0.011↓**	**0.046↓**	**0.017↓**	0.074↓	0.463
Motor strip β Power	0.674	0.314	**0.015↓**	0.753	**0.025↓**	0.116	0.345

(Note: Mu changes are highlight in yellow, beta changes are highlighted in green)

Table 5.1-4. Comparison of Persistent Spectral and Spatial Analyses of Non-BCI Subjects

	Subject 1	Subject 2	Subject 3	Subject 4	Subject 5	Subject 6	Subject 8	Subject 9	Subject 10
Spectral									
Total μ Proportion	**0.018**↓	0.178	**0.018**↓	**0.018**↓	**0.018**↑	0.398	0.735	0.237	0.866
Total μ Power	**0.018**↓	**0.043**↓	**0.018**↓	**0.018**↓	0.499	**0.028**↓	0.612	**0.043**↓	0.866
Total β Proportion	0.441	0.314	**0.038**↑	0.110	0.110	0.374	0.953	0.110	**0.021**↑
Total β Power	0.345	0.176	0.173	**0.008**↓	0.953	0.767	0.767	**0.038**↓	0.767
Spatial									
Left-brain μ Power	0.249	0.128	0.176	**0.018**↓	0.866	0.249	**0.028**↑	0.735	**0.028**↑
Motor strip μ Power	0.249	0.237	0.063	**0.018**↓	0.499	0.686	**0.046**↑	0.753	**0.028**↑
Motor strip β Proportion	0.999	0.575	0.655	0.461	0.093	**0.044**↓	0.128	0.074	0.285

(Note: Mu changes are highlight in yellow, beta changes are highlighted in green)

5.2. Motor Learning Discussion

The motor learning analysis supported the hypothesis that training on a BCI-robotic system could influence motor learning. The BCI group consistently outperformed the Non-BCI group in all measures.

5.2.1. Overall Trends

Rate of adaptation declined slower for the BCI group (Figure 4.2-3), meaning the BCI group was able to benefit from a higher capacity to adapt longer than the Non-BCI group. This related directly to the decreased learning error exhibited by the BCI group. In addition, this investigation showed that the BCI group adapted to the task greater than the Non-BCI by demonstrated a lower error after the learning phase (Section 4.2.2) and a greater difference between the catch-trials in the measure of degree of adaptation.

It appeared that the closed-loop system implemented in this investigation did have a positive effect on a subject's learning capacity. The following section discusses how learning varied between different age groups, possibly yielding unique implications of how BCI-robotic training might benefit the population more at risk of suffering from strokes.

5.2.2. Demographic Comparisons and Learning Differences

Further analysis of the motor learning data highlighted interesting trends based on the demographics of the subjects. Demographic groups based on age and activity level added content to the discussion of motor learning by indicating where the majority of the variance in the data originated. Two age groups and two activity groups comprised the demographic categorizations. Multi-comparisons ANOVA with Bonferroni corrections compared the daily

distributions for each motor learning analysis as outline in Section 3.4.2 (It should be noted that because each demographic group consisted of a considerably smaller sample size, the statistical power of this analysis was reduced). The most informative results occurred in the age group comparison, which is discussed below.

Age and Motor Learning in the BCI Group

Each study group was decomposed into two age groups, 19-40 and over 40. The distributions of each age group in each study group were tested for rate of adaptation, learning error and degree of adaptation. The results of the analyses were consistent with the literature for rate of adaptation and degree of adaptation; as expected, most of the statistical variance laid within the younger age group [139, 140]. The total error analysis; however, showed a unique difference between the age groups that deserved attention.

Total Learning Error

The decomposition of error analysis into two phases allowed for the revelation of a possible trend when it comes to BCI training, motor learning and age. When looking at the total learning error (El_d), it became apparent that 19-40 BCI group outperformed the 19-40 Non-BCI group, consistent with what was outlined in Section 4.2.2. In addition, the 19-40 BCI group demonstrated more statistically significant reductions in total learning error after the first day of assessment, which was consistent with previous studies that showed that younger subjects tend to learn tasks faster than their elder counterparts [139-141]. Figures 5.2-1 to 5.2-4 illustrate the multiple-comparisons ANOVA distributions for the BCI subjects ages 19-40, Non-BCI subjects ages 19-40, BCI subjects ages 40+ and Non-BCI subjects ages 40+ respectively. The 19-40 BCI

group had consistently significant reductions in learning error on each day after assessment began, including the 30-day Follow-up. All other groups showed less persistent reductions in error.

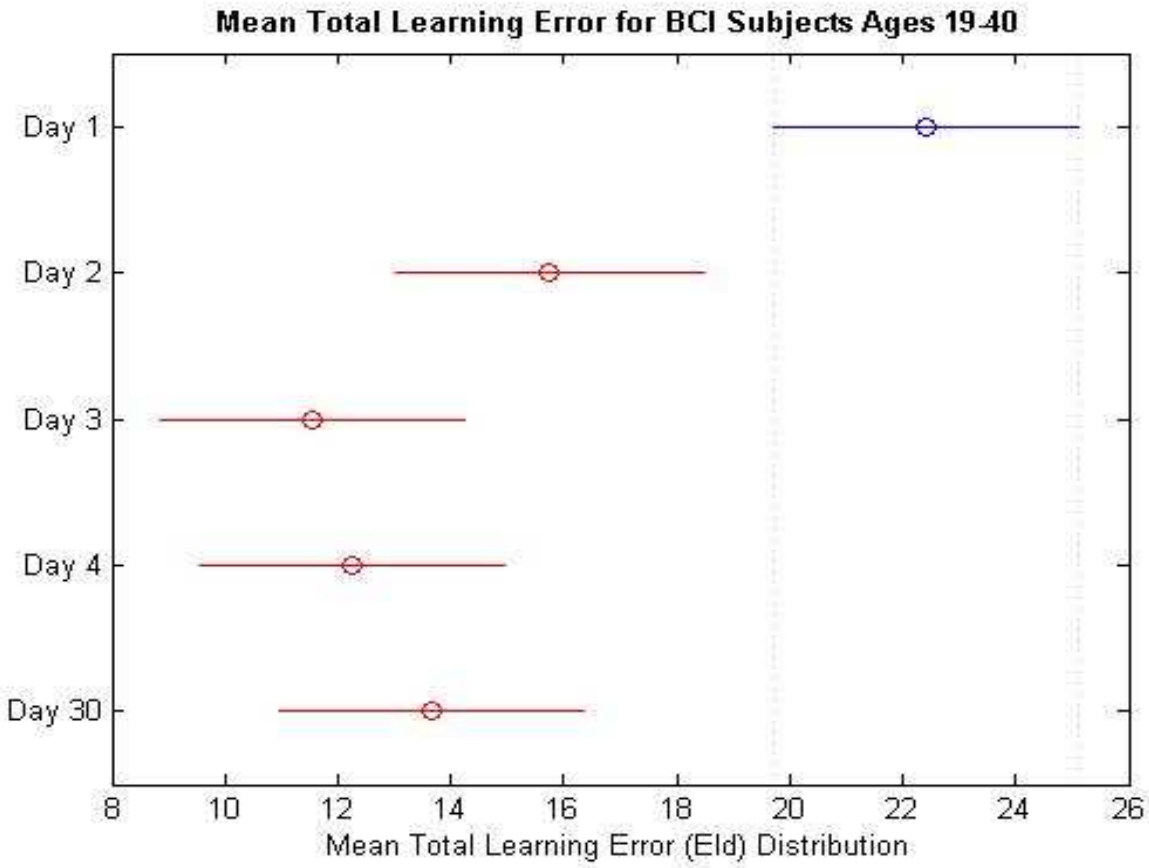

Figure 5.2-1. Multiple-comparisons ANOVA of total Learning Error (El_d) for BCI subjects ages 19-40. The blue line highlights the mean and 95% confidence intervals of the El_d on the first day (El_1) of MLA. All days highlighted in red had error distributions that were significantly lower than on the first day.

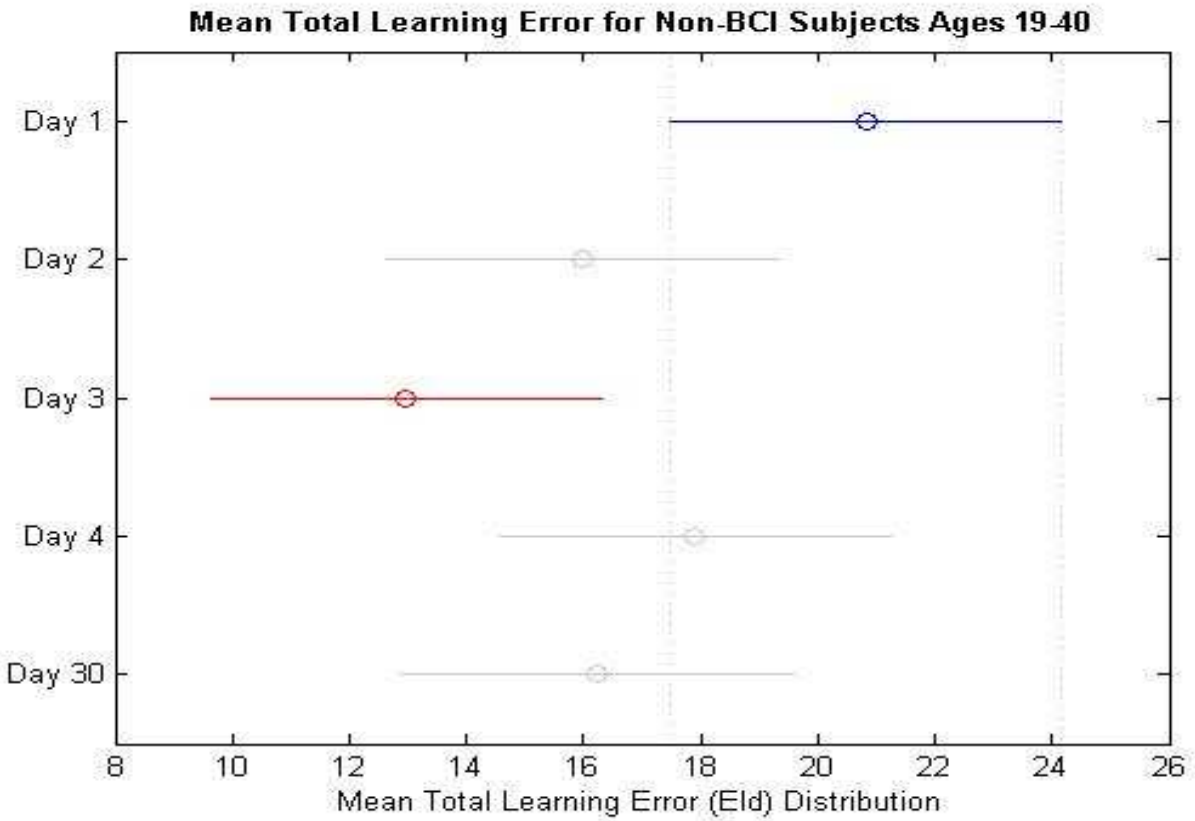

Figure 5.2-2. Multiple-comparisons ANOVA of total Learning Error (Eld) for Non-BCI subjects ages 19-40. The blue line highlights the mean and 95% confidence intervals of the Eld on the first day (El_1) of MLA. Only the third day (highlighted in red) had a significantly lower error than day one; similar to the aggregate analysis discussed in Section 4.2.2.

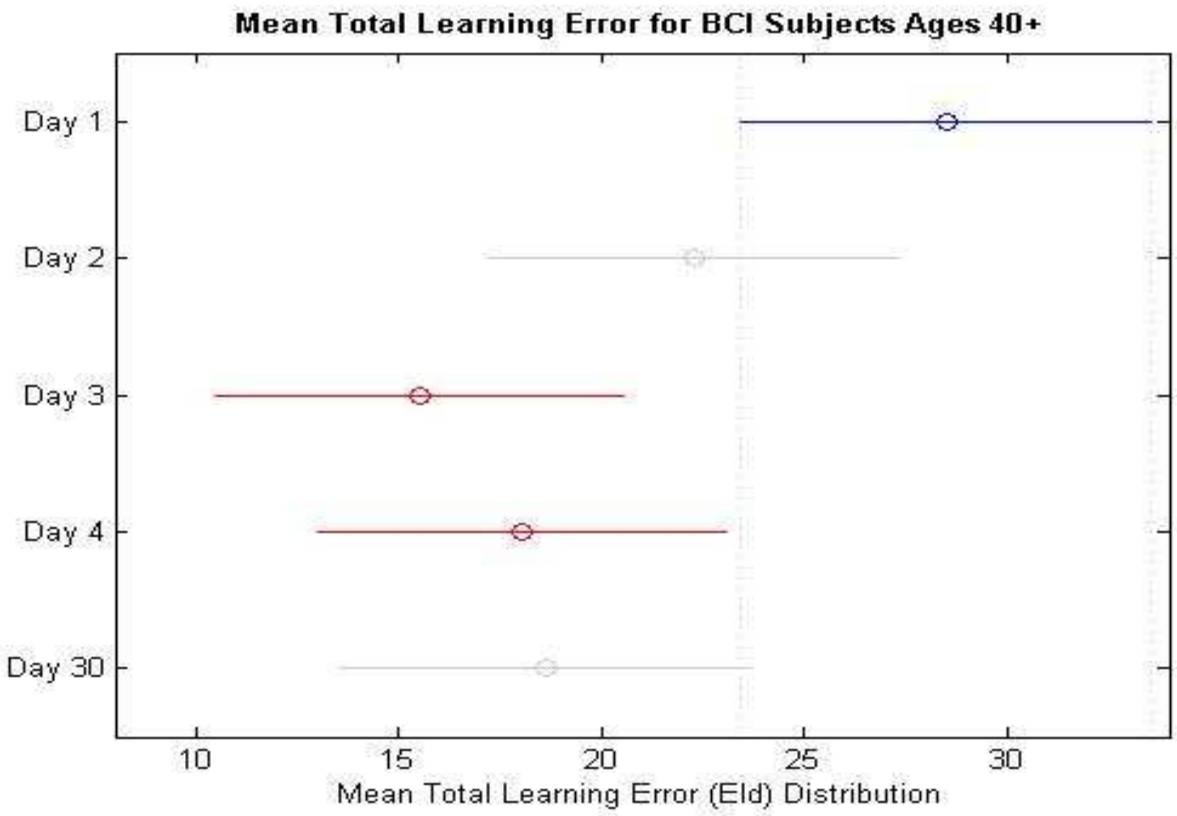

Figure 5.2-3. Multiple-comparisons ANOVA of total Learning Error (Eld) for BCI subjects ages 40+. The blue line highlights the mean and 95% confidence intervals of the Eld on the first day (El1) of MLA. All days highlighted in red had error distributions significantly lower than on the first day. Note that significance in lost after Day 4.

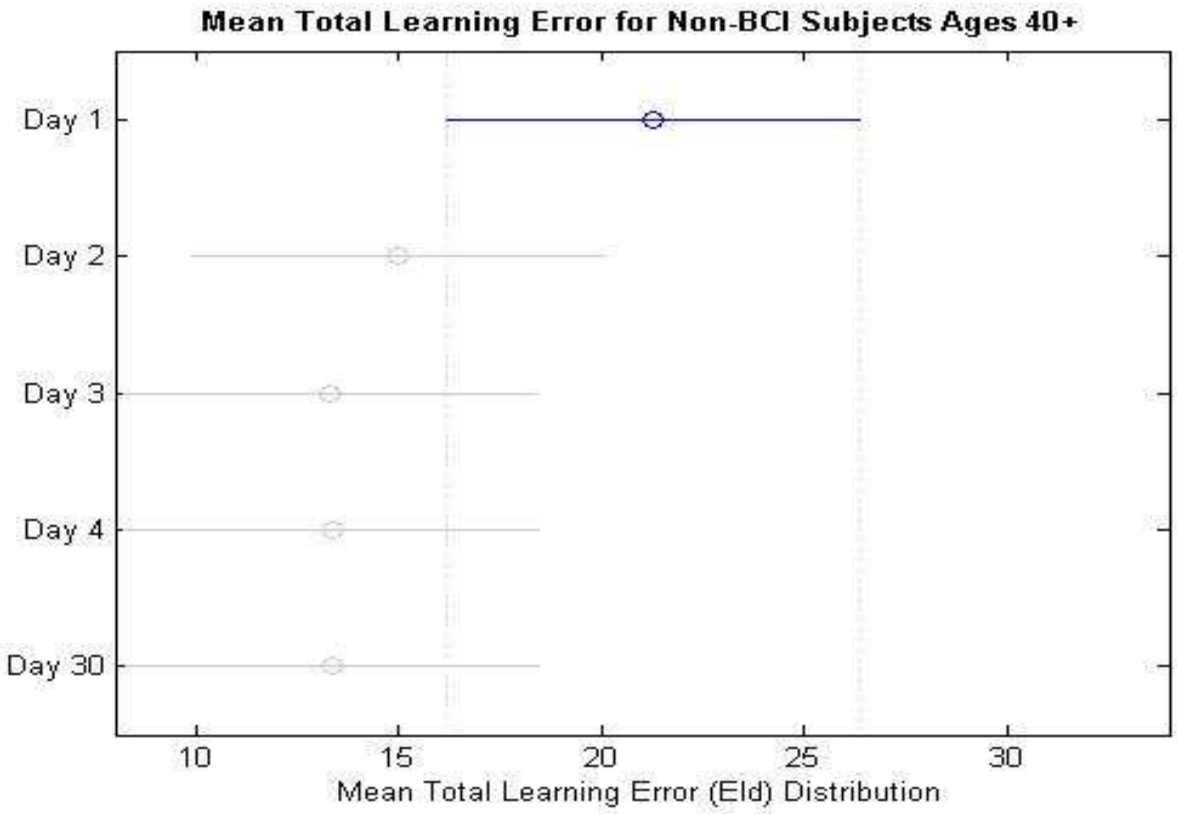

Figure 5.2-4. Multiple-comparisons ANOVA of total Learning Error (Eld) for Non-BCI subjects ages 40+. The blue line highlights the mean and 95% confidence intervals of the Eld on the first day (El1) of MLA. There were no significant reductions in learning error any of the following days of assessment for this group.

Total Adapted Error

As mentioned in Section 4.2.2, the total adapted error (Ea_d) had less significant within-group changes but had more significant between-group changes. However, when decomposed into age groups, it becomes clear that the within-group significance laid within the more aged BCI subjects.

Figure 5.2-5 illustrates the multiple-comparisons ANOVA distribution of the 40+ BCI group for each day of assessment; this figure shows that the more aged group had consistent reductions in adapted error up to the fourth day of assessment where the reduction was statistically significant. This effect was not demonstrated in any other age group. As illustrated in Figure 5.2-6, the less aged BCI group showed consistent decreases in adapted error; however these changes were never statistically significant. Both age groups in the Non-BCI group showed inconsistent changes in the adapted error on each day.

The significance in the more aged BCI study has implications in regards to how BCI training could benefit the stroke-susceptible population.

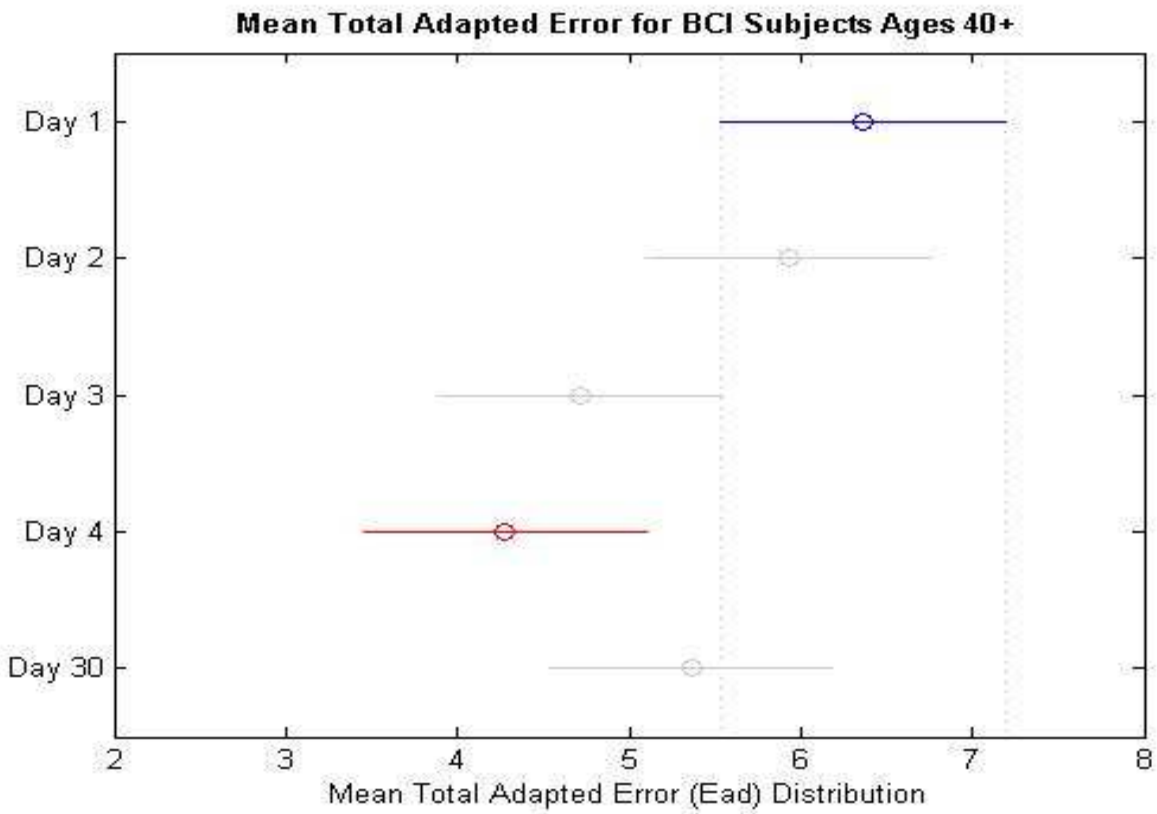

Figure 5.2-5. Multiple-comparisons ANOVA of total Adapted Error (Ea_d) for BCI subjects ages 40+. The blue line highlights the mean and 95% confidence intervals of the Ea_d on the first day (El_1) of MLA. The line highlighted in red shows that a significant reduction in adapted error was achieved on the fourth day of assessment.

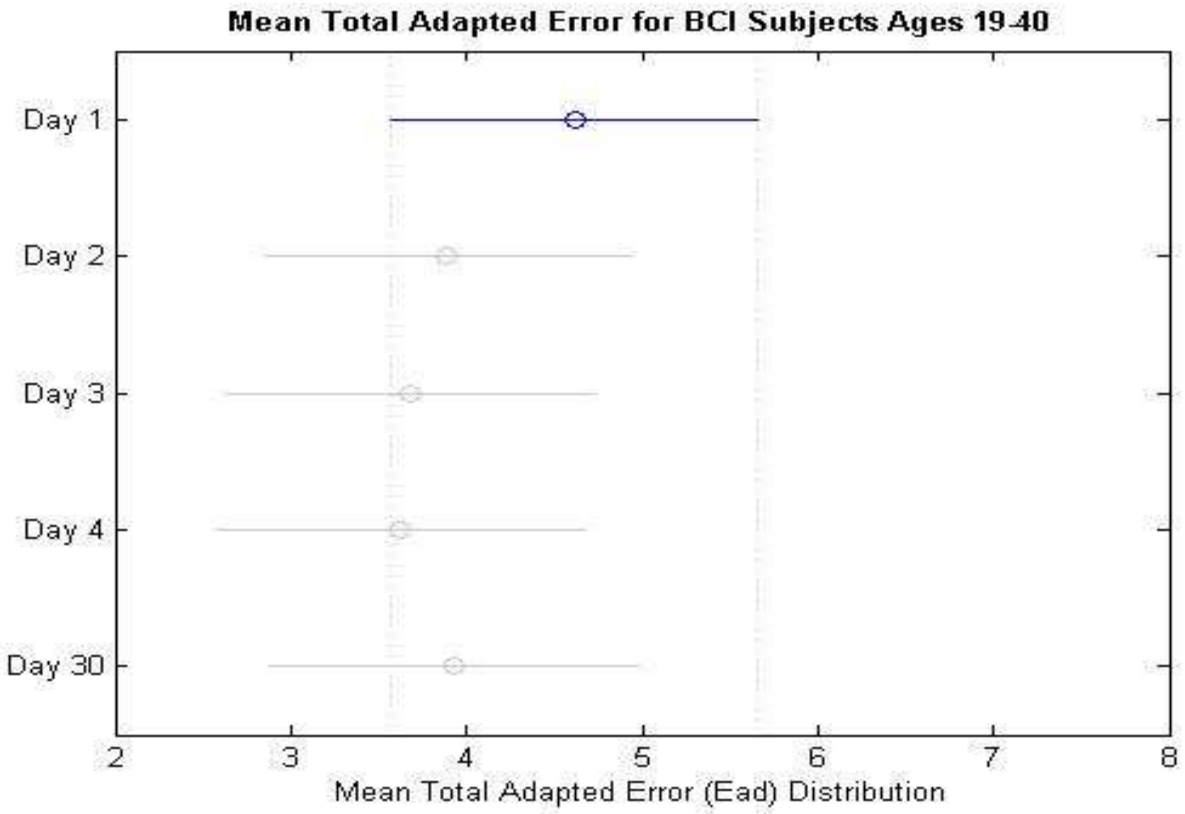

Figure 5.2-6. Multiple-comparisons ANOVA of total Adapted Error (Ea_d) for BCI subjects ages 19-40. The blue line highlights the mean and 95% confidence intervals of the Ea_d on the first day (El_1) of MLA. While there were consistent reductions in Ea_d on each of the following days, none were statistiscally significant

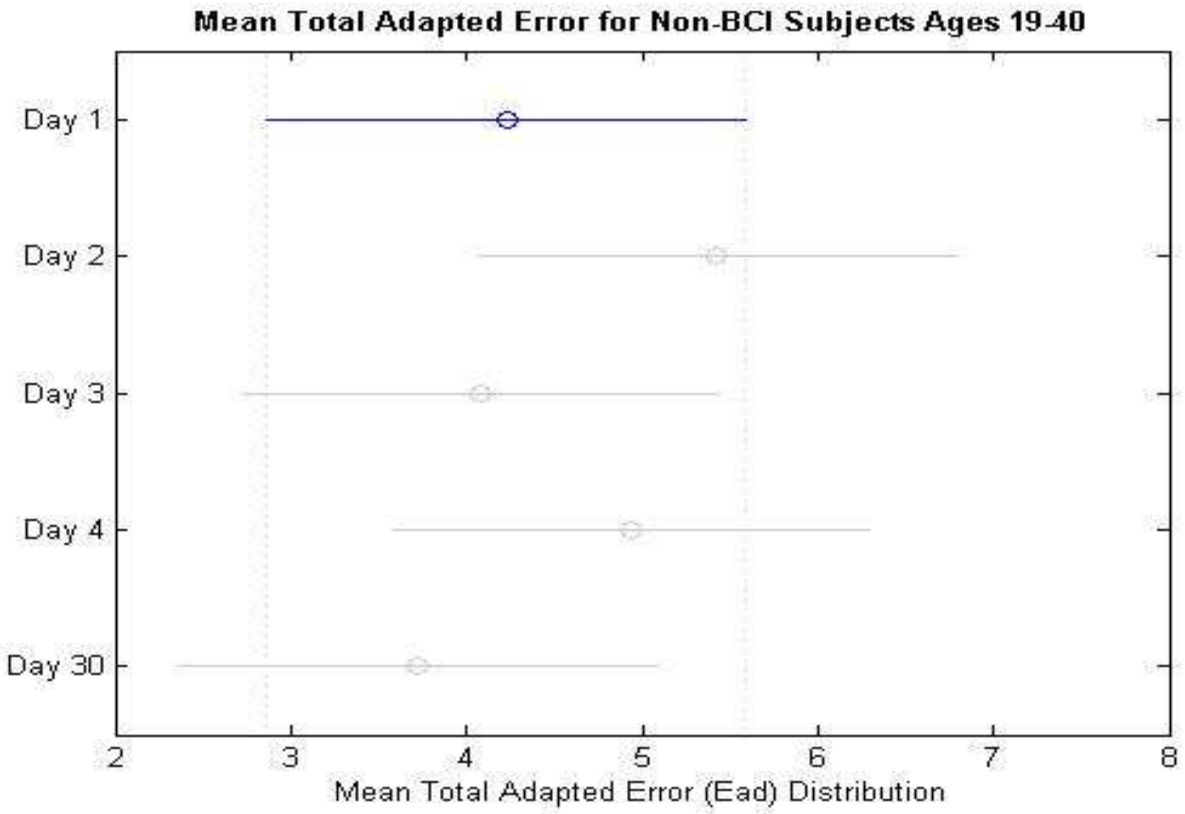

Figure 5.2-7. Multiple-comparisons ANOVA of total Adapted Error (Ea_d) for Non-BCI subjects ages 19-40. The blue line highlights the mean and 95% confidence intervals of the Ea_d on the first day (El_1) of MLA. Total adapted error did not decrease consistently on the following days.

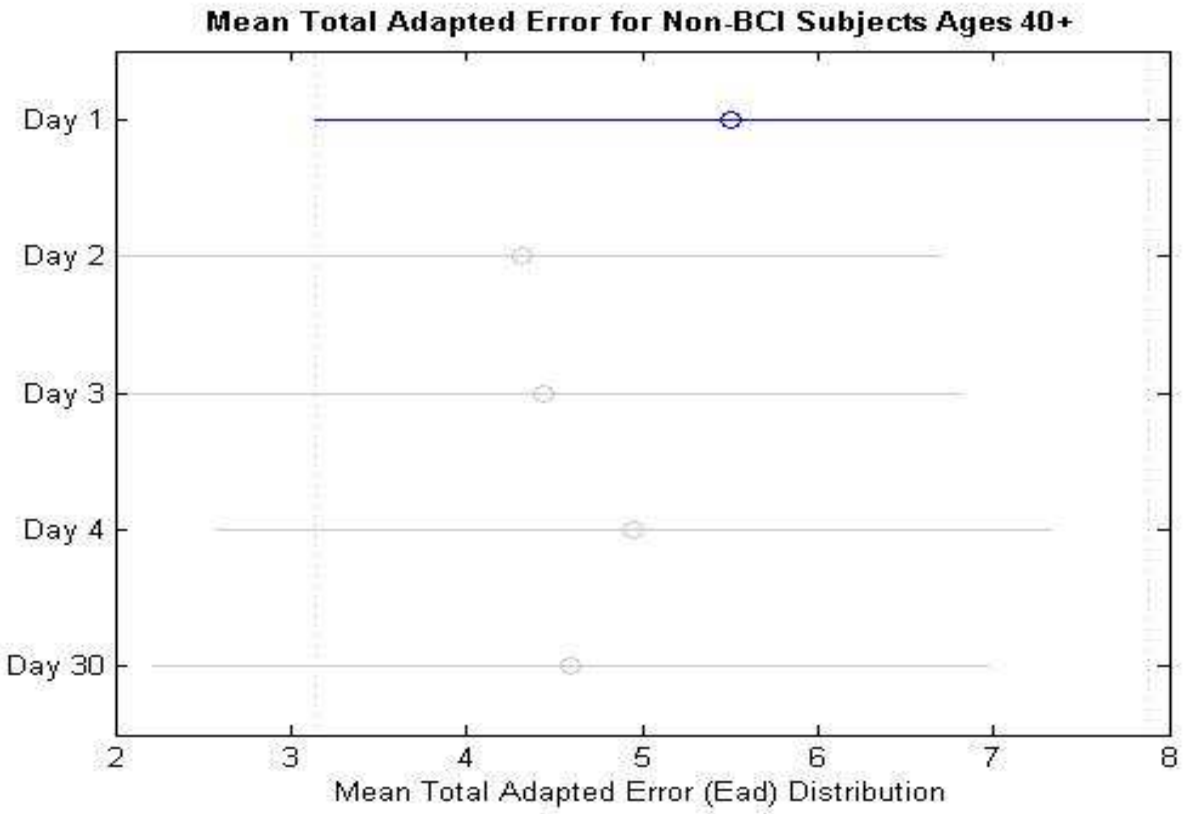

Figure 5.2-8. Multiple-comparisons ANOVA of total Adapted Error (Ea_d) for Non-BCI subjects ages 40+. The blue line highlights the mean and 95% confidence intervals of the Ea_d on the first day (El_1) of MLA. Total adapted error did not decrease consistently on the following days.

Chapter 6: Conclusions and Future Work

This investigation sought to determine whether training on a BCI-controlled robot can influence brain plasticity and motor learning. The results of this investigation have supported the hypothesis that BCI training does indeed influence brain plasticity and motor learning. The discussion below summarizes the contribution of each aim to the support of this hypothesis.

6.1 Brain Plasticity Conclusions

As discussed above, it appears that BCI training may have an influence on beta coherence as all BCI subjects who experienced changes in beta proportion showed spectral and spatial decreases. This was the most consistent observation in the plasticity analysis. Further study should explore this hypothesis by controlling the EEG channel layouts for all subjects.

As mentioned above, only one Non-BCI subject showed beta proportion decreases, however many Non-BCI subjects had decreased mu activity. It is possible the decreased mu activity in the Non-BCI subjects who had used two different caps phased out any observable beta activity that might show a consistent change in the Non-BCI group. However, considering that none of the Non-BCI subjects who used one EEG cap throughout the study showed significant beta changes, it is likely that this conclusion is not what was happening. More than likely, the decreased mu activity could be attributed to the fact that the older cap had more frontal and occipital channels; therefore, the increased mu activity during Screening was actually attributed to alpha.

6.2 Motor Learning Conclusions

The unique differences between to learning approaches of the two the age groups within the BCI group could have implications for how one would approach developing a new BCI protocol for training older stroke patients. The results of the demographic analysis above implied that while younger subjects predicted the learning task faster than their more aged counterparts; the learning abilities of the younger age group reached a plateau. The analysis above demonstrated that while older subjects did not predict the task as well as their younger counterparts, they tended to persistently reduce the amount of error they made in over time. This could suggest that BCI training has more lasting benefits for the elderly. This revelation implies that the population most susceptible to stroke may have more options for rehabilitation in the future with BCI training

The variability in the total error analysis between groups was likely attributed to the wide range of demographics covered in the sample population. The question of a plateau effect occurring during the analysis of error may surface when observing the differences between the within group comparisons. The between-groups analyses were presented to mitigate doubt associated with such questions by presenting a comparison that normalized the distributions and compared only difference ratios between the groups. These analyses highlighted the unique proportional changes that were occurring within the BCI group.

The Aim I analysis showed that a considerable portion of the BCI group demonstrated higher mu proportions of activity during the short-term analysis, this suggested that these individuals were likely more engaged while performing their tasks. This could account for the increased motor learning performance in the BCI group. Physiologically, it is possible that the increased cortical activity experienced by the BCI group preceding the daily MLA facilitated

some form of Hebbian learning that linked the MLA with the BCI task in the BCI subjects' brains (i.e. *"neurons that fire together wire together"*) [63]. Perhaps that link caused BCI training to naturally speed each subjects' adaptation to the MLA by engaging newly-formed neural pathways. Future studies should explore the physiological underpinnings of this possible phenomenon.

Overall, the motor learning analysis supported the hypothesis that BCI-controlled robotic training can influence motor learning. In all motor learning metrics presented in this investigation, the BCI group outperformed the Non-BCI group consistently. The findings of this investigation support the application of BCI to future rehabilitation protocols.

6.3 Guided-Imagery Analysis Discussion and Future Directions

The analysis in Section 4.3 showed that the classification techniques employed in this investigation had some success but could be improved. Aside for the fact that extracting reaching direction from EEG data is non-trivial, several limitations of the feature set may have contributed to the results of this study [142, 143].

The features extracted for the plasticity analysis were aggregated channel-frequency-r^2 values extracted during two seconds of a reaching task. This approach to feature extraction ignored phase and handled the issue of EEG non-stationarity by including all data from several time windows within each reach. This is a common feature extraction technique implemented in BCIs and has had considerable success in classifying fine motor imagery (i.e. hand movements); however, for gross activity, more complex features extraction and classification techniques may have produced more accurate classification results [105, 131, 134].

For instance, an alternative approach to classification would incorporate a phase analysis either of event related potentials or spectral activity (possibly through wavelet analysis). Rather than extracting a bin of similar features for one reach, one could incorporate several different types of features to characterize different stages of the reach (i.e. rest, initiation, action). Several studies have implemented these types of approaches in decoding EEG activity for other applications [132, 133, 144, 145].

Investigators are invited to use the data extracted in this investigation to formulate their own classification studies. Appendix C details the location and directions for retrieving the data.

Appendix A: Calculation of Inter-Reach r^2 for Plasticity Analysis

The feature set extracted for each imagined reach in the plasticity analysis was produced by taking the union of two measures of r^2. The first measure, the intra-reach r^2, was determined by Equation (7) in which the Hotelling t^2 measure was extracted from the *MATLAB® princomp* function. The second r^2 measure, the inter-reach r^2, had a slightly more complex calculation. Figure A-1 illustrates the method implemented to determine inter-reach r2.

The segmented line illustrates the windowed temporal reaching data in which one second of data comprised the pre-target period and, similarly, one second comprised the post-target period. Each second was windowed into eleven 200 millisecond windows that were overlapped by 50%. The *MATLAB®* function *pburg* extracted the power spectrum from each window for each EEG channel; each window was then bandpass filtered to transmit the frequencies from 5Hz to 35Hz. The 11 windows for the pre-target period were placed in a matrix as were the 10 windows for the post target period. These matrices were then passed as parameters to the *MATLAB® corrcoef* function.

Corrcoef produced a 992x992 square output matrix that estimated the correlation coefficient, *r*, of each feature (frequency-channel-r^2) in the pre-target period with itself (upper diagonal matrix) and with those in the post-target period (lower diagonal matrix). The negative 496^{th} diagonal (the main diagonal minus 496) of the corrcoef output matrix correlated each frequency of the pre-target period with its corresponding post-target period frequency. To produce r^2 estimates for all frequencies in each of the 16 channels, the algorithm squared the -496^{th} diagonal and extracted the corresponding p-values (probability of insignificance). As with the intra-reach case, frequencies that produced r^2 values less then 0.2 were removed from the feature set; to further filter the set, frequencies that had corresponding p-values greater than

0.05 (95% confidence that the *r* values were significant) were also removed. The remaining frequencies with corresponding channels comprised the inter-reach r^2 feature set for a single reach; the union of the intra-reach r^2 and the inter-reach r^2 produced the final feature set for a single reach. This investigation performed this process for every imagined reach performed during the Screening stage, Training Day One, Training Day Four and the 30-Day Follow-up to produce the aggregate feature set of each stage.

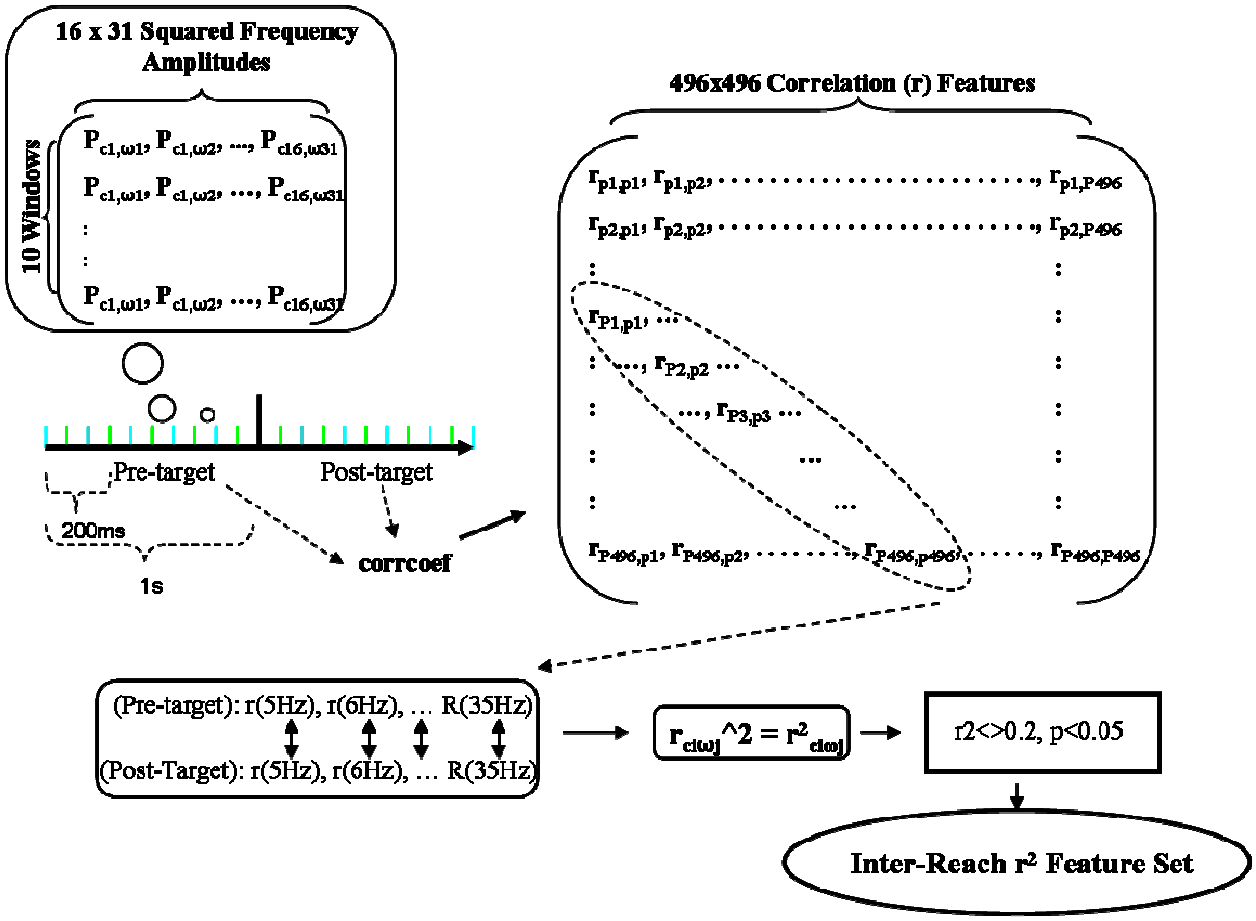

Figure A-1. Diagram of process implemented in this investigation to determine the inter-reach r^2.

Appendix B: Goodness-of-Fit Measures for Motor Learning

The motor learning analysis built its measurements off of the assumptions that data were accurately estimated by the exponential curves (Equation (11)) fitted to the data. The discussion in this section verifies the goodness-of-fit of the exponential. B-1 illustrates the mean residuals for the BCI group (blue) and the Non-BCI group (red) for each day of training. The solid red line illustrates a linear regression of the residuals and the solid black line is located at zero. The residuals are fairly well distributed about zero, which implies a good fit and supports the within-group comparisons performed in the motor learning analysis.

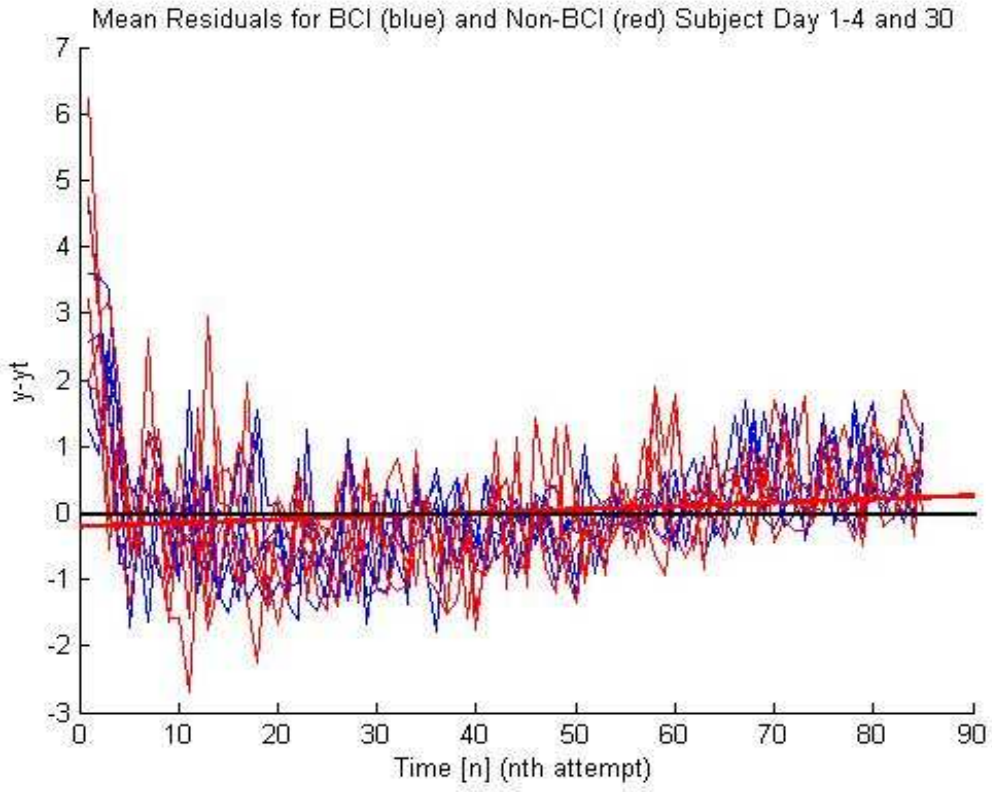

Figure B-1. Mean residuals for Days 1-4 and 30 of MLA. The BCI group (blue) and Non-BCI (group) have the same linear regression (solid red line), which is significantly approaching a zero mean (solid black line).

To further support the residual analysis, the coefficients of determination, r^2, were calculated for each subject on each day of motor assessment from the residuals ($y - y_t$) using the following formula:

$$r^2 = 1 - \frac{\sum_{1}^{85} (y_n - y_t)^2}{85\sigma_{yn}^2}$$

Where y_n represents the sample data, y_t represents the estimated data and σ^2_{yn} is the variance of the sample data. Table B-1 contains the coefficients of determination (r^2) of each subject on each day of motor assessment. Figure B-2 shows an ANOVA comparison between the mean daily r^2 distribution of the BCI group and that of the Non-BCI group. The ANOVA comparison yielded a p-value of 0.6259, which implies that there was no significant difference between the BCI r^2 distribution and Non-BCI r^2 distribution. Therefore, the between-group comparisons in the motor learning analysis were valid.

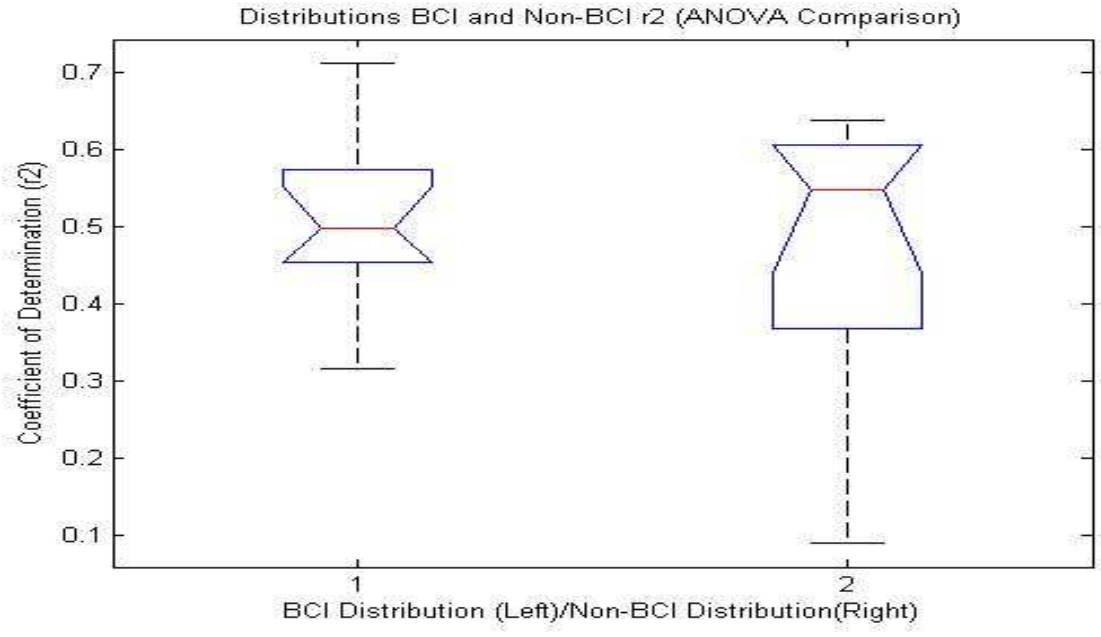

Figure B-2. Box-whisker plots of BCI (left) and Non-BCI (right) r^2 distributions. ANOVA comparisons implied no significant difference (p = 0.6294, F = 0.24) between the two distributions of the exponential fits.

Table B-1. Coefficients of Determination, r^2, for Daily Motor Assessment Estimated Exponential Fits.

BCI					
	Day 1	**Day 2**	**Day 3**	**Day 4**	**Day 30**
Subject 1	0.2637	0.2743	0.2415	0.5587	0.2811
Subject 2	0.3246	0.4367	0.6365	0.6260	0.3872
Subject 3	0.4035	0.2691	0.6526	0.6270	0.6241
Subject 4	0.2106	0.4537	0.7094	0.4188	0.5479
Subject 5	0.3519	0.4925	0.4633	0.4905	0.6114
Subject 6	0.3297	0.5922	0.8214	0.5452	0.6570
Subject 7	0.2827	0.6269	0.5915	0.3135	0.3910
Subject 8	0.1199	0.3207	0.5276	0.4745	0.1413
Subject 9	0.7093	0.6890	0.7537	0.6777	0.7306
Subject 10	0.4407	0.5147	0.5788	0.6194	0.6350
Subject 11	0.3520	0.6957	0.6272	0.6215	0.4595
Subject 12	0.5427	0.6949	0.6507	0.7396	0.6521
Non-BCI					
Subject 1	0.4260	0.6661	0.8087	0.5639	0.7236
Subject 2	0.0248	0.4706	0.5819	0.7201	0.5442
Subject 3	0.4221	0.2131	0.5562	0.4691	0.2044
Subject 4	0.4601	0.4537	0.6917	0.6035	0.6604
Subject 5	0.0590	0.1815	0.0886	0.1802	-0.0552
Subject 6	0.5542	0.6514	0.2719	0.5723	0.5639
Subject 7	0.5673	0.7852	0.7970	0.3987	0.5112
Subject 8	0.5245	0.6586	0.6686	0.5759	0.4526
Subject 9	0.4414	0.0614	0.5699	0.2056	0.5401
Subject 10	0.5286	0.7603	0.6633	0.7052	0.5011
Subject 11	0.4512	0.7403	0.6244	0.6685	0.5147
Subject 12	0.0321	0.0155	0.5114	0.3237	0.6213

Appendix C: Retrieval of EEG Data

The BCI data will be made available after July 8th, 20ll. Contact Karolyn Babalola at karolyn@gatech.edu for instructions on gaining access to the data after that time.

References

1. **Roger, V.L., et al., *Heart disease and stroke statistics--2011 update: a report from the American Heart Association.* Circulation, 2011. 123(4): p. e18-e209.**

2. **(CDC)., C.f.D.C.a.P., *Prevalence of disabilities and associated health conditions among adults: United States, 1999.* MMWR Morb Mortal Wkly Rep., 2001. 50: p. 120-125.**

3. **Muntner P, G.E., Klag MJ, Coresh J., *Trends in stroke prevalence between 1973 and 1991 in the US population 25 to 74 years of age.* Stroke, 2002(33): p. 1209-1213.**

4. **Smith, S.C.J., R.; Pearson, T.A.; Fuster, V.; Yusuf, S.; Faergeman, O.; Wood, D. A.; Alderman, M.; Horgan, J.; Home, P.; Hunn, M.; Grundy, S. M., *Principles for National and Regional Guidelines on Cardiovascular Disease Prevention: A Scientific Statement From the World Heart and Stroke Forum.* Circulation, 2004. 109: p. 3112-3121.**

5. **Stegmayr B, A.K., Kuulasmaa K, Rajakangas AM, Thorvaldsen P, Tuomilehto J., *Stroke incidence and mortality correlated to stroke risk factors in the WHO MONICA Project. An ecological study of 18 populations.* Stroke, 1997. 28(7): p. 1367-1374.**

6. **Ingall, T., *Stroke--incidence, mortality, morbidity and risk.* J Insur Med, 2004. 36(2): p. 143-52.**

7. **Asplund K, S.B., Peltonen M., *From the Twentieth to the Twenty-First Century: A Public Health Perspective on Stroke. In: Ginsberg MD*, in *Cerebrovascular Disease Pathophysiology, Diagnosis, and Management.*, B. J, Editor. 1998, Blackwell Science: Malden, Mass.**

8. **Kelley-Hayes M, B., A, Kase C, Scaramucci A, D'Agostino R, Wolf P, *The influence of gender and age on disability following ischemic stroke: the Framingham study.* J Stroke Cerebrovasc Dis, 2003. 12: p. 119-126.**

9. **Rosamond, W., et al., *Heart disease and stroke statistics--2007 update: a report from the American Heart Association Statistics Committee and Stroke Statistics Subcommittee.* Circulation, 2007. 115(5): p. e69-171.**

10. **Dobkin, B.H., *Strategies for stroke rehabilitation.* Lancet Neurol, 2004. 3(9): p. 528-36.**

11. **Wittenberg, G.F., et al., *Constraint-induced therapy in stroke: magnetic-stimulation motor maps and cerebral activation.* Neurorehabil Neural Repair, 2003. 17(1): p. 48-57.**

12. **Miltner, W.H., et al., *Effects of constraint-induced movement therapy on patients with chronic motor deficits after stroke: a replication.* Stroke, 1999. 30(3): p. 586-92.**

13. **Barreca, S., Wolf, S. L., Fasoli, S., and Bohannon, R., *Treatment interventions for the paretic upper limb of stroke survivors: A critical review.* Neurorehabilitation and Neural Repair., 2003. 17: p. 1-7.**

14. **Page, S.J., Levine, P., and Leonard, A. C., *Modified constraint-induced therapy in acute stroke: A randomized controlled pilot study.* . Neurorehabilitation and Neural Repair., 2005. 19: p. 27-32.**

15. **Taub, E.a.W., S. L., *Constraint-induced (ci) movement techniques to facilitate upper extremity use in stroke patients.* . Top Stroke Rehab., 1997. 3: p. 38-61.**

16. **Butler, A.J. and S.J. Page, *Mental practice with motor imagery: evidence for motor recovery and cortical reorganization after stroke.* Arch Phys Med Rehabil, 2006. 87(12 Suppl 2): p. S2-11.**

17. **Ward, N.S., *Plasticity and the functional reorganization of the human brain.* Int J Psychophysiol, 2005. 58(2-3): p. 158-61.**

18. **Kelley-Hayes M., B., A., Kase, C.S., Scaramucci, A., D'Agostino, R. B., Wolf, P.A., *The influence of gender and age on disability following ischemic stroke: the Framingham study.* Journal of Stroke and Cerebrovascular Diseases., 2003. 12: p. 119-126.**

19. **Thom, T., et al., *Heart disease and stroke statistics--2006 update: a report from the American Heart Association Statistics Committee and Stroke Statistics Subcommittee.* Circulation, 2006. 113(6): p. e85-151.**

20. **Lynch, J.K., et al., *Report of the National Institute of Neurological Disorders and Stroke workshop on perinatal and childhood stroke.* Pediatrics, 2002. 109(1): p. 116-23.**

21. **deVeber, G.A., et al., *Neurologic outcome in survivors of childhood arterial ischemic stroke and sinovenous thrombosis.* J Child Neurol, 2000. 15(5): p. 316-24.**

22. **Krakauer, J.W., *Motor learning: its relevance to stroke recovery and neurorehabilitation.* Curr Opin Neurol, 2006. 19(1): p. 84-90.**

23. **Randolph, A.B., *Individual-Technology Fit: Matching Individual Characteristics and Features of Biometric Interface Technologies with Performance*, in *Computer Information Systems*. 2007, Georgia State University: Atlanta, GA. p. 166.**

24. **Moore, M.M., *Real-world applications for brain-computer interface technology.* IEEE Trans Neural Syst Rehabil Eng, 2003. 11(2): p. 162-5.**

25. **Wolpaw, J.R., Birbaumer, N., McFarland, D.J., Pfurtscheller, G., Vaughan, T.M., *Brain-computer interfaces for communication and control.* Clinical Neurophysiology, 2002. 113: p. 767-791.**

26. **Kennedy, P.R., Kirby, M. T., Moore, M. M., King, B., Mallory, A., *Computer control using human intracortical local field potentials.* IEEE Trans Neural Syst Rehabil Eng, 2004. 12(3): p. 339-44.**

27. **Kennedy, P., Andreasen, D., Ehirim, P., King, B., Kirby, T., Mao, H., Moore, M., *Using human extra-cortical local field potentials to control a switch.* J Neural Eng, 2004. 1(2): p. 72-7.**

28. **Pfurtscheller, G., *Event-related synchronization (ERS): an electrophysiological correlate of cortical areas at rest.* Electroencephalogr Clin Neurophysiol, 1992. 83(1): p. 62-9.**

29. **Pfurtscheller, G., Neuper, C., & Birbaumer, N., *Human Brain-Computer Interface (BCI).* Motor Cortex in Voluntary Movements. A Distributed System for Distributed Functions, 2005.**

30. **Pfurtscheller, G. and F.H. Lopes da Silva, *Event-related EEG/MEG synchronization and desynchronization: basic principles.* Clin Neurophysiol, 1999. 110(11): p. 1842-57.**

31. **Pfurtscheller, G. and C. Neuper, *Event-related synchronization of mu rhythm in the EEG over the cortical hand area in man.* Neurosci Lett, 1994. 174(1): p. 93-6.**

32. **Page, S.J., et al., *Mental practice combined with physical practice for upper-limb motor deficit in subacute stroke.* Phys Ther, 2001. 81(8): p. 1455-62.**

33. **Page, S.J., P. Levine, and A. Leonard, *Mental practice in chronic stroke: results of a randomized, placebo-controlled trial.* Stroke, 2007. 38(4): p. 1293-7.**

34. **Oldfield, R.C., *The assessment and analysis of handedness: the Edinburgh inventory.* Neuropsychologia, 1971. 9(1): p. 97-113.**

35. **Lauer, R.T.P., P. H.; Kilgore, K. L., *EEG-based control of a hand grasp neuroprosthesis.* . Neuroreport, 1999. 10(8): p. 1767-1771.**

36. **Lauer, R.T.l.P., P.H.; Kilgore, K.L.; Heetderks, W.J. , *Applications of cortical signals to neuroprosthetic control: A critical review.* IEEE Transactions on Rehabilitation Engineering, 2000. 8(2): p. 205-208.**

37. **Ang, K.K., et al., *Clinical study of neurorehabilitation in stroke using EEG-based motor imagery brain-computer interface with robotic feedback.* Conf Proc IEEE Eng Med Biol Soc, 2010. 1: p. 5549-52.**

38. **Buch, E., et al., *Think to move: a neuromagnetic brain-computer interface (BCI) system for chronic stroke.* Stroke, 2008. 39(3): p. 910-7.**

39. **Krebs, H.I., et al., *Rehabilitation robotics: pilot trial of a spatial extension for MIT-Manus.* J Neuroeng Rehabil, 2004. 1(1): p. 5.**

40. **Lo, A.C., et al., *Robot-assisted therapy for long-term upper-limb impairment after stroke.* N Engl J Med, 2010. 362(19): p. 1772-83.**

41. **Birbaumer, N. and L.G. Cohen, *Brain-computer interfaces: communication and restoration of movement in paralysis.* J Physiol, 2007. 579(Pt 3): p. 621-36.**

42. **Fabiani, G.E., et al., *Conversion of EEG activity into cursor movement by a brain-computer interface (BCI).* IEEE Trans Neural Syst Rehabil Eng, 2004. 12(3): p. 331-8.**

43. **Guger, C., et al., *How many people are able to operate an EEG-based brain-computer interface (BCI)?* IEEE Trans Neural Syst Rehabil Eng, 2003. 11(2): p. 145-7.**

44. **McFarland, D.J., A.T. Lefkowicz, and J.R. Wolpaw, *Design and operation of an EEG-base brain-computer interface with digital signal processing technology.* Behavior Research Methods, Instruments, & Computers, 1997. 29(3): p. 337-345.**

45. **Schalk, G., et al., *BCI2000: a general-purpose brain-computer interface (BCI) system.* IEEE Trans Biomed Eng, 2004. 51(6): p. 1034-43.**

46. **Dobkin, B.H., *Brain-computer interface technology as a tool to augment plasticity and outcomes for neurological rehabilitation.* J Physiol, 2007. 579(Pt 3): p. 637-42.**

47. **Ang, K.K., et al., *A clinical evaluation on the spatial patterns of non-invasive motor imagery-based brain-computer interface in stroke.* Conf Proc IEEE Eng Med Biol Soc, 2008. 2008: p. 4174-7.**

48. **Ang, K.K., et al., *Clinical study of neurorehabilitation in stroke using EEG-based motor imagery brain-computer interface with robotic feedback.* Conf Proc IEEE Eng Med Biol Soc, 2010. 2010: p. 5549-52.**

49. **Ang, K.K., et al., *A clinical evaluation of non-invasive motor imagery-based brain-computer interface in stroke.* Conf Proc IEEE Eng Med Biol Soc, 2008. 2008: p. 4178-81.**

50. **Murase, N., et al., *Influence of interhemispheric interactions on motor function in chronic stroke.* Ann Neurol, 2004. 55(3): p. 400-9.**

51. **Duque, J., et al., *Transcallosal inhibition in chronic subcortical stroke.* Neuroimage, 2005. 28(4): p. 940-6.**

52. **Nudo, R.J. and G.W. Milliken, *Reorganization of movement representations in primary motor cortex following focal ischemic infarcts in adult squirrel monkeys.* J Neurophysiol, 1996. 75(5): p. 2144-9.**

53. **Johansson, B.B., *Brain plasticity and stroke rehabilitation. The Willis lecture.* Stroke, 2000. 31(1): p. 223-30.**

54. **Taub, E., G. Uswatte, and D.M. Morris, *Improved motor recovery after stroke and massive cortical reorganization following Constraint-Induced Movement therapy.* Phys Med Rehabil Clin N Am, 2003. 14(1 Suppl): p. S77-91, ix.**

55. **Kolb, B. and I.Q. Whishaw, *Brain plasticity and behavior.* Annu Rev Psychol, 1998. 49: p. 43-64.**

56. **Rossini, P.M., et al., *Post-stroke plastic reorganisation in the adult brain.* Lancet Neurol, 2003. 2(8): p. 493-502.**

57. **Rossini, P.M. and G. Dal Forno, *Neuronal post-stroke plasticity in the adult.* Restor Neurol Neurosci, 2004. 22(3-5): p. 193-206.**

58. **Liepert, J., M. Tegenthoff, and J.P. Malin, *Changes of cortical motor area size during immobilization.* Electroencephalogr Clin Neurophysiol, 1995. 97(6): p. 382-6.**

59. **Jenkins, W.M. and M.M. Merzenich, *Reorganization of neocortical representations after brain injury: a neurophysiological model of the bases of recovery from stroke.* Prog Brain Res, 1987. 71: p. 249-66.**

60. **Kaas, J.H., *Plasticity of sensory and motor maps in adult mammals.* Annu Rev Neurosci, 1991. 14: p. 137-67.**

61. **Munakata, Y. and J. Pfaffly, *Hebbian learning and development.* Dev Sci, 2004. 7(2): p. 141-8.**

62. **Pleger, B., et al., *Functional imaging of perceptual learning in human primary and secondary somatosensory cortex.* Neuron, 2003. 40(3): p. 643-53.**

63. **Hebb, D.O., *Physiological learning theory.* J Abnorm Child Psychol, 1976. 4(4): p. 309-14.**

64. **Taub, E., et al., *Technique to improve chronic motor deficit after stroke.* Arch Phys Med Rehabil, 1993. 74(4): p. 347-54.**

65. **Liepert, J., et al., *Motor cortex plasticity during constraint-induced movement therapy in stroke patients.* Neurosci Lett, 1998. 250(1): p. 5-8.**

66. **Sunderland, A. and A. Tuke, *Neuroplasticity, learning and recovery after stroke: a critical evaluation of constraint-induced therapy.* Neuropsychol Rehabil, 2005. 15(2): p. 81-96.**

67. **Wolf, S.L., et al., *Retention of upper limb function in stroke survivors who have received constraint-induced movement therapy: the EXCITE randomised trial.* Lancet Neurol, 2008. 7(1): p. 33-40.**

68. **Taub, E., *Somatosensory deafferentation research with monkeys: Implications for rehabilitation medicine.*, in *Behavioral Psychology in Rehabilitation Medicine: Clinical Applications*. 1980, Williams and Wilkins: New York. p. 371-401.**

69. **Dodds, T.A., et al., *A validation of the functional independence measurement and its performance among rehabilitation inpatients.* Arch Phys Med Rehabil, 1993. 74(5): p. 531-6.**

70. **Reinkensmeyer, D.J., J.L. Emken, and S.C. Cramer, *Robotics, motor learning, and neurologic recovery.* Annu Rev Biomed Eng, 2004. 6: p. 497-525.**

71. **Hogan, N. and H.I. Krebs, *Interactive robots for neuro-rehabilitation.* Restor Neurol Neurosci, 2004. 22(3-5): p. 349-58.**

72. **Hesse, S., et al., *Upper and lower extremity robotic devices for rehabilitation and for studying motor control.* Curr Opin Neurol, 2003. 16(6): p. 705-10.**

73. **Hogan N, K.H., Charnarong J, Sharon A., *Interactive robotic therapist.*, C.M.I.o. Technology, Editor. 1995: United States.**

74. **Lum, P.S., et al., *Robot-assisted movement training compared with conventional therapy techniques for the rehabilitation of upper-limb motor function after stroke.* Arch Phys Med Rehabil, 2002. 83(7): p. 952-9.**

75. **Reinkensmeyer, D.J., et al., *Understanding and treating arm movement impairment after chronic brain injury: progress with the ARM guide.* J Rehabil Res Dev, 2000. 37(6): p. 653-62.**

76. **Krebs, H.I., et al., *Robot-aided neurorehabilitation.* IEEE Trans Rehabil Eng, 1998. 6(1): p. 75-87.**

77. **Volpe, B.T., et al., *Robot training enhanced motor outcome in patients with stroke maintained over 3 years.* Neurology, 1999. 53(8): p. 1874-6.**

78. **Volpe, B.T., et al., *A novel approach to stroke rehabilitation: robot-aided sensorimotor stimulation.* Neurology, 2000. 54(10): p. 1938-44.**

79. **Fugl-Meyer, A.R., et al., *The post-stroke hemiplegic patient. 1. a method for evaluation of physical performance.* Scand J Rehabil Med, 1975. 7(1): p. 13-31.**

80. **Fugl-Meyer, A.R., L. Jaasko, and V. Norlin, *The post-stroke hemiplegic patient. II. Incidence, mortality, and vocational return in Goteborg, Sweden with a review of the literature.* Scand J Rehabil Med, 1975. 7(2): p. 73-83.**

81. **Brunnstrom, S., *Motor testing procedures in hemiplegia: based on sequential recovery stages.* Phys Ther, 1966. 46(4): p. 357-75.**

82. **Twitchell, T.E., *The restoration of motor function following hemiplegia in man.* Brain, 1951. 74(4): p. 443-80.**

83. **Roth, M., et al., *Possible involvement of primary motor cortex in mentally simulated movement: a functional magnetic resonance imaging study.* Neuroreport, 1996. 7(7): p. 1280-4.**

84. **Porro, C.A., et al., *Primary motor and sensory cortex activation during motor performance and motor imagery: a functional magnetic resonance imaging study.* J Neurosci, 1996. 16(23): p. 7688-98.**

85. **Lotze, M., et al., *Activation of cortical and cerebellar motor areas during executed and imagined hand movements: an fMRI study.* J Cogn Neurosci, 1999. 11(5): p. 491-501.**

86. **Rizzolatti, G. and L. Craighero, *The mirror-neuron system.* Annu Rev Neurosci, 2004. 27: p. 169-92.**

87. **Stevens, J.A. and M.E. Stoykov, *Using motor imagery in the rehabilitation of hemiparesis.* Arch Phys Med Rehabil, 2003. 84(7): p. 1090-2.**

88. **Hari, R., et al., *Activation of human primary motor cortex during action observation: a neuromagnetic study.* Proc Natl Acad Sci U S A, 1998. 95(25): p. 15061-5.**

89. **Rizzolatti, G., et al., *Premotor cortex and the recognition of motor actions.* Brain Res Cogn Brain Res, 1996. 3(2): p. 131-41.**

90. **Decety, J. and J. Grezes, *Neural mechanisms subserving the perception of human actions.* Trends Cogn Sci, 1999. 3(5): p. 172-178.**

91. **Lyle, R.C., *A performance test for assessment of upper limb function in physical rehabilitation treatment and research.* Int J Rehabil Res, 1981. 4(4): p. 483-92.**

92. **Ward, N.S., *Mechanisms underlying recovery of motor function after stroke.* Postgrad Med J, 2005. 81(958): p. 510-4.**

93. **Nicolelis, M.A., *Actions from thoughts.* Nature, 2001. 409(6818): p. 403-7.**

94. **Farwell, L.A. and E. Donchin, *Talking off the top of your head: toward a mental prosthesis utilizing event-related brain potentials.* Electroencephalogr Clin Neurophysiol, 1988. 70(6): p. 510-23.**

95. **Pfurtscheller, G. and C. Neuper, *Future prospects of ERD/ERS in the context of brain-computer interface (BCI) developments.* Prog Brain Res, 2006. 159: p. 433-7.**

96. **Birbaumer, N., et al., *EEG and slow cortical potentials in anticipation of mental tasks with different hemispheric involvement.* Biol Psychol, 1981. 13: p. 251-60.**

97. **Coyle, S.M., T.E. Ward, and C.M. Markham, *Brain-computer interface using a simplified functional near-infrared spectroscopy system.* J Neural Eng, 2007. 4(3): p. 219-26.**

98. **Hinterberger, T., et al., *An EEG-driven brain-computer interface combined with functional magnetic resonance imaging (fMRI).* IEEE Trans Biomed Eng, 2004. 51(6): p. 971-4.**

99. **Weiskopf, N., et al., *Physiological self-regulation of regional brain activity using real-time functional magnetic resonance imaging (fMRI): methodology and exemplary data.* Neuroimage, 2003. 19(3): p. 577-86.**

100. **Berger, H., *Uber das electrenkephalogramm des menchen.* Arch Psychiatrm Nervenkr, 1929. 87: p. 527–570.**

101. **Walter, W.G., et al., *Contingent Negative Variation: an Electric Sign of Sensorimotor Association and Expectancy in the Human Brain.* Nature, 1964. 203: p. 380-4.**

102. **Birbaumer, N., *Breaking the silence: brain-computer interfaces (BCI) for communication and motor control.* Psychophysiology, 2006. 43(6): p. 517-32.**

103. **Jasper, H.H., *The Ten Twenty Electrode System of the International Federation.* Electroencephalogr Clin Neurophysiol, 1958. 10: p. 371-375.**

104. **Hochberg, L.R. and J.P. Donoghue, *Sensors for brain-computer interfaces.* IEEE Eng Med Biol Mag, 2006. 25(5): p. 32-8.**

105. **Wolpaw, J.R. and D.J. McFarland, *Control of a two-dimensional movement signal by a noninvasive brain-computer interface in humans.* Proc Natl Acad Sci U S A, 2004. 101(51): p. 17849-54.**

106. **Babiloni, C., et al., *Human movement-related potentials vs desynchronization of EEG alpha rhythm: a high-resolution EEG study.* Neuroimage, 1999. 10(6): p. 658-65.**

107. **Vaughan, T.M., et al., *The Wadsworth BCI Research and Development Program: at home with BCI.* IEEE Trans Neural Syst Rehabil Eng, 2006. 14(2): p. 229-33.**

108. **McFarland, D.J., et al., *Spatial filter selection for EEG-based communication.* Electroencephalogr Clin Neurophysiol, 1997. 103(3): p. 386-94.**

109. **Florian, G. and G. Pfurtscheller, *Dynamic spectral analysis of event-related EEG data.* Electroencephalogr Clin Neurophysiol, 1995. 95(5): p. 393-6.**

110. **Jansen, B.H., et al., *Usefulness of autoregressive models to classify EEG-segments.* Biomed Tech (Berl), 1979. 24(9): p. 216-23.**

111. **Schlogl, A., D. Flotzinger, and G. Pfurtscheller, *Adaptive autoregressive modeling used for single-trial EEG classification.* Biomed Tech (Berl), 1997. 42(6): p. 162-7.**

112. Daniel, W.W., *Biostatistics, a foundation for analysis in the health sciences*. 4th ed. Wiley series in probability and mathematical statistics Applied probability and statistics. 1987, New York: Wiley. xiii, 733 p.

113. Wonnacott, T.H. and R.J. Wonnacott, *Introductory statistics for business and economics*. 4th ed. Wiley series in probability and mathematical statistics. 1990, New York: Wiley. xvi, 815 p.

114. Newell, K.M., Y.T. Liu, and G. Mayer-Kress, *Time scales in motor learning and development.* Psychol Rev, 2001. 108(1): p. 57-82.

115. Sainburg, R.L. and D. Kalakanis, *Differences in control of limb dynamics during dominant and nondominant arm reaching.* J Neurophysiol, 2000. 83(5): p. 2661-75.

116. Prilutsky B.I., K.A.N., Farrell B., Harley L., Phillips G., Bottasso C.L. , *Movement coordination in skilled tasks: Insights from optimization.*, in *Advances in Neuromuscular Physiology of Motor Skills and Muscle Fatigue.*, M. Shinohara, Editor. Unpublished manuscript., Transworld Research Network: Kerala, India.

117. Shanbao Tong, N.V.T., *Quantitative EEG Analysis Methods and Clinical Applications*. Artech House Series, Engineering in Medicine & Biology, ed. C.J. Martin Yarmush. 2009, Norwood, MA: Artech House.

118. Miller, K.J., et al., *Three cases of feature correlation in an electrocorticographic BCI.* Conf Proc IEEE Eng Med Biol Soc, 2008. 2008: p. 5318-21.

119. Leuthardt, E.C., et al., *A brain-computer interface using electrocorticographic signals in humans.* J Neural Eng, 2004. 1(2): p. 63-71.

120. Fay, M.P. and M.A. Proschan, *Wilcoxon-Mann-Whitney or t-test? On assumptions for hypothesis tests and multiple interpretations of decision rules.* Stat Surv, 2010. 4: p. 1-39.

121. Wilcoxon, F., *Individual comparisons of grouped data by ranking methods.* J Econ Entomol, 1946. 39: p. 269.

122. Flanagan, J.R., et al., *Prediction precedes control in motor learning.* Curr Biol, 2003. 13(2): p. 146-50.

123. Abe, S., *Support vector machines for pattern classification*. 1st ed. 2010, New York: Springer.

124. Bishop, C.M., *Pattern Recognition and Machine Learning*, ed. J.K. Michael Jordan, Bernhard Scho¨lkopf. 2006, New York, NY: Springer Science.

125. Boyle, B.H., *Support vector machines : data analysis, machine learning, and applications*. Computer science, technology, and applications. 2011, Hauppauge, N.Y.: Nova Science Publishers.

126. **Cristianini, N. and J. Shawe-Taylor, *An introduction to support vector machines : and other kernel-based learning methods*. 2000, Cambridge ; New York: Cambridge University Press. xiii, 189 p.**

127. **Thurstone, L.L., *The learning curve equation*. 1919, Psychological review company, University of Chicago: Princeton, N.J.,. p. 3 p. l., 51 p.**

128. **Perneger, T.V., *What's wrong with Bonferroni adjustments.* BMJ, 1998. 316(7139): p. 1236-8.**

129. **Carmer, S.G. and M.R. Swanson, *Detection of Differences Between Means: A Monte Carlo Study of Five Pairwise Multiple Comparison Procedures.* Agron. J., 1971. 63: p. 940–945**

130. **Tukey, J.W., *Comparing individual means in the analysis of variance.* Biometrics, 1949. 5(2): p. 99-114.**

131. **McFarland, D.J. and J.R. Wolpaw, *Sensorimotor rhythm-based brain-computer interface (BCI): feature selection by regression improves performance.* IEEE Trans Neural Syst Rehabil Eng, 2005. 13(3): p. 372-9.**

132. **Garrett, D., et al., *Comparison of linear, nonlinear, and feature selection methods for EEG signal classification.* IEEE Trans Neural Syst Rehabil Eng, 2003. 11(2): p. 141-4.**

133. **Lotte, F., et al., *A review of classification algorithms for EEG-based brain-computer interfaces.* J Neural Eng, 2007. 4(2): p. R1-R13.**

134. **Pfurtscheller, G., et al., *EEG-based discrimination between imagination of right and left hand movement.* Electroencephalogr Clin Neurophysiol, 1997. 103(6): p. 642-51.**

135. **Etnier, J.L., et al., *Changes in electroencephalographic activity associated with learning a novel motor task.* Res Q Exerc Sport, 1996. 67(3): p. 272-9.**

136. **Gliner, J.A., P.M. Mihevic, and S.M. Horvath, *Spectral analysis of electroencephalogram during perceptual-motor learning.* Biol Psychol, 1983. 16(1-2): p. 1-13.**

137. **Niedermeyer, E., D.L. Schomer, and F.H. Lopes da Silva, *Niedermeyer's electroencephalography : basic principles, clinical applications, and related fields*. 6th ed. 2011, Philadelphia: Wolters Kluwer/Lippincott Williams & Wilkins. xv, 1275 p.**

138. **Pineda, J.A., *The functional significance of mu rhythms: translating "seeing" and "hearing" into "doing".* Brain Res Brain Res Rev, 2005. 50(1): p. 57-68.**

139. **Etnier, J.L. and D.M. Landers, *Motor performance and motor learning as a function of age and fitness.* Res Q Exerc Sport, 1998. 69(2): p. 136-46.**

140. Tunney, N.T., Leslie F.; Gaddy, Mandy; Rosenfeld, Amie; Pearce, Neal; Tamanini, Jeff; Treby, Alison *Aging and Motor Learning of a Functional Motor Task.* Physical & Occupational Therapy in Geriatrics 2004. 21(3): p. 1-16.

141. Serrien, D.J., S.P. Swinnen, and G.E. Stelmach, *Age-related deterioration of coordinated interlimb behavior.* J Gerontol B Psychol Sci Soc Sci, 2000. 55(5): p. P295-303.

142. Wang, Y. and S. Makeig, *Predicting Intended Movement Direction Using EEG from Human Posterior Parietal Cortex*, in *Foundations of Augmented Cognition. Neuroergonomics and Operational Neuroscience*, D. Schmorrow, I. Estabrooke, and M. Grootjen, Editors. 2009, Springer Berlin / Heidelberg. p. 437-446.

143. Waldert, S., et al., *Hand movement direction decoded from MEG and EEG.* J Neurosci, 2008. 28(4): p. 1000-8.

144. Berndt, I., et al., *Effects of pointing direction and direction predictability on event-related lateralizations of the EEG.* Hum Mov Sci, 2002. 21(3): p. 387-410.

145. Hammon, P.S., et al., *Predicting Reaching Targets from Human EEG.* Signal Processing Magazine, IEEE, 2008. 25(1): p. 69-77.